**FOREIGN
BROADCAST
INFORMATION
SERVICE**

JPRS Report

Science & Technology

China

SCIENCE & TECHNOLOGY

CHINA

CONTENTS

BIOTECHNOLOGY

MICROELECTRONICS

Launch of Missile From Nuclear Submarine Detailed

40080166 Beijing HANGTIAN [SPACEFLIGHT] in Chinese No 1, 26 Jan 89 pp 2-3

[Article by Xi Qixin [1153 0796 2450]]

[Excerpt] In September 1988, China successfully conducted an underwater test of a missile launched from a nuclear submarine, becoming one of the few countries in the world with such a nuclear counter-strike capability. As a reporter assigned to cover activities in defense science and technology, I had the unusual opportunity to witness this great event.

A Day To Be Remembered

On a certain day in September, the sky over this ocean test site in northern China was crystal-clear, and visibility was unlimited. A fleet of escort vessels had arrived at the test site earlier and had set up a restricted zone several dozen nautical miles in radius. When the "August First" carrying this reporter reached the test area, the restricted zone had been completely cleared; the only vessel visible was the whale-like nuclear submarine tens of nautical miles from the observation ships, waiting for its command to submerge.

A command was issued by the control center: "Start countdown at minus 2 hours!" The giant whale began to submerge, and in a short time, white ripples appeared on the ocean surface where the submarine had been. When the countdown reached minus 5 minutes, all personnel at the control center, the monitoring center and the observation stations stopped to listen for the earth-shaking roar of rocket ignition.

With the final countdown: "5, 4, 3, 2, 1, ignition!", a milk-white rocket pierced through the water accompanied by a

thundering roar, and headed straight upward. The orange flame
from the rocket engine looked like a long scarf stretching from
the ocean to the sky.

The observation stations began to send back a series of
reports: "flight condition normal!", "first-stage cut-off,
second-stage ignition!", "second-stage cut off!" Soon the
rocket had disappeared from view; only a smoke trail continued
to linger in the sky.

A middle-aged scientists standing next to me let out a sigh of
relief. Shortly after, the control center issued the following
messages: "The target was spotted by one of the monitoring
ships!"; "The target landed in the water, close to the
designated impact point!" Immediately, all the ships in the
test region began blowing their whistles, and continued for as
long as 3 minutes. On the "August First," a military band
played the national anthem; everyone stood at attention, facing
the Chinese flag waving in the breeze. I was overwhelmed by a
sense of national pride. That evening, I wrote the following
comment in my diary: "This day will be remembered in history."

Developing the Nuclear Submarine Is a National Priority

The next day, I was permitted to board the nuclear submarine
which was now docked in the harbor. When I entered the main
cabin, I had the illusion of entering a scientific palace.
Large rocket launch tubes stood neatly in the missile
compartment; countless pipes and cables stretched across the
compartments like blood vessels in the human body; a variety of
electronic instruments, equipment, and computers exhibited the
marvels of modern technology.

The nuclear submarine is regarded as an indicator of a nation's
industrial and technological standards. It has many desirable
features including good concealment, long endurance, high
survivability, and the capability of initiating surprise
attacks; it has been called a mobile "underwater launch silo."
In the early 1950's, General Nieh Rongzhen had the courage and
foresight as a military strategist to propose to the Party
Central Committee that China should develop its own nuclear
submarine. This proposal was immediately approved by Chairman
Mao, Premier Zhou Enlai, and by General Peng Dehuai. At that
time, an attempt was made to obtain technical data on the
submarine from a major country, but the request was denied. To
show his determination, Chairman Mao said: "We shall develop
the nuclear submarine even if it takes 10,000 years!"

The difficult task of development fell on the shoulders of the Chinese scientists and engineers. One of the scientists who took part in the initial development told me: "In the early days, the only technical information we had were two photographs of a foreign nuclear submarine." But after many years of struggle and determined efforts, China finally succeeded in building a state-of-the-art nuclear submarine.

A key contributor to the nuclear submarine project was Huang Xuhua. Huang was a Communist Party member and graduate of Jiaotong University who had lived through many wars. He was given the responsibility as the chief technical manager for the project. The first challenge he encountered was to design the profile of the submarine. The profile of a submarine not only plays an important role in determining the drag force on the submarine when travelling through water, but also dictates the design and layout of the various subsystems of the vehicle. At the time, he was faced with a choice between the streamlined design of a conventional submarine and the advanced teardrop design of the nuclear submarine models. The former choice would be the easier task because there was a large amount of data available and considerable experience in its construction; the latter choice would be much more difficult because there was no information whatsoever except a few photographs in foreign magazines. However, in order to catch up with the state-of-the-art in nuclear submarines, Huang chose the more advanced design. As a consequence, he spent many sleepless nights and countless hours exploring, testing, and overcoming major technical obstacles before achieving success.

During the course of my interviews, I heard the following story: One of the scientists who participated in the development of the nuclear submarine died from exhaustion. On his deathbed, he made a request to his colleagues: "If one day the missile launch actually takes place, please call my name so my spirit can share the joy of victory with all of you." It was the loyalty and dedication of people like this scientist that China's defense industry is able to enjoy today's success.

Rocket Designer and Craftsman

In an introductory remark, chief rocket designer Chen Deren said: "A submarine-launched missile has some unique features which are not shared by conventional missiles because it is launched from under the water. First, it does not have the same degree of design freedom as a ground-based liquid-propellant rocket. Its dimensions must be kept very small to comply with the constraints of the submarine launch tubes; it

must also meet very strict reliability requirements because of the densely packed and long-term storage mode on the submarine. Second, the missile must be able to endure the stress as it is ejected from the launch tube into the water at high speeds and as it exits the water. Third, since the missile is launched from a moving platform, the launch system must be specially designed to compensate for the motion of the submarine; also, measures must be taken to ensure the stability of the missile attitude when traveling through rough seas. Chen also said: "In order to meet the special requirements of a submarine-launched missile, we have used a propulsion system with a solid-propellant engine. To convert from a liquid-propellant system to a solid-propellant system required some major modifications." [Passage omitted]

Chen's remarks reminded me of a young man named Wang Lin, who was the shop supervisor of a certain factory under the Ministry of Aerospace Industry. The shop was assigned the task of developing solid rocket fuels; it was a very dangerous assignment because without any prior knowledge, the research efforts were mostly exploratory, no one knew what the margin of safety was. During each test, Wang was stationed at the most critical post. One day, an accident happened; the fuel exploded, throwing the steel-reinforced safety door a distance of 80 meters, and Wang was crushed under the 1-ton steel door. This tragic accident, however, did not cause panic or grief among other members of the research team; they continued to press forward in the face of the unknown. Another engineer injured his face and lost all his fingers from burns, yet he refused to give up his job. Without the unselfish sacrifices of these researchers, there would have been no successful rocket flight today. [Passage omitted]

Telemetry Data-Processing Software Developed

[Article by Wang Juntao [3769 1498 3447]]

[Text] The real-time data-processing software package for a multi-channel telemetry system developed by the Linquan [2651 3123] Electric Machine Plant of the Guizhou Space Industries Corporation has been in use at the Nan Hang Remotely-Piloted Vehicle Institute and at a certain air force base for nearly three years. It has made significant contributions to the development and testing of China's aerospace and aviation products.

This package can be used for real-time data processing for both PAM-FM-FM [pulse amplitude modulation-FM-FM] and PCM-FM [pulse code modulation-FM] multi-channel telemetry systems. In particular, it can be used to perform verification and certification of space vehicles, aircraft and ground vehicles. Before using the software package, the user first keys into the computer the parameters of a telemetry channel (e.g., name, unit, channel position, input-output relationship, and the range of parameter values). To use the software, the user simply keys in the parameter code number and the processing-time segment to activate the various data-processing modes. The processing modes include: curve fitting of the data based on an order selected by the software package, inspecting the telemetry data quality, etc. The package also has the capability of verifying the timing mechanism of the telemetry system, testing the degree of linearity of the PAM demodulator, and processing in parallel the data from multiple telemetry channels. In addition, it has many flexible features such as operating in an interactive mode, printing data in different formats, performing data interpolation and removing unusual data points, displaying parameter curves in color on an 800x600 large screen, plotting time history curves of physical parameters, and automatically adjusting the coordinate system based on the parameter values to be plotted. In the past, processing telemetry data required several days or even several months, and the accuracy was rather poor. By using this software package, accurate results can be obtained in a timely manner at the data collection site. This software has been favorably received by Army commanders and by commercial users.

Advanced Guided Missile/Space Monitoring and Control Network Completed

40080173c Beijing KE JI RIBAO [SCIENCE & TECHNOLOGY DAILY] in Chinese
29 Apr 89 p 1

[Article by Liu Jianghai [0491 3068 3189] and Wang Hanlin [3769 5060 2651]]

[Text] The measurement and control technologies used by China's advanced
guided-missile/space monitoring and control network are considered to be
state-of-the-art. In a recent competition to provide monitoring and
control services for the International Maritime Satellite Organization,
China easily won the bid. This shows the competitive advantage China
has in this field.

The development of monitoring and control technologies in this country
began with the tracking and measurement of China's first surface-to-
surface missile. After 30 years of continuous progress in this area,
the current system not only can track missiles and rockets, but can also
direct the sending of a satellite into space and its retrieval back to
earth, and can accurately position it in a geosynchronous or sun-synchronous
orbit. Over the years, a team of nearly 10,000 scientists and engineers
with a wide range of special disciplines and the capability to conduct
various tests has been established; coordinated plans and documents to
support missile and satellite tests have been developed; a complete
set of technical management systems, methodologies and regulations is
being established; high-precision monitoring and control flight regions
and medium-precision networks of monitoring and control and data exchange
have also been established to support integrated tests of different missile
models and launch vehicles. Specifically, 30 space-monitoring and control
stations including the mobile tracking stations of the Xian Satellite
Monitoring and Control Center and the two "Yuan Wang" space-tracking ships
have been constructed. More than 500 large tracking facilities and
thousands of medium and small tracking facilities have been built, all
of which use exclusively Chinese-made equipment; most of these systems have
ranging, doppler, telemetry and remote-control capabilities.

In conjunction with the ground tracking stations and the fleet of tracking
ships, this monitoring and control network can accurately measure and
control rockets and satellites within a range of 9,000 km and up to an

altitude of 36,000 km above the earth; it can also command the spacecraft
to perform difficult maneuvers in space. Within the measurement range
of several thousand kilometers, the tracking-station positioning accuracy
has reached the meter level and the time-synchronization accuracy has
reached 1 micro-second.

The missile/space monitoring and control network has been used in several
hundred missile tests and 25 satellite launches including those of 11
retrievable satellites; the 100-percent success rate makes this system
one of the best in the world. It has also participated in the tracking
and monitoring of the U.S. "Spacelab" and the Soviet "Cosmos 1402" nuclear-
powered ocean reconnaissance satellite; prediction accuracies have been
comparable to those achieved by developed nations.

KRS-5 Crystal Growth in Various Atmospheres, Polycrystalline Fiber Preparation

[English abstract of article by Hou Yinchun [0186 0603 2504], et al., of Shanghai Institute of Optics and Fine Mechanics, Chinese Academy of Sciences]

[Text] KRS-5 single crystals have been grown in three kinds of atmospheres-- air, Ar and Ar+I_2. The scattering centers in crystals were examined and the metal impurities and oxygen content of the crystals were analyzed. The poly- crystalline fibers, 0.5-1 mm in diameter, have been prepared by an extrusion method. The stability and attenuation of the fiber are discussed.

References

1. Harrington, J.A., SPIE, Vol 266, "Infrared Fibers (0.8 - 12 μm)," 1981 p 10.
2. Ikedo, S., LASER RESEARCH, Vol 11 No 11, 1983 p 834.
3. Sakuragi, S., SPIE, Vol 32, "Advances in Infrared Fibers," 1982 p 2.
4. Wang Fengyun, et al., CHINESE JOURNAL OF LASERS, Vol 15 No 21, 1988 p 734.
5. Duthler, C.J., J APPL PHYS, Vol 45 No 6, 1974 p 2668.
6. Klein, P.H., Davisson, J.W., MAT RES BULL, Vol 11, 1976 p 1335.
7. Quan Ningsan, LASER AND INFRARED TECHNOLOGY, No 1, 1986 p 36.
8. Sparks, M.G., Deshazer, L.G., SPIE, Vol 266, "Infrared Fibers (0.8 - 12 μm)," 1981 p 3.

Study of Growth of LATGS/P Single Crystal by Means of Rotating Disk Method

[English abstract of article by Liao Yingliang [1675 2019 5328], et al., of Shanghai Institute of Technical Physics, Chinese Academy of Sciences]

[Text] A study involving modified TGS crystals has been conducted by means of the rotating disk method, partially substituting H_3PO_4 for H_2SO_4 and doping with an appropriate amount of L-lalanine. The growth habits of the modified crystals are examined and the optimum growth conditions are found. Therefore, a perfect and uniform single crystal of LATGS/P with high efficiency has been obtained. The area of this crystal is more than 100 x 50 mm^2. Its dielectric constant is 25-28, dielectric loss is $3 \times 10^{-4} - 1 \times 10^{-3}$, pyroelectric coefficient p is 4×10^{-8} $C/cm^2 \cdot$ K and internal bias E_b is 3-5 kV cm. The modified crystal has been used as a sensitive element in a pyroelectric detector and for targets of a pyroelectric vidicon.

References

1. Fang Changshui, et al., JOURNAL OF SHANDONG UNIVERSITY, Vol 4, 1983 p 112.
2. Lin Xueshi, INFRARED PHYSICS AND TECHNOLOGY, Vol 2, 1980 p 55.
3. NOAA-73040506.

Growth of Lithium Triborate Single Crystals by Flux Seeding Method

[English abstract of article by Jiang Aidong [3068 1947 2767], et al., of Fujian Institute of Research on the Structure of Matter, Chinese Academy of Sciences]

[Text] Plate-shaped lithium triborate single crystals with dimensions of 38 x 24 x 4 mm have been grown by the flux seeding method using a self-flux B_2O_3 of composition $LiB_3O_5 : B_2O_3 = 2 : 1$ (mol) at a constant temperature for a long time and then have been cooled very slowly. Although self-flux has the advantage of preventing contamination to the crystal, the viscosity of the solution is so high that it is very difficult to increase the growth rate for large crystals. Therefore, efforts have been achieved in this respect. Finally, a large crystal of up to 37 x 25 x 13 mm of superior quality has been grown using this new flux.

References

1. Mazzeti, C., Carli, F.D., CHIM ITAL, Vol 56, 1926 p 23.
2. Rollet, A.P., Bouaziz, R., COMPT RAND, Vol 240, 1955 p 2417.
3. Sastry, B.S.R., Hummel, F.A., J AMER CERAM SOC, Vol 41, 1958 p 7.
4. Bouaziz, R., ANN CHIM, Vol 6, 1961 p 345.
5. Koning, H., Hoppe, R., Z ANORG ALLG CHEM, Vol 439, 1978 p 77.
6. Ihara, M., et al., YOGYO KOYOKAISHI, Vol 88, 1980 p 179.
7. Jiang Aidong, ARTIFICIAL CRYSTALS, Vol 17 Nos 3-4, 1988 p 280.
8. Jiang Aidong, et al., J CRYST GROWTH, Vol 79, 1986 p 963.
9. Jiang Aidong, et al., ARTIFICIAL CRYSTALS, Vol 17 Nos 3-4, 1988 p 280.

$Cr^{3+}:LiGaW_2O_8$ Crystal Grown by Flux Method

[English abstract of article by Wang Guofu [3769 0948 1381], et al., of Fujian Institute of Research on the Structure of Matter, Chinese Academy of Sciences]

[Text] The growth of a $Cr^{3+}:LiGaW_2O_8$ crystal by the flux method is studied in this paper, and the growth temperature curve for the $LiGaW_2O_8-Li_2B_2O_4$ system has been de ermined by DTA. The size of the crystals is 6 x 11 x 35 mm. The peak wavelength of the $^4T_2-^4A_2$ transition vibronic spectrum and the fluorescence lifetime for $Cr^{3+}:LiGaW_2O_8$ crystals have been determined to be 9400 Å and 5 µs, respectively. $Cr^{3+}:LiGaW_2O_8$ crystals may be used as tunable phonon terminal infrared laser crystals.

References

1. Klevtsov, P.V., et al., SOVIET PHYS CRYST, Vol 16, 1971 p 440.
2. Luo Zundu, et al., CHINESE PHYSICS, Vol 6 No 4, 1986 p 991.

Study of Hepatitis B Virus DNA Structure

40081036a Beijing ZHONGGUO KEXUE [SERIES B] in Chinese No 1, Jan 89 pp 57-66

[Article by Qi Zuhe [3823 4371 0735] et al., Institute of Basic Medical Sciences, Chinese Academy of Medical Sciences, Beijing]

[Summary] Having successfully cloned the Hepatitis B virus strain subtype adr (adr NC-1) and determined the DNA sequences, researchers are trying to ascertain the variations among six subtypes including the Chinese-cloned adr NC-1 strain and five other subtypes isolated in other countries: pHBr 330, pBRHBadr-4, pADR-1, adw, and ayw.
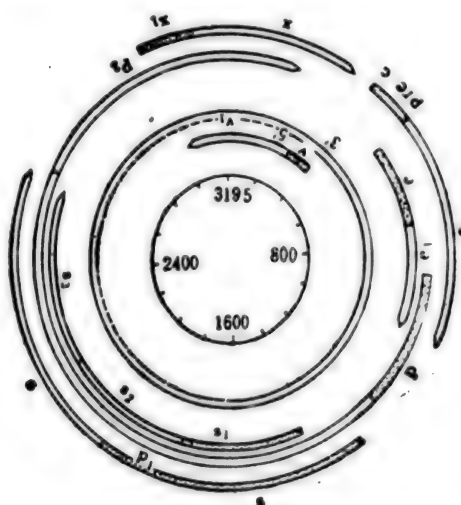
Figure 4.   adr NC-1 DNA gene and its frame structure

Table 1 shows that the average point mutation between different adr strains of adr subtype is 3 percent, and 10 percent between the subtypes. The homogeneity in the above cases was 97 percent and 90 percent respectively, from which the kinship between the subtypes can be explained.
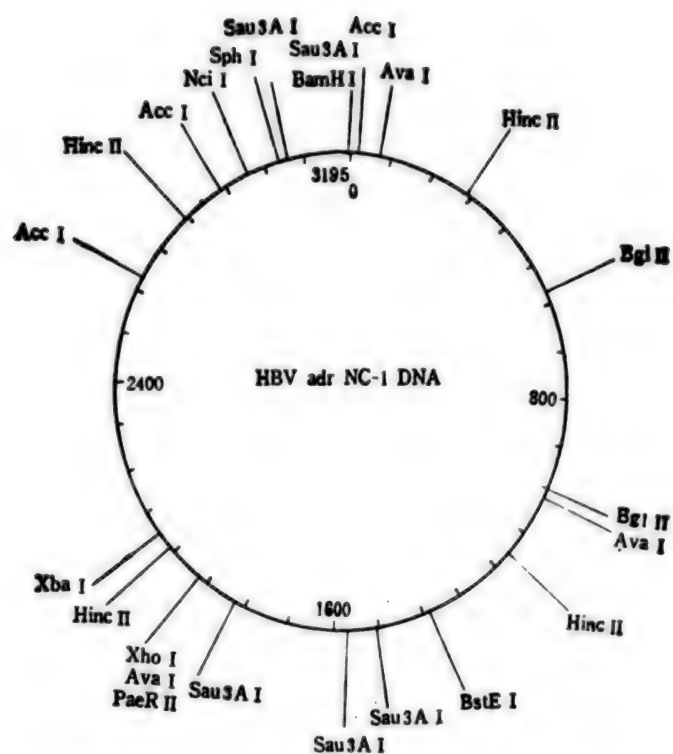
Figure 6. adr NC-1 HBV enzyme incision

Table 1. Homology of adr NC-1 and Other HBV DNA Sequences

| Subtype | No. of nucleotide | Point mutation | | % homology |
		No.	%	
adr pHBr330	3118	94	2.9	97.1
adr pADR-1	3215	98	3.1	96.9
adr adr4	3215	103	3.2	96.8
adw	3200	313	9.8	90.2
ayw	3182	363	11.4	88.6
adr NC-1	3195			

References

1. Siddiqui, A. et al., Proc. Natl. Acad. Sci. USA, 76 (1979), 4664.

2. Ono, Y. et al., Nucl. Acid. Res., 11 (1983), 1747.

3. Fujiyama, A. et al., Nucl. Acid. Res., 11 (1983), 4601.

13

4. Wu Xiangfu, et al., ZHONGGUO KEXUE [Scientia Sinica-Series B], 1983, 12: 1114.

5. Gan Renbao, et al., ACTA BIOCHIMICA ET BIOPHYSICA SINICA, 16 (1983), 316.

6. Cai Liangwan, et al., JOURNAL OF CHINESE ACADEMY OF MEDICAL SCIENCES, 6 (1984), 4: 251.

7. Qi Zuhe, et al., ZHONGGUO KEXUE [Scientia Sinica-Series B], 1988, 12: 1300-1304.

8. Galibert, F. et al., NATURE, 281 (1979), 646.

9. Steden, R., Nucl. Acid. Res., (1979), 6: 2601.

10. Hawley, D. K. et al., Nucl. Acid. Res., 118 (1983), 8: 2237.

11. Takahashi, K. et al., J. Gen. Virol., 57 (1981), 325.

12. Gerety, R. J. et al., Hepatitis B, Academic Press, 1985.

13. Yamada, E. et al., J. Gen. Virol., 64 (1983), 895.

14. Stibbie, W. et al., J. Virol., 46 (1983), 626.

15. Neurath, A. R., NATURE, 315 (1985), 1154.

16. Persing, D. H., Proc. Natl. Acad. Sci. USA, 82 (1985), 3440.

17. Weiher, H. et al., Science, 219 (1983), 626.

Fourth Annual Biomembrane Conference

40081036b Shanghai XIBAO SHENGWUXUE ZAZHI [CHINESE JOURNAL OF CELL BIOLOGY] in Chinese Vol 11 No 1, Mar 89 p 47

[Summary] The Chinese Fourth Annual Biomembrane Conference sponsored by the Chinese Society of Biophysics, the Society of Biochemistry, and the Society of Cell Biology, is scheduled to be held in December 1989 in order to exchange ideas on biomembrane development from the aspects of physics, chemistry, and biology. Areas to be concentrated on are:

1. Biomembrane structures

2. Biomembrane and energy transfer

3. Ion and small molecule transmembrane movement

4. Ion passage

5. Protein transmembrane transport

6. Biomembrane and message transmission (CAMP System, Inositol Phospholipid System)

7. Receptors

8. Membrane fusion

9. Early stage metamorphosis during embryonic development

10. Biomembrane and cell aging

11. Artificial cells and liposomes

12. Biomembranes and crop resistance to cold, drought, and disease

13. Biomembrane research techniques (fluorescence, nuclear magnetism, paramagnetism, freeze etching, and use of differential scanning calorimeter in membrane protein conformation studies

Synthesis, Antimalarial as well as Antitumor Activities of 2,4-Diamino-6-(N-Methyl-Substituted Benzylamino) Quinazolines*

[English abstract of article by Zhou Weicheng [0719 0251 3397], et al., of Shanghai Institute of Pharmaceutical Industry; Dai Zurui [2071 4371 3843] of Second Military University, Shanghai]

[Text] Sixteen 2,4-diamino-6-(N-methyl-substituted benzylamino) quinazolines (I) were synthesized by two different methods. 2-Nitro-5-chloro-benzonitrile was treated with the appropriate N-methyl-substituted benzylamines and I was formed after reduction and cyclization. The other method involved reductive methylation, i.e., 2,4-diamino-6-substituted benzylaminoquinazolines reacted with formaldehyde and sodium cyanoborohydride at pH 6.3.

Suppressive therapeutic tests on mice infected with <u>Plasmodium</u> <u>berghei</u> showed that four ($I_{6,7,10,16}$) of these compounds suppressed all the parasites when administered orally at a dose of 5 mg/kg and produced more than 99 percent suppression at 2.5 mg/kg. Eight compounds ($I_{1,2,4,5,8-10,15}$) were found to have antitumor effects against leukemia cells in cultures comparable to or superior to those of the positive control methotrexate.

References

1. Elslager, E.F., et al., "Folate Antagonist 9. 2,4-Diamino-6-[(aralkyl) alkylamino] Quinazolines, a Potent Class of Antimetabolites with Prodigious Antimalarial Effects," J MED CHEM, Vol 15, 1972 p 1138.
2. Dai Zurui, et al., CHINESE JOURNAL OF PHARMACOLOGY, Vol 3, 1982 p 210.
3. Yan Huifang, et al., MEDICINE INDUSTRY, Vol 19, 1988 p 396.
4. Li Guangyun, et al., ACTA PHARMACEUTICA SINICA, Vol 19, 1984 p 108.
5. Davoli, J., et al., "Folate Antagonist 2. 2,4-Diamino-6-{[aralkyl ana (heterocyclic) methyl] amino} Quinazolines, a Novel Class of Anti-metabolites of Interest in Drug-resistant Malaria and Chagas' Disease," J MED CHEM, Vol 15, 1972 p 812.

6. Zhang Xiuping, et al., ACTA PHARMACEUTICA SINICA, Vol 19, 1984 p 792.
7. Elslager, E.F., et al., "Synthesis of Fused Pyrimidines as Folate
   Antagonists," in Castle, R.N., ed., "Heterocyclic Chemistry," Vol 2,
   1st Ed, Orem, Utah, Hetero Corp, 1974, pp 97-133.
8. Zhang Xiuping, et al., ACTA PHARMACEUTICA SINICA, Vol 15, 1980 p 711.

Preliminary Study of HBsAg-Specific T Cell Clones*

[English abstract of article by Zhang Dingfeng [1728 1353 7685], et al., of the Institute of Viral Hepatitis, Chongqing Medical University]

[Text] Clones of HBsAg-reactive CD8+ and CD4+ T cells were obtained from the PBM of a hepatitis B immunized individual whose PBM proliferated when cultured with HBsAg. Lymphocytes were activated by culturing for 2 weeks with HBsAg and high concentrations of IL-2, then cloned in the presence of irradiated HBsAg-activated PBM and autologous EBV-transformed B cells, together with antigen and IL-2. All clones examined exhibited proliferation in an antigen-specific manner. Of the seven clones examined by flow cytometry, four were CD4+, CD8-, while three were CD4-, CD8+. Several clones produced IL-2 activity after stimulation with HBsAg. Since the development of CD8+ T-cell clones specific for soluble antigens has been difficult, the high frequency with which CD8+ cells were cloned in these experiments suggests that the cloning strategy employed may be of general use for the development of CD8+ clones. The availability of HBV-specific T cell clones of different phenotypes may help explain the mechanism of immunotolerance in HB infection.

References

1. Celis, E., et al., "Hepatitis B Virus-Reactive Human T Lymphocyte Clones: Antigen Specificity and Helper Function for Antibody Synthesis," J IMMUNOL, Vol 132, 1984 p 1511.
2. Zarling, J., et al., "Human Cytotoxic T Cell Clones Directed Against Herpes Simplex Virus Infected Cells," J IMMUNOL, Vol 136, 1986 pp 4669-4673.
3. Mohagheghpour, N., "Generation of Antigen Receptor-Specific Suppressor T Cell Clones in Man," J EXP MED, Vol 164, 1986 pp 950-955.
4. Ting, C.C., "Induction of Suppressor T Cells by Interleukin 2," J IMMUNOL, Vol 133, 1984 p 261.

5. Van de Griend, R.J., et al., "Rapid Expansion of Human Cytotoxic T Cell Clones: Growth Promotion by a Heat-Labile Serum Component and by Various Types of Feeder Cells," J IMMUNOL METHODS, Vol 66, 1984 p 285.
6. Chen, B.P., et al., "Presentation of Soluble Antigen to Human T Cells by Products of Multiple HLA-Linked," IMMUNOL, Vol 132, 1984 p 1511.

Studies of Enzymic Synthesis of Oligopeptides. II. Thermolysin-Catalyzed Synthesis of Peptides Containing Side Chain Free Carboxyl Group

[English abstract of article by Wang You [3076 3731], et al., of Shanghai Institute of Organic Chemistry, Chinese Academy of Sciences]

[Text] A number of peptides were synthesized from the carboxyl component containing a free side chain carboxyl group of aspartyl or glutamyl residue through thermolysin catalysis. The effects of neighboring residues situated near a C-terminal glutamic or aspartic acid in the carboxyl component on the formation of peptide bonds have been studied. The efficiency of coupling by thermolysin was found to vary with the nature of the amino component and the carboxyl component. Strict stereospecificity was observed.

References

1. Wang You, et al., ACTA CHIMICA SINICA, 1985 p 246.
2. a) Morihara, K., et al., BIOCHEM BIOPHY RES COMMUN, Vol 92, 1980 p 396.
    b) Oka, T., Morihara, K., J BIOL CHEM, Vol 82, 1977 p 1055.
3. Wang You, et al., "Collected Abstracts from the First Symposium on Organic Synthesis," August 1985, Kunming.
4. Schön, Il, Kisfaludy, L., INT J PEPT PROTEIN RES, Vol 14, 1979 p 485.
5. Fruton, J.S., "Advances in Enzymology," Vol 53, ed by Meister, A., John Wiley and Sons, New York, 1982 p 239.
6. Oyama, K., et al., GEN OFFEN, 3 012 693, 1980.
7. Schröder, E., ANN CHEM, Vol 679, 1964 p 207.
8. Yamada, S., Tekeuchi, Y., TETRAHEDRON LETT, 1971 p 3595.

Observation of Immunogenic Effect of Intradermal Inoculation of Small Dose of Hepatitis B Vaccine

[English abstract of article by Liu Peiyan [0491 0160 6056], et al., of the Sanitary and Anti-epidemic Station of Daxing County, Beijing]

[Text] The immunogenic effect of intradermal inoculation of a small dose of HB vaccine was evaluated in 120 seronegative villagers (men: 55, women: 65) whose ages were from 3 to 70. These participants were randomly divided into a subcutaneous group (I) and intradermal group (II). The results showed that the anti-HBs seroconversion rates and P/N ratios of those who showed seroconversion for group I, II were 98.4 percent, 98.3 percent and 88.0, 89.4, respectively, after the third injection. There was no significant difference between the groups in the seroconversion rates and their P/N ratios ($p > 0.05$). It is concluded that, in these two groups, small doses of HB vaccine stimulate high immune responses. The intradermal small dose regime is safe, more economical and will make the HB vaccine available to more people.

References

1. Konishi, K., et al., IGAKU NO MEHAMI, Vol 134, 1985 p 253.
2. Yin Deming, et al., CHINESE JOURNAL OF EPIDEMIOLOGY, Vol 6, 1986 p 367.
3. Ding Zhengrong, et al., JOURNAL OF PUBLIC HEALTH AND DISEASE CONTROL, Vol 3, 1984 p 37.
4. Xu Huafang, et al., CHINESE JOURNAL OF INFECTIOUS DISEASES, Vol 3, 1985 p 253.
5. Hashimoto, E., et al., LIVER, Vol 26, 1985 p 157.
6. Wang Jingming, et al., JOURNAL OF THE ACADEMY OF MILITARY MEDICINE, Vol 11 No 5, 1987 p 338.
7. Liu Peixin, et al., "Study of New Signs of Rural HBV Infection," 1987 p 40.
8. Coudeau, A., et al., "Immunogenicity of Low Dose (1.25 and 0.31 μg) Hepatitis B Vaccine," LANCET, Vol 2, No 8411, 1984 p 1091.

First Isolation of Vibrio Alginolyticus from Samples Causing Food Poisoning

[English abstract of article by Ji Shuping [4764 5289 5493], et al., of the Hygiene and Anti-epidemic Station, Harbin]

[Text] The authors report an event of food poisoning which has been traced to the ingestion of salted shrimp. Vibrio alginolyticus was shown to be the causative agent through epidemiological investigations and etiological tests. Vibrio alginolyticus can bring about human septecemia and wound infection and it has been found in the feces of patients with diarrhea, but no determination of its pathogenicity has previously been made. Vibrio alginolyticus was isolated from the samples of food which led to food poisoning and, for the first time, it was determined to be a pathogen of food poisoning.

References

1. Lennette, E.H., et al., "Manual of Clinical Microbiology," 3rd edition, Washington, American Society for Microbiology, 1980 pp 231-234.
2. Krieg, N.R., et al., "Bergeys Manual of Systematic Bacteriology," Vol 1, London, Williams, 1984 pp 518-534.
3. Matsumoto, K., et al., "Clinical Examination," Tokyo, 1985 pp 556-558.
4. Zhou Guilian, et al., CHINESE JOURNAL OF MICROBIOLOGY AND IMMUNOLOGY, Vol 2, 1982 p 299.

Studies of Safety Assessment of Pesticides by Means of Immunological Criteria

[English abstract of article by Zhou Yunzhen [0719 7291 3791], et al., of the Department of Nutrition and Food Hygiene, Tongji Medical University, Wuhan]

[Text] The immunological responses induced by the pesticides HCH, Sevin and Malathion have been studied. The results show that the pesticides can produce immunological changes, even in low doses. These responses appeared more sensitive to toxicants than did other biological responses indicated by biochemical parameters. The sensitivity found by the authors is especially significant when setting up an early sensitivity criterion for detecting the toxicity of chemicals whose low toxicity is known, but cannot be determined due to the lack of specific criteria. In addition, the authors' studies show the dose-response relationship, and that this relationship produces the same results as the specific criterion. Therefore, the authors suggest that immunological criteria be thought of as part of the toxicological assessment criteria for food safety.

References

1. Han Chengyuan, "Indirect Coagulation Techniques," Beijing, Science Press, 1979 p 1.
2. Lin Feiqing, et al., JOURNAL OF SHANGHAI HOSPITAL NO 1, Vol 3, 1957 p 161.
3. Simpson, M.A., "Spectrophotometric Determination of Lymphocyte Mediated Sheep Red Blood Cell Hemolysis In Vitro," J IMMUNOL METH, Vol 21, 1978 p 159.
4. Lefford, M.L., et al., "The Measurement of Tuberculin Hypersensitivity in Rats," IN ARCH ALLERGY, Vol 47, 1974 p 570.
5. Zhou Rulin, et al., JOURNAL OF WUHAN MEDICAL COLLEGE, Vol 10 No 3, 1981 p 74.
6. Yu He, "Clinical Immunology Technology," Shanghai Science and Technology Press, 1983 p 388.
7. Xu Shuyun, et al., "Pharmacological Testing," Beijing People's Public Health Press, 1982 pp 945-946.
8. Gong Wei, et al., SHANGHAI JOURNAL OF IMMUNOLOGY, Vol 1, 1981 p 131.

9. Ji Jinlin, et al., JOURNAL OF WUHAN MEDICAL COLLEGE, No 3, 1984 p 197.
10. Zhou Yunzhen, et al., CHINESE JOURNAL OF PREVENTIVE MEDICINE, Vol 19, 1985 p 338.
11. Zhou Yunzhen, et al., HEALTH RESEARCH, Vol 6, 1972 p 9.
12. Vinogradov, FOREIGN MEDICINE AND PUBLIC HEALTH, Vol 3, 1985 p 159.
13. Xue Bin, OVERVIEW OF FOREIGN IMMUNOLOGICAL AND TOXICOLOGICAL RESEARCH, Vol 3, 1987 p 136.

Study of Mutagenicity of Toxoflavin from Pseudomonas Farinofermentans

[English abstract of article by Yue Qi'an [1471 0796 1344], et al., of the Department of Microbiology, Weifang Medical College]

[Text] Fermented corn flour containing toxoflavin and bongkretic acid produced by P. farinofermentans can cause acute food poisoning, but no studies on the mutagenicity of toxoflavin have yet been reported. The authors studied the mutagenicity of toxoflavin by Tradescantia Paludosa and animal micronucleus tests. The results show that toxoflavin exhibits distinct mutagenic action in both plant and animal cells. The mutagenic action of toxoflavin in cells may have an important bearing on food hygiene examination.

References

1. HEILONGJIANG MEDICINE, No 4, 1978 p 15.
2. JOURNAL OF CHINESE ACADEMY OF MEDICAL SCIENCES, Vol 2, 1980 p 77.
3. Zhao Naixin, et al., CHINESE PUBLIC HEALTH, Vol 6, 1987 p 65.
4. Hu Wenjuan, HEALTH RESEARCH, Vol 13, 1984 p 34.
5. Hu Yuhua, et al., JOURNAL OF HUAXI MEDICAL COLLEGE, Vol 17, 1986 p 314.
6. Shi Liming, et al., ADVANCES IN BIOCHEMISTRY AND BIOPHYSICS, No 3, 1975 p 33.
7. Gollapudi, B., Kamra, O.P., "Application of a Simple Giemsa Staining Method in the Micronucleus Test," MUTAT RES, Vol 64, 1979 p 45.
8. Li Shouqi, et al., CHINESE JOURNAL OF PREVENTIVE MEDICINE, Vol 19, 1985 p 24.
9. Huang Xingshu, "'Sanzhi' Testing of Environmental Chemicals," Zhejiang Science Press, 1985.
10. Ma Dexiu, et al., JOURNAL OF SHANDONG COLLEGE OF OCEANOLOGY, Vol 11 No 2, 1981 p 65.
11. Hou Jialong, BULLETIN OF BIOLOGY, No 5, 1987 p 15.
12. Chen Dengqin, et al., JOURNAL OF SHANDONG COLLEGE OF OCEANOLOGY, Vol 11 No 2, 1981 p 80.

Effect of Pyrethroids on Rat Brain Synaptosomal ATPase Activities

[English abstract of article by Tang Cuyue [0781 0191 6460], et al., of the Department of Environmental Toxicology, Tongji Medical University, Wuhan]

[Text] The in vitro effects of several pyrethroids on rat brain synaptosomal ATPase activities have been investigated. No significant changes in Na^+, K^+-ATPase or oligomycin-insensitive Mg^{2+}-ATPase activities were observed under the current experimental conditions, but all pyrethroids tested caused significant inhibition of oligomycin-sensitive Mg^{2+}-ATPase activity with a certain concentration dependence. The results suggest the possibility that pyrethroids may alter the cellular energy metabolism of the nervous system. One of the pesticides (Beijing pyrethroid) is Chinese made.

References

1. Casida, J.E., et al., "Mechanisms of Selective Action of Pyrethroid Insecticides," ANN REV PHARMACOL TOXICOL, Vol 23, 1983 p 413.
2. Crofton, K.M., et al., "Pyrethroid Insecticides and Radioligand Displacement from the GABA Receptor Chloride Ionophore Complex," TOXICOL LETT, Vol 35, 1987 p 183.
3. Abbassy, M.A., et al., "Pyrethroid Action on the Nicotinic Acetylcholine Receptor/Channel," PESTIC BIOCHEM PHYSIOL, Vol 19, 1983 p 299.
4. Staatz, C.G., et al., "Effect of Pyrethroids on [^{3}H] Kainic Acid Binding to Mouse Forebrain Membranes," TOXICOL APPL PHARMACOL, Vol 64, 1982 p 566.
5. Mishria, S.K., et al., "Effects of Vanadium on Different ATPases and Binding of ^{8}H-Labeled Ouabain and Calcium-45 to Rat Brain Synaptosomes," J TOXICOL ENVIRON HEALTH, Vol 8, 1981 p 449.
6. Desaiah, D., et al., "Effect of Acute and Continuous Morphine Administration on Catecholamine-Sensitive ATPases in Mouse Brain," J PHARMACOL EXP THER, Vol 208, 1979 p 80.
7. Lowry, O.H., et al., "Protein Measurement with the Folin Phenol Reagent," J BIOL CHEM, Vol 193, 1951 p 265.

8. Clark, J.M., et al., "Two Different Types of Inhibitory Effects of Pyre-throids on Nerve Ca and Ca+Mg-ATPase Activity in the Squid, Loligo Pealei," PESTIC BIOCHEM PHYSIOL, Vol 18, 1982 p 180.
9. Yu Lan, BIOCHEMISTRY, Vol 4, 1988 p 161.
10. Boyer, P.O., et al., "Oxidative Phosphorylation and Photophosphorylation," ANN REV BIOCHEM, Vol 46, 1977 p 955.

Detection of Typhi Antibodies by Latex Agglutination

[English abstract of article by Geng Yu [5105 1502], et al., of Hospital No 302 of the PLA, Beijing]

[Text] A latex test for the immunodiagnosis of murine typhus, using a erythrocyte-sensitizing substance from Rickettsia prowazekii absorbed in latex particles, has been developed. The test was evaluated using a total of 234 healthy persons and non-typhus patient sera, 89 single and 63 paired typhus patient sera. The positive rate was 92.1 percent for paired and 80.9 percent for single sera from patients with typhus. The test produced results consistent with those given by the microimmunofluorescence (Micro-IF) and microagglutination (MA) tests. The sensitivity of the test was higher than that of the Weil-Felix (P < 0.05) test. This test is simple, rapid, sensitive and specific.

References

1. Hechemy, K.E., et al., "Detection of Rocky Mountain Spotted Fever Antibodies by a Latex Agglutination Test," J CLIN MICROBIOL, Vol 12, 1980 p 144.
2. Hechemy, K.E., et al., "Evaluation of Latex-Rickettsia rickettsii Test for Rocky Mountain Spotted Fever in 11 Laboratories," J CLIN MICROBIOL, Vol 18, 1983 p 938.
3. Rawlings, J.A., et al., "Comparison of a Latex Agglutination Procedure with the Microimmunofluorescence Test for Rickettsia typhi," J CLIN MICROBIOL, Vol 21, 1985 p 470.
4. Hechemy, K.E,, et al., "Detection of Typhus Antibodies by Latex Agglutination," J CLIN MICROBIOL, Vol 13, 1981 p 214.
5. Geng Yu, et al., CHINESE JOURNAL OF HUMAN AND ANIMAL DISEASES, Vol 2 No 4, 1986 p 49.
6. Shirai, A., et al., "Indirect Hemagglutination Test for Human Antibody to Typhus and Spotted Fever Group Rickettsiae," J CLIN MICROBIOL, Vol 2, 1975 p 430.
7. Geng Yu, et al., CHINESE JOURNAL OF MEDICAL TESTING, Vol 11, 1988 p 25.
8. Oreskes, I., et al., "Influence of pH, Ionic Strength and Human Gamma Globulin Concentration on Stability of Polystyrene Latex Particle Suspensions," PROC SOC EXP BIOL NED, Vol 115, 1964 p 753.

Biotechnology Strategic Goals

40081037a Beijing RENMIN RIBAO [OVERSEAS EDITION] in Chinese 6 May 89 p 4

[Summary] The strategic goals for China's biological technology development were worked out at a national meeting held in Shanghai on 3 May 1989. These goals include the development of high-yield, high-quality and disease-resistant animal and plant species; development of new medicines, vaccines and gene therapy; and research on protein engineering. By the end of this century, it is expected that these areas of biotechnology including plant gene technologies, gene separation, gene modification and gene expression will attain international level; and these areas as hybrid paddy rice, breeding of transcribed gene organism, hepatitis B and liver cancer research and treatment will lead the world. In order to increase its annual rice production value to 30 billion yuan, China will develop a new recombinant paddy rice species superior to the current three-line hybrid species which will raise crop yield 20 percent per harvest, and crop areas will be expanded to 100 million mu (about 16.5 million acres), the newly developed resistant plant species will promote agricultural production, and the newly established biotechnology industries will be able to increase annual production value 1 billion yuan and produce effective drugs for treating such common diseases as tumor, hepatitis B, and cardiovascular disease.

Progress in Biotechnology

40081037b Beijing RENMIN RIBAO [OVERSEAS EDITION] in Chinese 11 May 89 p 1

[Summary] According to sources at a national conference on strategic goals in biotechnology recently held in Shanghai, China has made major advances in three fields of biotechnology. In basic research, China has mastered all the technology in more than 20 of the most advanced fields, including polypeptide sequencing, DNA synthesis, gene augmentation, molecule hybridization, and engineered enzyme manufacture and its application. China has also developed 14 instruments including those for DNA synthesis, laser scanners, biosensors, and bioreactors. In agriculture, China now ranks first in hybrid rice research. In medicine, China is now able to make 65 of 80 new biotechnological medicines created in developed countries, including blood-derived hepatitis B vaccine. Recently, a new type of hepatitis B vaccine and polyvalent vaccines have been developed. A highly efficient interlukin-2 has been developed by Shanghai Institute of Biochemistry, the expression rate of which is "world class." Two kinds of interferons, alpha-1 (α1) and alpha-A (αA) were produced, the interferon α1 has been put in clinical tests for treating phase I and phase II hepatitis B, and will be marketed in 1990-1991.

Removal of Radioactivity from Lanthanum Oxide. IV. Pilot-Plant Scale
Experiment for Removal of Radioactivity from Lanthanum Oxide in HNO$_3$ Medium
by HEHEHP

[English abstract of article by Liang Junfu [2733 0193 4395], et al., of the
Institute of Nuclear Energy Technology, Qinghua University, Beijing;
Zhang Feiming [1728 7378 7686], et al., of Shanghai Yuelong Chemical Plant]

[Text] The process flowsheet for removing radioactive nuclides from
lanthanum oxide is given and a pilot-plant-scale experiment has been
completed in Shanghai Yuelong Chemical Plant. The results indicate that
the decontamination factors of α-radioactivity, iron and calcium are higher
than 1000, the recovery of lanthanum is greater than 96 percent, α-radio-
activity in the La$_2$O$_3$ product is lower than 1 count per hour, and the
Fe$_2$O$_3$ and CaO contents are lower than 5 ppm. High quality phosphor grade
La$_2$O$_3$ is obtained.

The results show that this technological process is feasible and reliable, and
the operation is simple and stable

References

1. Zhu Yongjun, et al., JOURNAL OF NUCLEAR AND RADIOCHEMISTRY, Vol 9 No 2,
    1987 p 80.
2. Wang Wenyi, et al., JOURNAL OF NUCLEAR AND RADIOCHEMISTRY, Vol 9 No 3,
    1987 p 129.
3. Liang Junfu, et al., JOURNAL OF NUCLEAR AND RADIOCHEMISTRY, Vol 9 No 4,
    1987 p 207.
4. Zhuang Yongneng, et al., JOURNAL OF NUCLEAR AND RADIOCHEMISTRY, Vol 8 No 1,
    1986 p 20.
5. Liang Junfu, et al., Chinese patent, 85100148.

Effect of Organic Water-Miscible Solvents on Extraction of Uranium by TOA

[English abstract of article by Shi Xiukun [4258 4423 0981], et al., of the Technical Physics Department, Beijing University]

[Text] The effects of organic water-miscible solvents, such as methanol, ethanol, acetone, dioxane, glycol, dimethylsulfoxide (DMSO), dimethyl-formamide (DMF), and tetrahydrofurance (THF), in the aqueous phase, on the extraction of uranyl sulphate by tri-n-octylamine (TOA) has been investigated. All data obtained showed that the addition of alcohols, ketones, etc., into the aqueous phase brings about an increase in the distribution ratio of uranium, whereas the addition of DMSO, DMF, etc., brings about a decrease. In the current study, the regularity and mechanism of the extraction with TOA are further studied and discussed from the measurements of some physical properties, such as the dielectric constant, interface tension, etc.

References

1. Alian, A., Snanad, W., TALANTA, Vol 14, 1967 p 659.
2. Hala, J., "Ion Exchange and Solvent Extraction," Vol 8, Chapter 5, Marcel Dekker, Inc., New York, 1981.
3. Zhu Buyao, et al., CHEMISTRY, No 6, 1981 p 21.
4. Hogfeldt, E., "Stability Constants of Metal-Ion Complexes. Part A: Inorganic Ligands," Oxford, Pergamon Press, 1982.
5. Akhadov, Y.Y., "Dielectric Properties of Binary Solutions," Oxford, Pergamon Press, 1981.
6. Chen Yude, et al., "Nuclear Fuels Chemistry," Atomic Energy Press, 1985, p 246.
7. Huang Ziqing, "Dielectric Solution Theory," Science Press, 1983 p 127.
8. Agami, C., Caillot, M., BULL SOC CHIM FRANCE (1990, 1969).
9. Gutmann, V., Wychera, E., INORG NUCL CHEM LETTERS, Vol 2, 1966 p 257.
10. Tanaka, N., et al., "Ions and Molecules in Solution," Elsevier, Amsterdam, 1983, p 223.

Distributed Transportation Control System Debuts

[Article by [surname] Xuan [1357]: "The DTDS-1 Distributed
Transportation Control System Passes Evaluation at Qinghua"]

[Text] The DTDS-1 distributed transportation control system developed
under the responsibility of the Qinghua University Computer Department
recently passed its Beijing evaluation, signifying completion of one
stage of research on "distributed knowledge bases and structures" as
part of "Project 863."

DTDS-1 is a distributed knowledge-based system for transportation
control. The system has been implemented under a single-node
transportation-control expert system and the QDUNIX-75 distributed
operating system in a three-unit PCS-68000 hardware environment
connected via Ethernet.

Trends toward distributed processing and parallel processing that have
appeared in the field of artificial intelligence in recent years have
stimulated the development of research into distributed artificial
intelligence and distributed knowledge bases. There is a broad
applications future for distributed knowledge bases in all aspects of
national defense and the civilian economy, but because they are quite
comprehensive and very difficult, the major nations of the world are
actively fostering research in these areas. Although this research has
come about later in China, it is still considered important. Personnel
from relevant areas at Qinghua University cooperated on this project
involving knowledge bases and their structures as part of Project 863,
and in just over a year had built the DTDS-1 system.

There is a company node (also a mobile field node) and two mobile field
nodes, where each node is a PCS-68000 microcomputer. The mobile field
nodes are composed of a single mobile field transport-control expert
system, complementary components, instructional components, primary
knowledge components, and user and network interfaces, as well as a

blackboard communications component. The company component also has problem resolution and distribution components, as well as result integration and evaluation components. The DTDS-1 system uses a framework to indicate the primary knowledge and the blackboard knowledge. Processes and generation are used to indicate related transportation control and complementary knowledge. The entire system is written in C.

The DTDS-1 system can function as a distributed knowledge-based system in a development and experimental environment, and it uses a distributed knowledge-based system structure to produce algorithms for the solution of transportation control problems. It has a single-node (expert system) control method, which coordinates inter-node communications through the blackboard structure under control of the knowledge base, and also does comprehensive evaluations of control results.

After preliminary experiments and analysis, experts felt that when viewed from the implementation methods of system structure, task resolution, communications mechanisms, and coordination nodes, this system is at the forefront of domestic systems. The primary control specifications of the DTDS-1 are quite satisfactory, and it can be used for transportation control in medium to large cities. They recommended that it be implemented as soon as possible.

Progress With Expert Systems, New Generation Systems

40080168b Beijing JISUANJI SHIJIE [CHINA COMPUTERWORLD] in Chinese
No 15, 19 Apr 89 p 34

[Article by Ye Lu [0673 6424]: "Expert Systems and the New-Generation
Computer Systems"]

[Excerpt] Artificial intelligence technology is technology that uses
computers to simulate human learning, reasoning, and problem solving,
and that adds channels and methods to decision making. The subject
matter of its research involves such things as natural language
comprehension, knowledge representation and pattern recognition, plan
generation and problem resolution, machine translation and speech
synthesis, theorem proof and inductive reasoning, learning systems and
discovery systems, recognition models and expert systems, robot vision
and intelligent robots, and intelligent speech and automation
programming. This paper gives a simple introduction to the development
of artificial intelligence expert systems in China, and also presents
opinions on what effect the research and development of expert systems
will have on research for the new generation of computer systems.

I. China Has Broadly Initiated Research on Expert Systems

Artificial intelligence technology began to appear in the 1950s, and
from the perspective of contemporary society, world science and
technology has entered a new stage of development. One of the primary
problems mankind has encountered has been the startling increase in
volumes of information, the day-by-day hastening of information
transfer, and the transformation of many categories thereof. In a
situation like this, to rely merely on natural human intelligence is to
be unable to rapidly process and understand information of such enormous
volumes. Aided by computer systems, people have begun to study expert
systems, and China's computer technology research personnel and research
personnel of other disciplines began study of expert systems beginning
in the 1960s.

1. An expert system is one kind of intelligent computer software system

With the rapid development of microcomputer and integrated circuit technologies in the 1970s, expert systems also saw great development in China. Because knowledge in those systems has been obtained from the minds of experts in areas of different professions and specialties and then programmed in software, after which it is sent to computers, expert systems are therefore a special kind of software. They are able to provide people with knowledge, recommendations, reasoning, and judgments or decisions. The comprehensive systems just described can act as a complete, independent intelligent tool to engage in development efforts with systems concerned with artificial intelligence technology, serving as human helpers for certain functions, and they can also be parts of new-generation computers or development tools.

2. Fields of development for expert system applications

Chinese domestic expert systems are primarily being used in such application fields as medicine and hygiene, geological prospecting, weather forecasting, transportation and shipping, education cultural, and social science research, and legal consulting.

At present, aside from a minority of provinces and [autonomous] regions, most areas have colleges and research institutes that are specifically engaged in artificial-intelligence technology and expert-systems research.

Some of the better areas for research efforts in expert systems include Beijing, Shanghai, Changchun, Changsha, and Harbin. In the Beijing area, the Institute of Artificial Intelligence at the Beijing Industrial Academy and the Computer Department at Qinghua University are most representative. The computer departments of Changchun and Jilin Universities began research work on expert systems earliest; in the Shanghai area, both the Fudan University Computer Department and the Computer Department at Jiaotong University have also been doing research in this field. The Computer Institute of Harbin Polytechnical University has done research on expert systems for several years; and Changsha Industrial Institute has begun research on expert systems in certain fields of applications.

3. Some representative expert systems for medical diagnosis

Expert systems have been more broadly used in China's medical and hygiene fields. Among them, the more representative are Chinese-medicine diagnostic expert systems. For example, the Institute of Artificial Intelligence at the Beijing Industrial Academy has long been doing research on a diagnostic expert system for Chinese medicine. This institute wrote dozens of programs using the lifelong skills, knowledge, and diagnostic secrets of the famous doctor of Chinese medicine, Guan

Youbo [7070 1635 3134], then provided them for use at some domestic medical facilities, where they were very effective.

In the field of weather forecasting, some departments within this country have been successful using "middle-scale meteorological experiments" for research on the rules of weather disasters, from which they have developed thunderstorm-forecasting expert systems having artificial intelligence capabilities. This kind of system uses computers to automatically process satellite cloud pictures, radar images, and large amounts of data from local weather forecasts. It is capable of giving a 72-hour thunderstorm forecast, where accuracy during a test period reached 80-90 percent; the [overall] success index has been greater than 50 percent.

[Passage omitted]

State of RISC Research, Development in China Reviewed

40080174 Beijing JISUANJI SHIJIE [CHINA COMPUTERWORLD] in Chinese No 16,
26 Apr 89 p 33

[Article by Wang Xinhe [3769 2450 3109] and Lin Xiaofeng [2651 2556
1490], North China Computing Institute: "The Significance of
Developmental Research on RISC Technology and the State of China's
Research Thereof"]

[Text] Research on RISC [reduced instruction set computing] and the
development of products based on RISC technology have become trends in
the computer-architecture research field and in computer industrial
circles, and have attracted the strong interest of computer specialists
in China. By participation in relevant academic conferences and studies
of some units in China, we have done a brief review of the significance
of Chinese research on RISC technology and its current status.

I. The Significance of China's Development of RISC Technology

Even though the origins of the concept of RISC technology can be traced
to the design of the Cray-1 and the IBM 801 during the 1970s, the true
indication of its birth was decided by the research results of such
people as Patterson at Berkeley during the early 1980s. These results
included: proposing a design philosophy and design for RISC system
architectures; a description of the basic characteristics of RISC
machines; and development of the world's first RISC processor chip--the
RISC-I. Over the past 10 years, processors and computers designed with
this technology have had the features of simple structure, easy
implementation in LSI and VLSI techniques, short development times, low
production costs, and a high performance-cost ratio. And they are
increasingly drawing the attention of areas within the computer
industry. Especially during the last few years, various high
performance 32-bit microprocessors, workstations, and minicomputer
products based on RISC technology have increasingly sprung up; all major
computer companies and semiconductor firms have followed this new course
and have competed to market new products based on RISC technology.

Competition is increasing, providing great vitality and prospects for broad-ranging growth for RISC technology.

So far, the growth of RISC technology has become a major field of the fourth-generation computer industry. It is our belief that proceeding from the state of China's current computer industry, further strengthening of domestic research into RISC technology and development of RISC products would be highly significant for the following two reasons:

1. Using the relatively low-level technologies of LSI and VLSI to manufacture equipment and to develop high-performance microprocessors improves reliability.

The fundamental basis for RISC technology is the so-called "20-percent-to-80-percent rule" in program design. Using simple, register-oriented operations and a uniform command instruction set allows a great improvement in rule-based modification of controller architecture, which is then quite suitable for implementation in LSI and VLSI; at the same time, bringing in pipelined parallel-processing architectures reduces the number of machine cycles needed for execution of instructions, from which an even higher processing speed can be obtained.

The streamlining and regularization of the command set means the lowering of the complexity of the controller architecture, and based on foreign design experiences, when processors using RISC designs are equal in performance to CISC-designed [complex instruction set computer] processors there can be a savings of 20-30 percent of chip area. This means that when the demand for level of technology and degree of integration do not change the remaining chip area can be used for broader data channels and more registers or for incorporating even more parallelism to make processors that have even higher performance-cost ratios. In other words, when using RISC-designed processors under conditions where performance is no less than that of CISC designs, they can be manufactured using later, less demanding levels of technology and degrees of integration.

Due to limitations in levels of IC technique and design conditions, China is at present only able to design and build 16-bit microprocessors, while foreign countries are generally building 32-bit microprocessor chips using 1.5-1.0-micron technology. To update our equipment would require tremendous outlays and a great deal of time. Furthermore, according to certain foreign materials and statistics, the design time for new CISC 32-bit microprocessor chips is about 3-5 years. But when RISC designs are used, then on the basis of China's existing equipment manufacturing technology we can add some necessary equipment and design tools without needing to replace everything, which will greatly reduce our investment. At the same time, development times can be reduced to 1-2 years, according to foreign experience. 32-bit chips are currently in the mainstream of microprocessors, and if we are to use

39

our existing equipment and design situation as much as possible in the short run as a basis for developing our own 32-bit microprocessors, then RISC can provide the technological feasibility.

2. We should take hold of the development of RISC-based fourth-generation computer products as an effective way to reduce the gap between China's computer system designs and levels of manufacturing and those abroad.

Although RISC technology was born nearly 10 years ago, actual use of RISC chips to design computer systems is a matter of the last few years. Current computer products using RISC microprocessors as CPUs number only a few. There are primarily two reasons for this: the first is that industrial circles had long been skeptical of this technology; the second is the difficulty caused by software incompatibility. With the growth of RISC, this technology has now been acknowledged and confirmed in industrial circles. But because RISC-designed computers have broken up the continuity of architectures required for software compatibility, this has led to an increase in the degree of difficulty for that compatibility. A lack of software support has caused computer production plants to maintain a cautious attitude toward developing RISC-based computer products. This has created a sharp contrast with the rapid development of RISC-based high-performance microprocessors, from which has arisen a situation in which the levels of software development and development of systems products has lagged behind that of software and chip development, which for awhile will be difficult to change. This reflects the fact that the development of RISC-based computer products abroad is still in early stages.

What we have just described means that we might take advantage of this opportunity and use RISC technology to develop our own fourth-generation computer products and to more quickly reduce the gap between China and other countries. This is true for the following reasons: 1. The RISC-based fourth-generation computer products we develop will not be as severely limited by software incompatibility as those abroad. System design and software development efforts can proceed without burdens, and energy can be focused on developing high-performance computer systems. 2. Unix provides an excellent environment for the porting of software. There is currently a program abroad called "Open Software Environment" that is based on Unix. Its goal is to solve problems due to porting the writing and running of software among different computers. Any software developed in accordance with the interface standard provided by this environment can truly divorce software development from machines and architecture. This is good news for China, where we are developing fourth-generation computer products in a situation where the level of hardware and systems design is higher than that of software development. This means that the design of architectures can consider less the compatibility with various foreign products and can provide the means by which to design fourth-generation computer products with our own characteristics.

II. The Situation in China Regarding Basic Research on RISC Technology

Five years ago the university community in China began to notice the importance of RISC technology. In his 1984 book "Computer Architectures," Professor Su Dongzhuang [5685 2639 8369] mentioned the characteristics of RISC technology. In his 1985 paper "RISC Technology and Architectures," Qinghua University Professor Li Sanli [2621 0005 4539] brought RISC technology to the attention of computer circles within China. According to our incomplete statistics, by 1988 more than 30 papers on RISC technology had been published in various domestic professional journals. Their contents may be largely divided into two categories: one is the kind of comprehensive article describing the characteristics of RISC technology, development trends abroad and the performance of some representative RISC microprocessor chips; another kind of article is a study of a particular RISC microprocessor product from a certain foreign company, in which the structure and performance are detailed, analyzed, and evaluated. Sources for the articles are primarily centered in some colleges and large research organizations in Beijing and Shanghai. Looked at overall, these articles fundamentally reflect the newest trends in research progress, new product information, and market changes for foreign RISC technology. This is an excellent aid for China's computer circles for understanding and harnessing of progress and changes in RISC technology, as well as for carrying out in-depth research.

At the same time, some colleges and research departments in China have set up special project groups for more thorough study of RISC technology and key problems within, which has yielded some preliminary results. Efforts in this area have been divided primarily into two lines [of research]: one is to set up a helpful environment for the design of RISC microprocessor chips. Hardware structure models for RISC chips will be developed to provide hardware descriptions and design verifications for their use. There is, for example, the RISC computer instruction simulator created by the Shanghai Jiaotong University computer department in the C language, which is used to simulate and verify the design and rationality of computer instruction sets, as well as the coordination between instruction sets and other architectural facilities. Another example involves the Fudan University Department of Computer Science, where a register-level hardware description language ERES has been used to build a RISC-II simulator; this simulator is able to simulate and verify key performance aspects of RISC-II data channels, control channels and instruction execution efficiency. This has been helpful for studying and understanding the structures, design philosophies and methods of foreign RISC processors, and at the same time has brought the means to help with domestic development of RISC processor chips. Efforts along another line of research began on key problems in RISC architecture. These are primarily concentrated in research on pipeline efficiency and structures, as well as on analyses of register management strategies and register window techniques. This

kind of work has been developed more deeply at Fudan University and Central China Institute of Engineering. In addition, the China Hewlett-Packard Company (CHP) and Institute No. 6 of the Ministry of Machine-Building and Electronics Industry, as well as Qinghua University, have each done thorough analyses and research on the Hewlett-Packard HPPA Precision Architecture computer product series and on SPARC [scalable processor architecture] chips.

We can see from the aforementioned situation that basic domestic research efforts toward RISC technology have made definite progress. There are now a distinct number of technical personnel who are engaged in work of this sort, and we can also see that the trend is for this contingent to increase in size. The level of research efforts is also on the rise. But for the moment, the following insufficiencies exist: the first is that the pace and depth of basic research is still some distance from that done abroad. Primary domestic efforts are still at a stage limited to gathering and analyzing foreign materials and doing overall evaluations. Not many in-depth research efforts have been forthcoming. Groups are dispersed and the subject matter is highly complex. Second, there has been little research work on compilers optimized for RISC architectures. This is without question a major insufficiency in domestic RISC research. We know that RISC architecture may be said to be a compiler-oriented architecture. If a RISC computer does not have the support of a good optimized compiler it is difficult to make much of its high efficiency. Third, there is insufficient understanding of and support for RISC research in the domestic computer world. It is our understanding that projects in RISC basic research are seldom supported by industry. Actually, the goals of RISC technology are not to study architectures but are to make computers with a high performance-cost ratio. RISC technology is an extremely useful technology that is capable of quickly generating economic returns.

III. The Current Situation Regarding Chinese Development of RISC Microprocessor Chips

The development of RISC microprocessor chips is based upon VLSI. The VLSI manufacturing industry in China is limited by three factors: one is a low level of equipment, which for the most part can only reach a standard of 3-5 microns; a second is that we are deficient in CAD design capability, as manual design efforts still occupy a considerable portion of chip design work; and the third is low funding, as well as fierce competition from foreign chips. These unfavorable conditions have brought great hardship to the development of RISC microprocessor chips. We understand that only the Lishan [7537 1472] Micro-electronics Institute in Shaanxi [Province] and the Beijing Duosi [1122 1835] Software Company are engaged in work of this sort. The former has developed a degree of integration sufficient for the 10,000-transistor Transputer microprocessor chip for which they have developed an Occam-language compiler; the latter is currently jointly developing a RISC-design processor with a foreign firm for use in supporting

processing with the FORTH language. It is additionally predicted that some units within China will more thoroughly take apart and analyze the SPARC chip.

Although some preliminary results have been obtained from work in these areas in China, we still have quite a way to go before we can manufacture 32-bit RISC microprocessor chips. What is more, we lack industrial support and are faced with competition from foreign products. The road ahead will still be quite bumpy.

iv. The Current Situation Regarding Domestic Development of and Research On RISC Computers and Computer Systems

Actually, RISC technology is not revolutionary architecture, but rather proposes a new architectural design strategy, so the purpose of using RISC technology is to design computers and computer systems that are refitted with new hardware functions. We have begun little of this work so far in China. Primary directions for research are toward how to use RISC microprocessors to construct parallel-processing computers and multi-processor computing systems, which would satisfy the demands of certain specific applications. For example, Qinghua University is currently researching how to use the RISC 32-bit Transputer processor to construct a multi-processor system for real-time image processing; and the Nanjing Marine Simulator Company is also working in this area. In addition in the work of some college and research organizations to study VLSI parallel-processing structures, they are also considering how to use RISC chips as processing units. It can be said in general that by using existing foreign chip products, and especially the Transputer chips of the Inmos Company, to develop multi-processor and parallel-processing systems is the primary focus of domestic research in this area. This work is currently still at an experimental stage.

V. Conclusion--Some Comments

We have said above that at present China is still at a preliminary stage regarding RISC technology research. Faced with truly abrupt trends in growth, whether we should passively accept foreign products or should use the two opportunities we have detailed above to advance the growth of China's computer industry is a question we believe is worth consideration regarding strategies for computer development. We can offer some opinions for everyone's consideration.

1. Basic research on RISC technology needs state support. Basic research is a power and life-source that can allow this branch of technology to continue to develop. The state should make RISC technology a special topic in its 5-year planning, should provide definite research expenses, should encourage colleges and research organizations to study and develop RISC technology, and should permit royalties for patents on research results. And provisions should be made for specific research topics of a guiding nature. Priority funding

should avoid great multiplicity of research directions and topics, waste of personnel and funds, and loss of opportunities.

2. Close cooperation between large enterprises in the computer industry and research departments and colleges will bring practicality to research directions and results; it can transform results into products as quickly as possible, it can generate profits, and it is the key to the sustained growth of this technology. Without the support of generous funding from large enterprises, as well as the strong sense of purpose coming from the demand to turn results into products, basic research in RISC technology will be difficult to continue.

3. We should have a stable research contingent that shares its labor so that we may enable the research and development of RISC technology to progress in all directions avoiding an aura of "S&T guerilla warfare."

4. By close cooperation with foreign interests we can quicken the pace of China's development of RISC technology. For example, by using domestic research results, we can make use of advanced foreign VLSI techniques and equipment, that is, design domestically and manufacture abroad. At the same time, software development should make as much use of common international standards as possible so that we can develop our own RISC-based fourth-generation computer products as quickly as possible.

New Magneto-Optical Memory Material Developed for Optical Disks

40080190c Beijing KE JI RIBAO [SCIENCE & TECHNOLOGY DAILY] in Chinese 20 May 89
p 2

[Article by Wan Xinjun [8001 2450 6511]]

[Text] Wang Yinjun [3769 5593 0689] and other scientists and engineers at the
Chinese Academy of Sciences' Institute of Physics recently developed an optical-
disk magneto-optical memory material consisting of a manganese-bismuth-aluminum-
silicon film; its magneto-optical Kerr angle of rotation is as high as 2.04
degrees. This value is five times that of the amorphous rare-earth and iron-
based-alloy film now being tested abroad for use as an optical-disk material,
and the material has therefore aroused the interest of specialists at home and
abroad.

Optical disks, in comparison to ordinary magnetic disks, have a superhigh
memory density, which can reach 100 million to 1 billion bits per square inch--
100 to 1000 times that of a floppy disk, or 10 to 100 times that of a hard disk.
The aforementioned [amorphous rare-earth and iron-based-alloy] material, first
reported by the U.S. firm IBM, has a Kerr angle of rotation of only 0.3-0.4
degree, and can easily change in actual application of the process. This key
project in China's Seventh 5-Year Plan has potential significance both in
application and in science.

Computer "Virus" Programs Discovered One after Another in China

40080194 Beijing JISUANJI SHIJIE [CHINA COMPUTERWORLD] in Chinese No 20, 24 May 89 p 1

[Article by Jiang Mingfu [3068 2494 1381] and Gao Guoming [7559 0948 2494]]

[Text] Computer viruses have attracted a great deal of attention in computer circles worldwide. Recently, one after another computer virus has appeared in China, and quite a few computers have already been infected.

Not long ago, a computer virus spread through microcomputers in the national statistical system. This virus was able to infect IBM-PC's and compatible computers using the MS-DOS [operating system]. At a certain time during operation of the infected computer, a small globe appeared on the screen and began to continuously roll around. This sphere resembled a table[-tennis] ball unobstructedly moving around on the table, up until the system was reset or turned off.

The virus spread quite fast. When a floppy disk used with an infected computer was passed to another computer, it could act as the virus carrier. Since this virus in the statistics system was discovered at the end of last year, the situation has now [come to the point where] the microcomputers at statistical-bureau computer installations in the great majority of provinces nationwide and at computer installations in some of the prefectures and cities have been infected by this virus.

According to analysis, this virus belongs to the benign category since it does not destroy programs or data within the computers. However, since it causes the small sphere to keep rolling around the screen, it has an effect on the screen display, and reduces the machine's operating efficiency. This is especially true wh - the 10-line CCDOS [Chinese-character disk operating system] is used: the sma.. sphere's movement causes the screen display to continuously roll up or down. In effect, the sphere fills the screen, and the contents on the monitor cannot be read; moreover, so much time is lost by the screen's rolling that it produces a marked reduction in the processing speed of the computer. In a [time] trial with an operator at a 4.77MHz IBM-PC, after the activity of the virus, the computer had almost no time left to run the user's program.

Also, in early March of this year, at the computing center of the Southwest Aluminum Machining Plant in Chongqing [Sichuan Province], another "virus" program

was discovered. That virus program caused interference with the use of the computer system. In the English mode, the effect on system operation was not very great. In the Chinese-character system operating mode, however, the virus seriously affected normal computer operation when Chinese characters were displayed on middle-resolution monitors, so much so, as to produce a phenomenon in which the machine "played dead." The screen displayed a round spot resembling a billiard ball; the spot's movement resembled that of the billiard ball in its path [around the table].

This "virus" program had a strong capability for contagion. All that was needed was for a disk not bearing the virus to be inserted into the [disk] drive, and the inventory of each and every file on the disk would catch the "virus"; this new disk then would also be capable of carrying the infection. As a result, within one month, the computing center had six hard disk drives infected, and over 100 diskettes had caught the "virus." All the offices in the three units (counting the control office) and four branch plants subordinate to the main plant detected the "virus."

After a detailed analytical study of the infected disks, the transmission of the "virus" can now be controlled, and the disks can be given immunity marks to prevent them from becoming contagious again. Recently, research on an "anti-virus" program has also been carried out, so as to resist and eradicate this "virus" in an extraordinarily efficient way.

In order to lessen the opportunity for infection by computer "viruses," it is suggested that computer specialists pay attention to two points: 1, not to use a disk bootstrap system [ci pan yindao xitong] with an unknown history; 2, not to run software with an unknown history.

Jiannan Machinery Plant's State-of-the-Art Winchester Disk Technology

40MB-Disk Servosurface Encoding Device

40080184 Beijing RENMIN RIBAO [PEOPLE'S DAILY] (Overseas ed.) in Chinese
5 May 89 p 4

[Article by Wang Xiyuan [3769 3305 0337]: "China's External Computer Storage
Technology Takes a New Step Forward--40MB-Disk Servo Code Inscribing Device
Developed"]

[Summary] A 40Mbyte-disk servosurface encoding device, a type of inscribing
device which can write 1000 magnetic tracks on a 26.5-mm ring-type disk, was
recently developed jointly by Central China Science & Engineering University and
the Jiannan [1696 0589] Machinery Plant. The tracks are inscribed on the surface
of a [Winchester] minidisk which can store the information equivalent of 400
books, each book having 100,000 Chinese characters. The positioning precision
required for this device is 0.3 micron, and only two or three other countries in
the world can manufacture this product with such precision.

More on Device, Other Products

40080184 Beijing ZHONGGUO DIANZI BAO in Chinese 9 May 89 p 1

[Article by Yang Bin [2799 2430] and Tian Feng [3944 0023]: "Jiannan Plant
Continues to Develop State-of-the-Art High-Tech Products"]

[Summary] Located in western Huaihua [County] in Hunan [Province], the Jiannan
Machinery Plant, China's largest production facility for computer magnetic
recording equipment, has this year already developed four world-class products,
including its Winchester minidisk servosurface encoding device, jointly perfected
with Central China Science & Engineering University. Now, the Winchester disk
head and float plate [assembly]--two new major series of products exported by
the plant--have also advanced to the world's forefront.

Jiannan has recently adopted a "three-points-in-a-line" [san dian yi xian]
export-oriented enterprise set-up, with the plant itself as the main support,
with the Shekou [Guangdong Province] S&T Development Company and other enter-
prises as bridges, and with sales companies in the U.S., Japan, and other
foreign countries as windows. Since 1984, the plant has developed over 40
high-tech products; this has ended a long period in which China had to import

such technology. The plant's gross industrial output value and profits taxes paid have grown yearly, and its products have captured over 50 percent of the domestic market.

Discovery of High Concentration Uranium

[Article by Zhou Zhonghuai [0719 0112 2037], Xu Lijun [1776 7787 0689], and Liu Xingjun [0491 5281 0193] of the Institute of Oceanology, the Chinese Academy of Sciences, Qingdao; manuscript received 21 Oct 87, Survey Report No 1529: "The Discovery of High Concentration Uranium in Concentrated Underground Seawater and Geochemical Anomaly of the Laizhou Bay"]

[Abstract] This article describes the results of a study conducted between January 1986 and September 1987 on the distribution of uranium content in concentrated underground seawater along the coast of Laizhou Bay.

Concentrated underground seawater samples were collected from five different areas. The concentration of each sample was measured with a Baume hydrometer. The sample was then diluted and its uranium concentration was determined by a laser-based analyzer. It is the most accurate, simple and fast way to directly measure uranium in water and its detection limit is 5×10^{-11} g.

Our results showed that concentrated underground seawater samples collected in the Laizhou Bay area contained high concentration of uranium, approximately 5-30 times higher than that in normal seawater. It ranges from about 20 µg/L to as high as 100 µg/L. The distribution of uranium concentration by area is shown in Figure 1. It rose from west to east from the Caiyangzi salt factory and peaked at the Chahe salt factory and then began to drop down. Figure 2 shows that the distribution of uranium concentration in concentrated underground seawater samples collected from different wells at the Yankou salt factory was not uniform.

Table 1 shows the comparison between the chemical composition of evaporated normal seawater at the Yankou salt factory and those of the undergound seawater samples collected in this work. Unlike other chemical constituents, the concentration of uranium is not proportional to the salinity of concentrated underground seawater. The probable causes include 1) seawater evaporation, 2) permeation of high concentration uranium from surrounding river and seawater, and 3) possible existence of uranium source in the sediment. Several mechanisms were proposed to explain this geochemical anomaly.
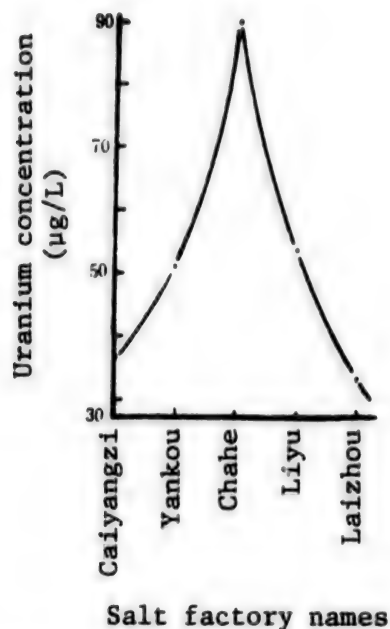
Figure 1.   Uranium Concentrations at Different Salt Factories
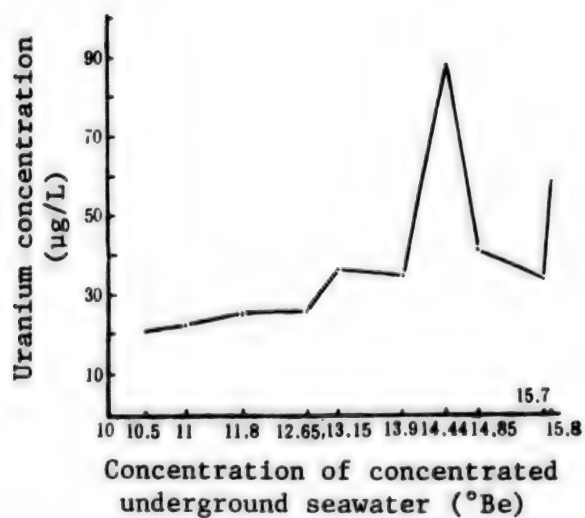
Figure 2.   Uranium Concentration in Underground Seawater Samples
Collected at the Yankou Salt Factory

51

Table 1. Comparison of Chemical Composition of Evaporated Seawater at the Yankou Salt Factory to the Compositions of Concentrated Underground Seawater Samples

Salt factory		Coastal seawater at Yankou	Yexian	Weixian	Chahe	Yankou	Caiyangzi	Guangrao	Normal seawater
°Be'		14.59	14.73	14.07	14.40	14.49	14.27	14.32	3.5
Primary ion (g/L)	Ca^{2+}	1.34	1.10	0.88	1.05	1.34	1.10	0.82	0.4
	Mg^{2+}	6.56	6.77	6.69	6.61	7.77	6.99	7.03	1.35
	Cl^-	97.15	99.57	89.40	90.85	91.12	89.06	92.64	19.00
	SO_4^{2-}	12.26	7.59	9.40	10.10	10.79	11.81	10.60	2.71
	K^+	1.86	1.49	1.37	1.39	1.10	0.83	1.22	0.38
	Na^+	53.92	53.35	49.21	49.50	48.21	48.66	51.00	10.50
	Br^-	0.33	0.31	0.30	0.32	0.31	0.29	0.33	0.065
Minute element ($n \times 10^3$ g/L)	I^-	0.46	0.23	0.45	0.37	0.42	0.38	0.46	0.06
	Li^+	0.26	0.25	0.22	0.25	0.15	0.18	0.16	0.17
	Sr^{2+}	15.36	12.55	10.50	10.50	15.30	12.50	10.50	8.0
	B^{3+}	7.60	4.60	/	/	/	4.40	5.22	4.6

52

Reflection, Transmission, Absorption of Light by Epidermis, Dermis, and the Whole Skin

[Article by Tang Jianmin [0781 1696 3046], Fu Changyu [0265 2490 0151], Jiao Li [3542 4539], and Chen Zulin [7115 4371 2651] of the Third Military Medical College, manuscript received on 7 May 88: "Light Reflection, Transmission and Absorption by Epidermis, Dermis and the Whole Skin"]

[Text] Abstract: Results of this experiment show the reflection and transmission of light in the 330-820-nanometer range by human epidermis, dermis and the whole skin. The experiment provides certain useful parameters either for studying the optical properties of skin, or for treatment of and protection against laser light on the skin.

An experimental report on the reflection, transmission and absorption of light and lasers by human skin[1] has provided certain parameters in the study of biological effects, treatment dosage and the protection threshold for light and lasers. However, the reflection, transmission and absorption of light by epidermis and dermis has not been studied in detail in China. Six skin samples taken from three different parts of the body were used in this experiment. Despite the fact that these samples came from different parts of the body of people with considerable age difference, their reflectance and transmittance curves showed similar patterns. Therefore, this report should in general be applicable to the yellow race. Since tissue absorptance is equal to one minus reflectance minus transmittance, it is only necessary to experimentally determine reflectance and transmittance. People are interested in finding out the absorption coefficient of each tissue layer,[1] i.e. $\mu = (1/X)\ln[(1-R)/(I/I_0)]$ where X is the thickness of the tissue layer, R is its reflectance, and (I/I_0) is its transmittance.

Experimental Apparatus and Results

1. Separation of Skin

After removing subcutaneous fat, skin samples were immersed in EDTA
solution at 37 °C for 2.5 hours. They were taken out of the solution
and placed on a glass plate. A pair of tweezers were used to separate
the epidermis, dermis and whole skin. Then they were rinsed in
distilled water and then dried by white paper towel or in air. The
epidermis, dermis and whole skin samples were allowed to unfold
naturally. Light was shone along the direction of the epidermis to
measure reflectance and transmittance. The skin samples from the
outside portion of the thigh and the neck were not rinsed in distilled
water after they were separated. Instead, they were directly air-dried
and then used in the experiment. Our experimental results showed that
the measured curves were not affected by rinsing the sample in distilled
water.

2. Experimental Apparatus for Measuring Tissue Reflectance and
Transmittance

The experiment was carried out using a Model UV-210A dual-beam-scanning
spectrophotometer with an integrator.[1] The range of scan is 330-820 nm.

3. Reflectance, Transmittance and Absorptance Curves and Absorption
Coefficient of the Epidermis

The specimen was a spare saved at the Burn Department; it was taken from
the outside portion of the leg of an adult male and had been stored at
4 °C in a refrigerator. The curves are shown in Figure 1. (a) is the
reflectance curve. It increases gradually with wavelength between 330
and 700 nm. The increase becomes more significant between 700 and 790
nm. In the range 790-820 nm, it decreases gradually with wavelength.
There is a flat peak at approximately 790 nm. (b) is the transmittance
curve. The transmittance rises with wavelength between 330 and 770 nm
and decreases with wavelength between 770 and 820 nm. (c) is the
absorptance curve which drops significantly with increasing wavelength
between 330 and 780 nm and rises between 780 and 820 nm. The absorption
coefficient of the epidermis μ is calculated from the equation
$\mu = (1/X)\ln[(1-R)/(I/I_0)]$. From 330 to 780 nm, μ continues to drop by
a factor of approximately 56. From 780 to 820 nm, the value of μ
increases.

wavelength (nm)

Figure 1. Reflectance, Transmittance and Absorptance Curves of the
Epidermis on the Skin From the Outside Leg

(a) reflectance curve
(b) transmittance curve
(c) absorptance curve

4. Reflectance, Transmittance and Absorptance Curves and Absorption
Coefficient of the Dermis

The specimen used is the same as that used in the previous experiment.
The measured curves are shown in Figure 2. (a) is the reflectance
curve. Between 330 and 820 nm, it fluctuates slightly. There are two
valleys at 415 and 560 nm, respectively. (b) is the transmittance
curve. Between 330 and 760 nm, the curve is generally rising. However,
there are two relatively flat valleys at 415 and 560 nm, respectively.
Between 760 and 820 nm, the curve declines gradually. (c) is the
absorptance curve which shows a general decreasing trend between 330 and
820 nm. However, there are three valleys at 380, 520 and 760 nm,
respectively. The absorption coefficient μ of the dermis continues to
drop from 330 to 760 nm by a factor of approximately 293. From 760 to
820 nm, the value of μ rises.

Figure 2. Reflectance, Transmittance and Absorptance Curves of the Dermis on the Skin From the Outside Leg

(a) reflectance curve
(b) transmittance curve
(c) absorptance curve

5. Reflectance, Transmittance and Absorptance Curves and Absorption Coefficient of the Whole Skin

The same specimen was used in this experiment. Figure 3 shows the measured curves. (a) is the reflectance curve and (b) is the transmittance curve. Both curves go up with wavelength between 330 and 780 nm and decline gradually between 780 and 820 nm. (c) is the absorptance curve, which decreases significantly between 330 and 780 nm and rises back up between 780 and 820 nm. There is a valley at 780 nm. The absorption coefficient of the whole skin, μ, keeps dropping from 330 to 780 nm by a factor of 10. Between 780 and 820 nm, the value of μ rises.
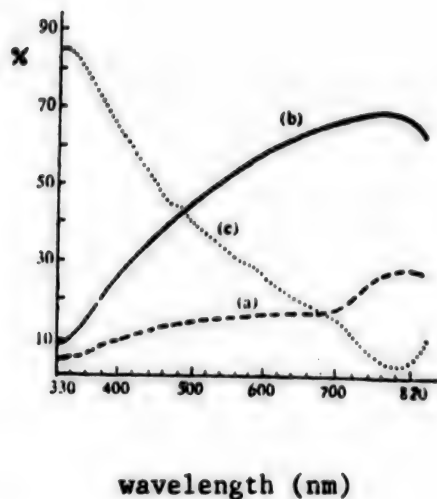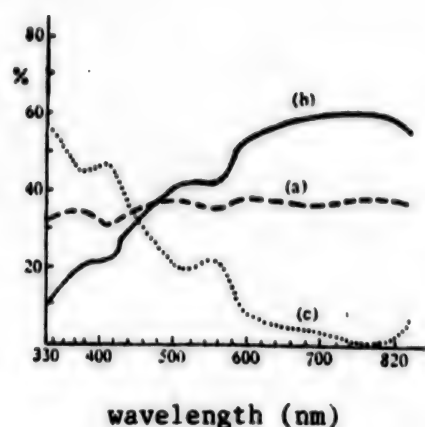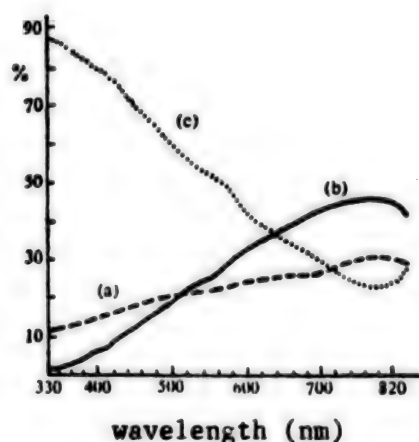

Figure 3. Reflectance, Transmittance and Absorptance Curves of the Whole Skin From the Outside Leg

(a) reflectance curve
(b) transmittance curve
(c) absorptance curve

56

We also measured the reflectance, transmittance and absorptance curves of epidermis, dermis and the whole skin with samples from an adult neck (spare skin kept at the Burn Department) preserved in a refrigerator at 4 °C for 36 hours. In addition, we measured reflectance and transmittance curves of epidermis, dermis and the whole skin using samples from the inner hip, upper inner arm, chest and head of a 13-month-old boy which were stored in a refrigerator at 4 °C for 30 hours. The reflectance and transmittance curves of epidermis, dermis and the whole skin more or less exhibit the same behavior as described above.

Analysis of Experimental Results

From the experimentally obtained curves, we reached four conclusions.

1. As far as reflectance is concerned, as shown in Figure 4, the dermis has the highest reflectance between 330 and 820 nm. The whole skin is next and the epidermis is the lowest. The reason is that the dermis is whiter than the epidermis. Therefore, its reflectance is higher than that of the epidermis. The whole skin has the same surface as the epidermis. The reflectance of the whole skin is higher than that of the epidermis because of multiple reflections.[1] Furthermore, the reflectance curves of epidermis, dermis and the whole skin have similar dependence upon wavelength. The dermis has two shallow valleys at 415 and 560 nm.

wavelength (nm)
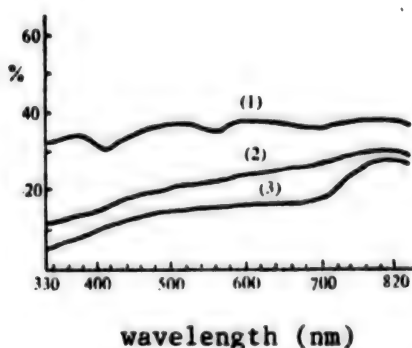
Figure 4. Reflectance Curves of Dermis, the Whole Skin and Epidermis of Sample From the Outer Leg

(1) dermis
(2) the whole skin
(3) epidermis

2. As far as transmittance is concerned, as shown in Figure 5, epidermis is the highest, dermis is next and the whole skin is the lowest between 330 and 820 nm. However, the transmittance of dermis is higher than that of epidermis at 330 to 385 nm. The three transmittance curves also vary following more or less the same pattern. The dermis, however, has two relatively shallow valleys (at 415 and 560 nm).

57

wavelength (nm)
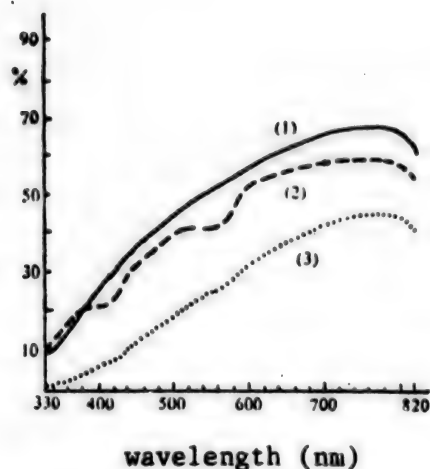
Figure 5. Transmittance Curves of Epidermis, Dermis, and the Whole Skin of Sample from the Outer Leg

(1) epidermis
(2) dermis
(3) the whole skin

3. As far as absorptance is concerned, as shown in Figure 6, the whole skin is the highest, epidermis is next and dermis is the lowest in the 330-820-nm range. The three curves also vary based on more or less the same trend. However, the dermis curve shows two relatively shallow peaks at 415 and 560 nm.
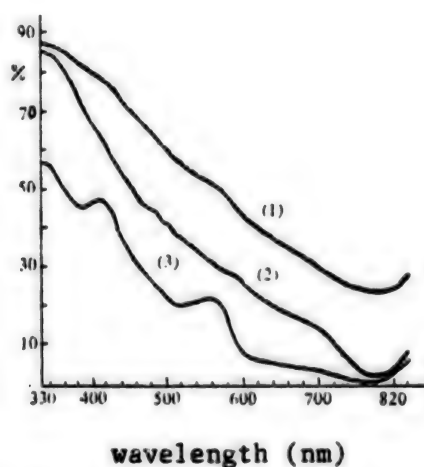
wavelength (nm)

Figure 6. Absorptance Curves of the Whole Skin, Epidermis and Dermis; Sample From the Outer Leg

(1) the whole skin
(2) epidermis
(3) dermis

58

4. As far as the absorption coefficient is concerned, at the same wavelength (330 to 820 nm), epidermis is the highest, the whole skin is next and dermis is the lowest. The absorption coefficient of the epidermis is 7 to 20 times higher than that of the dermis. In spite of the fact that epidermis is much thinner than dermis, the total absorptance of the epidermis is still higher than that of dermis.

Applications

When human skin is irradiated by light from 330 to 820 nm, the absorption of the skin varies greatly depending on the wavelength. It is highest in the near-ultraviolet region between 330 and 400 nm, which reaches as high as 80 to 90 percent for the whole skin (see Figure 6). When human skin is irradiated with light or lasers[1] in this band, 80-90 percent of the energy is absorbed by the skin. (The energy absorbed by the epidermis is 1.5 times that by the dermis.) In addition, more than 10 percent of the energy is reflected (see Figure 4). Therefore, less than 10 percent of the energy penetrates the skin to reach the subcutaneous tissue. Thus, this band of light can be used to treat skin diseases (by photochemical disinfection) without damaging any subcutaneous tissue. The skin has the lowest absorption in the red, i.e., 700 to 750 nm, and near-infrared, i.e., 750 to 820 nm; it is only about 23-30 percent (see Figure 6). Its reflectance is approximately 30 percent (see Figure 4). The energy penetrating the skin can be as high as 42-47 percent. This means that approximately one half of the energy can penetrate the skin. When light or a laser is used to treat a disease in the subcutaneous tissue (using the thermal effect of light), it is more appropriate to use the red and near-infrared band at 700-820 nm. The light would not cause much damage to the skin because only about 25 percent of the energy is absorbed by the skin.

The curves obtained in this work can provide a valuable reference to those studying the optical properties of the skin and the treatment, protection and biological effects of light and lasers[1] on the skin.

REFERENCES

1. Tang Jianmin, et al., ZHONGGUO JIGUANG [CHINESE JOURNAL OF LASERS], Vol 9, pp 440, 435 (1987).

2. Tang Jianmin, et al., JIGUANG ZAZHl [LASERS], Vol 7, p 213 (1986).

3. Fu Changyu, et al., YINGYONG JIGUANG [APPLIED LASER TECHNOLOGY], Vol 7, p 278 (1987).

4. L. Goldman, et al., "Laser in Medicine," New York, 1971, p 163.

IMM Analysis of Guided Modes of Dielectric Waveguides with Arbitrary Cross Section

40090054a Shanghai GUANGXUE XUEBAO [ACTA OPTICA SINICA] in Chinese Vol 9 No 2, Feb 89 pp 120-127

[English abstract of article by She Shouxian [0152 1343 2009] of the Department of Physics, Northern Jiaotong University]

[Text] In this paper the author presents an iterated moment method (IMM) for evaluating dispersion relations of dielectric waveguides with arbitrary cross sections. The numerical results are given for fibers of various shapes, such as circles, ellipses, equilateral triangles, chipped circles and oval cross sections. The results agree well with the exact computer-aided numerical results obtained by the finite element and point-matching methods. This method is simple and saves computing time.

References

1. She Shouxian, ACTA OPTICA SINICA, Vol 7 No 6 (June), 1987 pp 544-550.
2. She Shouxian, Qiao Li, "Sino-Japanese Joint Meeting on Optical Fiber Science and Electromagnetic Theory," Nanjing, 12-14 May 1987, pp 453-457.
3. Qiao Li, She Shouxian, OPT LETT, Vol 13 No 2 (February), 1988 pp 167-168.
4. She Shouxian, OPTICAL AND QUANT ELECTRON, Vol 20 No 2 (February), 1988 pp 125-136.
5. Kendall, P.C., et al., PROC IEE, Pt A, Vol 134, 1987 pp 699-702.
6. Kumar, A., Varshney, B.K., OPTICAL AND QUANT ELECTRON, Vol 16 No 4 (July), 1984 pp 349-354.
7. Yeh, C., et al., APPL OPT, Vol 18 No 10 (May), 1979 pp 1490-1504.
8. Yamashita, E., et al., IEEE TRANS MICROWAVE THEORY AND TECH, Vol MTT-27 No 4 (April), 1979 pp 352-356.
9. Wang Jingyi, She Shouxian, OPT COMMUN, Vol 64 No 4 (November), 1987 pp 297-301.

Study of Multifrequency Acoustooptic Interaction

[English abstract of article by Zhao Qida [6392 0796 1129] of the Department of Applied Physics, Beijing Polytechnic University]

[Text] Multifrequency acoustooptic coupled mode equations, including normal and abnormal acoustooptic interactions, are presented in this paper. Solutions for the equations of two independent acoustic signals in the Bragg limit are derived, and linear and nonlinear effects of the multifrequency acoustooptic interactions are analyzed theoretically. These include the diffraction efficiency, compression, cross modulation and additional intermodulation intensities. In particular, the differences between abnormal and normal diffraction are pointed out and analyzed. The experimental results are in good agreement with theoretical analyses.

References

1. Klein, W.R., Cook, B.D., IEEE TRANS SONICS AND ULTRASONICS, Vol SU-14 No 3 (July), 1967 pp 123-134.
2. Uchida, N., Niizeki, N., PROC IEEE, Vol 61 No 8 (August), 1973 pp 1073-1092.
3. Chang, I.C., IEEE TRANS SONICS AND ULTRASONICS, Vol SU-23 No 1 (January), 1976 pp 2-21.
4. Hecht, D.L., IEEE TRANS SONICS AND ULTRASONICS, Vol SU-24 No 1 (January), 1977 pp 7-18.
5. Xu Jieping, "Principles, Design and Applications of Acoustooptical Devices," Science Press, 1982, No 2, Chapter 4.
6. Sapriel, J., "Acousto-Optics," John Wiley & Sons Ltd., Chichester, New York, 1979, Chapter 7.
7. Dixon, R.W., IEEE J QUANT ELECTRON, Vol QE-3 No 2 (February), 1967 pp 85-93.

Phase-Matching Topology of Sum-Frequency Generation in Biaxial Crystals

[English abstract of article by Ren Hongwen [0117 4767 2429], et al., of the Institute of Crystal Materials, Shandong University, Jinan]

[Text] The properties of phase-matching (PM) faces for sum-frequency genera- tion (SFG) are analyzed according to the refractive indices and phase-matching conditions of two fundamental waves and their second-harmonic waves in normal acentric biaxial crystals. The authors derived 29 PM topological diagrams and existing conditions, 15 non-critical phase-matching (NCPM) topological diagrams, existing conditions and polarization relations. The topology and NCPM conditions for SFG in LAP and KB_5 are also presented.

References

1. Hobden, M.V., J APPL PHYS, Vol 38 No 11 (October), 1967 pp 4365-4372.
2. Xu Dong, "Collection of Academic Papers by Shandong University Graduate Students," Shandong University Press, 1984 p 102.
3. Cook, W.R.,Jr., Hubby, L.M.,Jr., J.O.S.A., Vol 66 No 1 (January), 1976 pp 72-73.

Decoding Model of Color Vision, Its Verifications

[English abstract of article by Lu Chenguang [7627 2525 0342] of the Computer Center, Changsha University]

[Text] In this paper, a decoding model of color vision is briefly introduced. The θ-r-z color system, which is based on the decoding model and has features of both the Munsell color system and the XYZ system, is proposed. The θ^*-r$^*_c$-z* color system obtained from the nonlinear transformation of B, G, R is provided. The decoding model is verified both by the reflection of z and z* to lightness and by the distribution of the color samples of the Munsell system in the θ^*-r$^*_c$-z* system.

References

1. Lu Chenguang, "Fuzzy Switching Quasi-Boolean Algebra and Vision Simulation Color Discernment," "Proceedings of International Symposium on Fuzzy System and Knowledge Engineering," Guangzhou University, Guangzhou Higher Education Publishing House, 1987 pp 436-459.
2. Lu Chenguang, TRENDS IN PSYCHOLOGY, No 14, 1986 pp 36-45.
3. Lu Chenguang, ROBOTS, Vol 1 No 6, 1987 pp 39-41.
4. Shu Yuexin, "Fundamental Principles of Color Optics," Shandong Science Press, Jinan, 1981 pp 310-603.
5. De Monasterio, F.M., Gouras, P., J PHYSIOL, Vol 251 No 1, 1975 pp 167-195.

Self-Mode-Locking in Phosphate Glass Laser

[English abstract of article by Zhang Guoxuan [1728 0948 6513], et al., of Shanghai Institute of Optics and Fine Mechanics, Chinese Academy of Sciences]

[Text] The phenomenon of self-mode-locking in a phosphate glass laser is reported. The experimental results show that the probability of self-mode-locking can reach 100 percent when the pumping power is sufficiently high and the resonator length is longer. The experimental results have been analyzed and are discussed in this paper.

References

1. Crowell, M.H., IEEE J Q E, Vol QE-1 No 1 (April), 1965 p 12.
2. Walf, E., "Progress in Optics," North-Holland Publishing Company, Vol IX, 1971, p 179.
3. Personal correspondence.
4. Li Shifang, et al., ACTA OPTICA SINICA, Vol 6 No 7 (July), 1986 p 585.
5. Linford, G.J., et al., APPL OPT, Vol 13 No 6 (June), 1974 p 1378.
6. Statz, H., J APPL PHYS, Vol 38 No 12 (December), 1967 p 4648.
7. Statz, H., et al., J APPL PHYS, Vol 38 No 5 (May), 1967 p 2212.

Optimum Pump Condition for Shortest Light Pulses From Laser Diodes

[Article by Shan Zhenguo [0830 2182 0948] of Shanghai Institute of Optics and Fine Mechanics, Chinese Academy of Sciences]

[Abstract] The Longe-Kuta method is used to solve for the photon and electron speed equation of the laser diode (LD). As shown in the results, by utilizing the gain switch principle, the shortest light pulses emitted from a LD is determined by equipment parameters, such as the excited radiation factor, cavity length, catastrophic destruction threshold value, and gain saturation effect. Generally, users can achieve this shortest light pulse only under certain pumping conditions. However, if one considers the effect of delay time on producing ultrashort light pulses, and adopts the corresponding measures proposed in the article, the shortest light pulses determined by equipment parameters can be readily generated.

Six figures show the direct current deviation with the superimposition of rectangular pulses (DCD+RP), the results of calculating DCD+RP driving an LD, relation between light pulse width and DCD, results of calculating an LD driven by rectangular current pulses of DCD with pulse width variation, results of calculating an LD driven by leading edge varying pulses, and results of calculating an LD driven by a DCD with a sine wave current.

Stimulated Amplification of Electromagnetic Waves in Foil Stack Systems for Transition Radiation and the Prospects of X-ray Lasers

[Article by Yan Zuqi [0917 4371 4388] and Yuan Kefei [7086 0668 1173] of Department of Physics, Shanghai University of Science and Technology]

[Abstract] As presented in LIANGZI DIANZIXUE [QUANTUM ELECTRONICS], 2(4), pp 321-326 (1985) by Yan Zuqi, in a multifoil stack resonance transition radiation system, two gain regimes are discussed. In one regime, when electromagnetic waves are propagated in a system, interaction may result with high energy electron beams for stimulated amplification. In another regime, with the addition of modified reactivation electron beam and multisystem transition radiation electromagnetic waves produced in various foil stacks, the intensity of resonance transition radiation of the system is enhanced. The article discusses the stimulated amplification problems of electromagnetic waves in the transition radiation foil stack system. Calculations were performed on the gain and radiation intensity of electromagnetic waves in this system. A qualitative analysis was made of the possible use of the stimulated resonance transition radiation to construct an X-ray laser; corresponding physical modes are introduced.

Six figures show the stimulated amplification of monochromatic plane polarized electromagnetic waves, restoration of its propagation direction after the electromagnetic waves pass through a pair of foils, stimulated amplification within and between foil stacks in a multifoil stack resonance transition radiation system, a five-lens Bragg resonance cavity containing a resonance transition radiation system, reflectivity in a particular direction as the reflected light is basically concentrated into a very narrow region in the neighborhood of mirror surface reflected angle, and rapid attenuation (owing to absorption by lens surfaces) of X-rays slightly deviated from the optimum wavelength of reflected light.

The paper was received for publication on 22 November 1987.

Theory of Injection-Locked Short Pulsed Dye Lasers

[Article by Zhang Tiejun [1728 6993 6511] of Changchun Institute of Optics and Fine Mechanics, Chinese Academy of Sciences]

[Abstract] The article presents a new model of the speed equation on mismatch effect between the injection light frequency of the principal laser, and the longitudinal mode frequency of a compression laser; a numerical solution is given. The discussion is concerned with the factors of injection power, injection wavelength and mismatch frequency, on the one hand, and the effect of a short pulse injection dye-locked laser, on the other. One table lists stationary parameters. Eleven figures show models of the energy levels and resonant cavity, S_1 and S_0 state spectra of rhodamine 6G, relations between injection-locked output and injection power (and wavelength), relations between injection-locked output and mismatch frequency, and the injection-locked output of waveform oscillation.

New Scanning Infrared Thermometric System Developed

40080173a Beijing JISUANJI SHIJIE [CHINA COMPUTERWORLD] in Chinese No 16, 26 Apr 89 p 2

[Article by Qin Ling [4440 1545]]

[Text] The HJW-1 is a state-of-the-art, high-speed, non-contact-type scanning infrared thermometric system developed by the Xian Hongda [1347 6671] Electronics Institute of the Ministry of Machine-Building and Electronics Industry. It is now in batch production.

The system is based on far-infrared radiation technology, and is operated by a computer with two-dimensional control. Specifically, it collects one-dimensional samples of the surface temperature of the measured object and processes the data using a microcomputer. The temperature values are shown on an electronic display unit, and hardcopy plots of temperature variations of the measured object can also be generated. If the temperature exceeds a certain threshold value, a warning signal is issued by the alarm unit. The operator can then make the proper adjustments to avoid possible damage to the fire-sensing device caused by overheating. Tables and plots of measured temperatures provide the raw data for fire-equipment research, and play an important role in the modernization of national defense. This is an integrated system which combines the technologies of optics, mechanics and electronics. Its sampling rate is 35 Hz, the measured temperature range is from 0° to 1800°C with a measurement accuracy of 0.5 percent, and the temperature resolution is 1°C; the entire temperature measurement process is automated. Based on the results of certification tests by experts in the field, the design, capability and performance of this system are considered to be comparable to the standards of foreign products of the 80's. This system can be used to replace imported systems, and its application in other commercial industries should be promoted.

Guangzhou, Hong Kong Scientists Cooperate: New Breakthrough in Research on
Gas-Sensitive Fiber-Optic Materials

40080182 Beijing KE JI RIBAO [SCIENCE & TECHNOLOGY DAILY] in Chinese 14 May 89
p 1

[Article by Chang Zheng [1603 1767]]

[Text] Guangzhou, 13 May--Cooperation between scholars Zheng Shunxuan [6774
7311 2467], Guo Sigan [6753 2448 3227], and Liang Zhenbin [2733 2182 2430] from
the Physics Department of Guangzhou's Zhongshan (Sun Yat-sen) University and
specialist Yü Yungan [0151 3057 1344] from the Physics Department of Hong Kong's
Chinhui [3190 2585] Institute has resulted in a new breakthrough in research on
gas-sensitive fiber-optic materials. The scientists announced today that certain
physical phenomena involving the optical properties and gas-sensing characteris-
tics of a tin-oxide thin film were observed for the first time in the world.

For the tin oxide, the researchers used a high-temperature spray-painting method
or sintering technique to produce a gas-sensitive fiber-optic sensor film. When
the light going through an optical fiber was transmitted to one side of the
sensitive film, the other side of the film could be used in connection with an
optical fiber to gather the light and send it to the detector. The strength or
weakness of the output light could be read on a monitor [connected to the
detector]. When there are combustible gases near the sensor film, the intensity
of the light passing through the thin film can undergo a change. With different
kinds of gases or with other oxides and different reduction properties, the
intensity changes in a regular fashion.

This "gas-sensitive optical" law was discovered by the scientists in May of last
year. After a year's time, the experiment has been repetitively confirmed, and
a theoretical explanation has been offered. This discovery ends the almost
half-century-long period in which gas sensitivity of oxides has been demonstrated
only in certain models of resistance, and opens up the [new] physics research
field of "gas-sensitive adsorption optics." This makes it possible to use
optical measurement techniques to study the not yet clearly understood gas-
sensitive properties of oxides and is quite significant for high-tech industry.

Shanghai Institute Develops Silicon Schottky Barrier Infrared Focal-Plane Device

40080198 Beijing GUANGMING RIBAO [GUANGMING DAILY] in Chinese 25 May 89 p 2

[Article by Yue Ziqiang [2867 1311 1730]]

[Summary] The Chinese Academy of Sciences' Shanghai Institute of Technical Physics has announced a new breakthrough: the development of a silicon Schottky barrier infrared focal-plane device meeting international standards of the eighties. This ingenious device has the vision functions of a super sensory organ: both in daylight and in the dark of night, it can transmit the infrared radiation from objects invisible to the human eye. The signals are optoelectronically converted into real-time imagery, widely applied in areas such as aeronautical and astronautical remote-sensing, missile guidance, night visual reconnaissance, mineralogical prospecting, forestry surveying, medical treatment, and industry.

New Long-Range Radar System Certified

40080197b Beijing ZHONGGUO DIANZI BAO in Chinese 23 May 89 p 1

[Article by Zhang Danbin [1728 0030 2430]: "Scientific Research & Production at Ministry of Machine-Building & Electronics Industry's Research Institute 38 Bears Fruit"]

[Text] The Ministry of Machine-Building & Electronics Industry's Research Institute 38, relocated to Hefei City just at New Year's Day this year, has already achieved several scientific research results at its new address, even before the completion of the capital construction. [One such result is] the recent manufacture and installation of a large-scale automatically controlled long-range radar system, which has been tested to certify it to advanced international standards. The new display instrument, which uses a microcomputer to control input of topographic maps that are displayed on the screen as coordinates, is now in batch production. These results have all been obtained even with a severe shortage of funds and imperfect production conditions.

New High-Sensitivity GaAs Hall Device Fabricated by Stable Domain Method

[Article by Zheng Yiyang [6774 0001 7122] of Institute of
Semiconductors, Chinese Academy of Sciences, Beijing; manuscript
received 30 January 88: "New High-Sensitivity GaAs Hall Devices
Fabricated by Stable Domain Principle"]

[Text] Abstract: The operating principle of a GaAs Hall device is
analyzed by means of computer modeling in this paper. When stationary
[i.e., "stable"] domain exists in the bulk and extends to the voltage-
control terminal of the Hall device, the output impedance of the device
increases and its sensitivity goes up by an order of magnitude. High-
sensitivity stationary-domain-type GaAs Hall devices have been prepared
to experimentally confirm this result. This new device will be widely
used.

1. Introduction

Sensitivity is an important parameter of a Hall device. Although the
sensitivity of a GaAs Hall device is generally higher than that of a
germanium-silicon Hall device, it can only reach 30 mV/mA·kg.

We used the electron transfer principle in GaAs devices to study the
characteristics of the domain. Through computer modeling, it was
discovered that when there is stationary domain in a Hall device and
when the depletion layer of that domain reaches the voltage-control
terminal, the impedance of the voltage-control terminal increases
significantly and the sensitivity of the device is approximately one
order of magnitude higher than before. It is in a new operating mode.
Since the high impedance at the output terminal of the device is
achieved by electron transfer effect, it is possible to use higher-
concentration materials to fabricate samples in order to overcome
unfavorable factors introduced by the ohmic contact.

We performed computer modeling to analyze the operating principle of this new device and fabricated samples for testing. Both theoretical and experimental work are essentially in agreement. The same result was also observed at the Tokyo Electrochemical Laboratory in Japan.[1] However, they did not perform any theoretical analysis. This operating mode will improve the characteristics of the device and lead to a wide range of applications.

2. Computation Method and Discussion

The analysis of a Hall device is usually limited to the low-electric-field area, i.e., the ohmic region. When analyzing the high field, GaAs Hall devices are different from Ge-Si Hall devices. GaAs Hall devices behave like Gunn devices in the high field. The formation of domain takes place due to electron transfer beyond the threshold and the effect of the domain must be taken into consideration in the Hall effect.

This paper focuses on the behavior of the device in the high field. Figure 1 shows the cross-shaped pattern that we used in this work. For simplicity and without distortion from reality, we used one-dimensional computer simulation. Moreover, the operating mode of the device is primarily influenced by the electric field which causes the electron-transfer effect to raise the impedance of the device. The impedance effect caused by the magnetic field is secondary and can be neglected in the calculation. The current-continuity equation and Poisson equation are used in the computation.

$$J(t) = en(x,\ t)v(E) - eD(E)\frac{\partial n(x,\ t)}{\partial x} + \varepsilon\frac{\partial E(x,\ t)}{\partial t}$$

$$\frac{\partial E(x,t)}{\partial x} = \frac{e}{\varepsilon}\ [n(x,\ t) - N_s(x)], \qquad (1)$$

where x is a space variable, t is a time variable, e is the electron charge (1.602×10^{-19} Coulomb), $\mathcal{E}$ is the dielectric constant of GaAs (1.1094×10^{-12} Faraday/cm), n(x,t) is the carrier concentration, N(x) is the dopant concentration, E(x,t) is the electric field, and D(E) is the diffusion coefficient. Based on the equation given in references 2 and 3 for the relationship of velocity and the electric field, v(E) can be expressed as:

$$v(E) = \frac{2.25 \times 10^9}{T}\ E \cdot \frac{1 + \dfrac{0.265}{1 - 5.3 \times 10^{-7}T}\ (E/E_s)'}{1 + (E/E_s)'}. \qquad (2)$$

In our computation, T = 300 K.

73
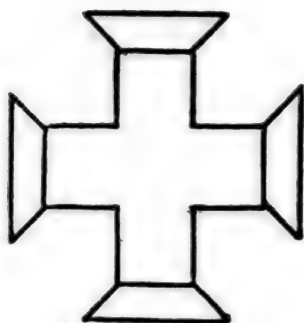
Figure 1.   Device Used in Modeling

In solving the above non-linear equation, the following terminal voltage condition was used.

$$V(t) = \int_0^l E(x, t)dx \qquad (3)$$

In addition, because the ohmic contact at the current terminal of a GaAs Hall device is usually good and the electric field has dropped to zero at the electrode, the following boundary condition is valid:

$$E(0, t) = E(l, t) = 0 \qquad (4)$$

Another treatment in the computation is that the change of geometry at the voltage output terminal of the Hall device is approximated by a concentration change. In reality, either a concentration or geometric change will result in an electric field change.

Devices of different concentrations and source region lengths were calculated. We first modelled the transition domain [i.e., region] in a long specimen. In this case, even when both ends of the device have exceeded the threshold, the sensitivity of the Hall device would not increase. This is because the high field domain starts from the cathode and the depletion layer passes by the voltage terminal of the Hall device and disappears at the anode. The depletion layer only passes by the voltage terminal over a short period of time and macroscopically the impedance of the device is not increased. Consequently, its sensitivity is not enhanced. Therefore, it is not possible to improve the performance of a Hall device with transition domain.

In order to change the impedance a the voltage terminal of a GaAs Hall device, it is natural to consider the stationary domain mode. In this case, the domain remains stationary in the device. If the depletion layer of the domain is at the voltage output terminal of the device, it is possible to raise the impedance and increase the sensitivity of the

device. We will consider two stationary domain modes, i.e., anode formation in the anode stationary domain and deeply doped cavity stationary domain.

Let us first discuss the anode formation and anode stationary domain. In our computation, we chose a short sample which is 9.0 μm in length. The transition region at the electrode is 1.0 μm. The Hall voltage terminal is at 4.0 to 5.0 μm. The external bias is 5.0 volts. The source region concentration is 1.0×10^{15} cm^{-3}. When the domain becomes stationary, it exhibits an electric field and carrier concentration distribution as shown in Figure 2. In this case the region between 4.0 μm and 5.0 μm is still in the low field and the device is equivalent to a pure resistor. Since there is no electron transfer effect due to high field, the resistance would not increase. However, from the current terminal of the Hall device the impedance has already increased. Nevertheless, the increase in the overall impedance makes no contribution to the Hall output. On the contrary, the output of the Hall device is reduced because the current is lowered due to the increase in the overall impedance of the device.

relative value of electric field E(x)

relative values of $N_0(x)$ and $n(x)$

distance (μm)
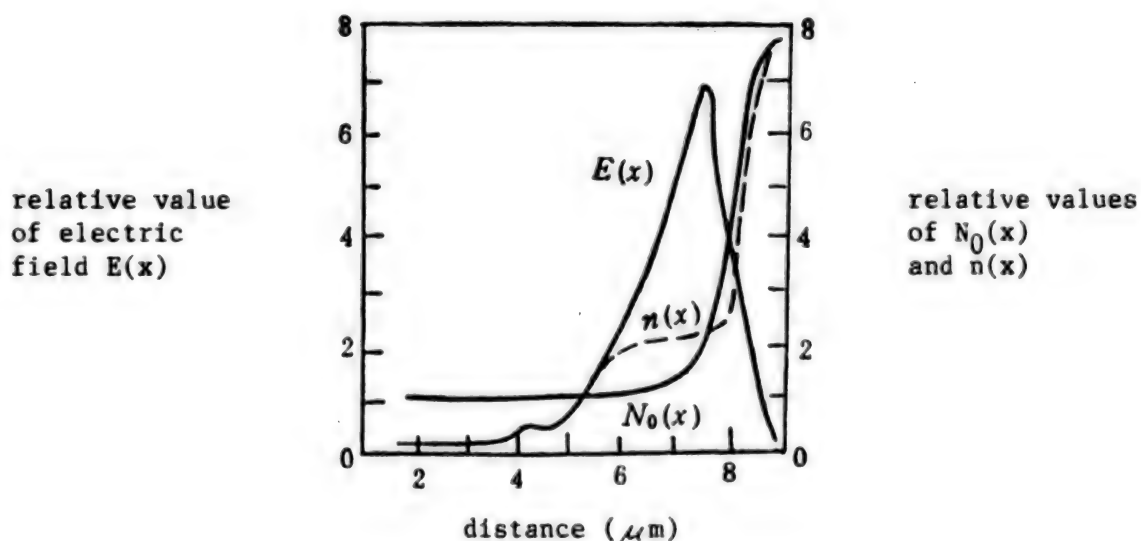
Figure 2. Electric Field and Concentration Distributions in a Stationary Domain Formed at the Anode

The electron transfer effect is caused by the energy band of N-type GaAs. In bulk-effect GaAs devices (primarily Gunn and Hall devices), there two upper energy valleys and one lower energy valley in the conduction band. The differences between the lower energy valley and the two upper energy valleys are $\Delta E_1 = 0.31$ eV and $\Delta E_2 = 0.36$ eV, respectively. The energy difference in the [111] lattice direction is smaller, i.e., $\Delta E_1 = 0.31$ eV. The effective mass of the electron is less in the lower energy valley and thus its mobility is higher. The values are $m_1^* = 0.067\, m_0$ and $\mu_1 = 0.8$ m^2/V·S, respectively. m_0 is the

75

rest mass of the electron. Since the effective state density is 94 times higher in the upper energy valley than in the lower energy valley, the upper energy valley can accommodate all the electrons transferred from the lower energy valley.

When the mean electric field exceeds its threshold (i.e., 3 kV/cm) in an N-type GaAs device, a high field domain begins to form in the device. Under the influence of the high electric field, electrons in the lower energy valley are transferred to the upper energy valley in massive quantity. This lowers the electron concentration in the lower energy valley and reduces the mobility in the upper energy valley, which increases the impedance of the device. By this time, the Hall output also increases accordingly.

However, our computation shows that in the stationary domain formed at the anode the carrier concentration does not decrease. Instead, it rises, as shown in the Figure as $n(x)$ (dotted curve). It also shows that the source of this carrier increase comes from the anode boundary. The carrier distribution curve $n(x)$ is pushed more inward compared to the dopant concentration curve $N_0(x)$, indicating that the depletion layer of the domain enters the boundary of the anode.

As we discussed earlier, the stationary domain formed at a deep notch could yield GaAs Hall devices of high sensitivity.[4-6] Since there is a concentration notch in the device, the accumulation layer of the domain fills the notch, while the depletion layer is distributed in the bulk to cause the bulk concentration to drop as shown in Figure 3. A low concentration region is also formed at the voltage output terminal of the Hall device to significantly increase the impedance of the voltage output terminal of the Hall device. Because the Hall output is proportional to the impedance of the Hall voltage terminal, the Hall output would also increase significantly. Based on our computation, it is easier for the depletion layer of the domain to reach the Hall voltage terminal to produce a new type of high-sensitivity Hall device when the device is shorter.
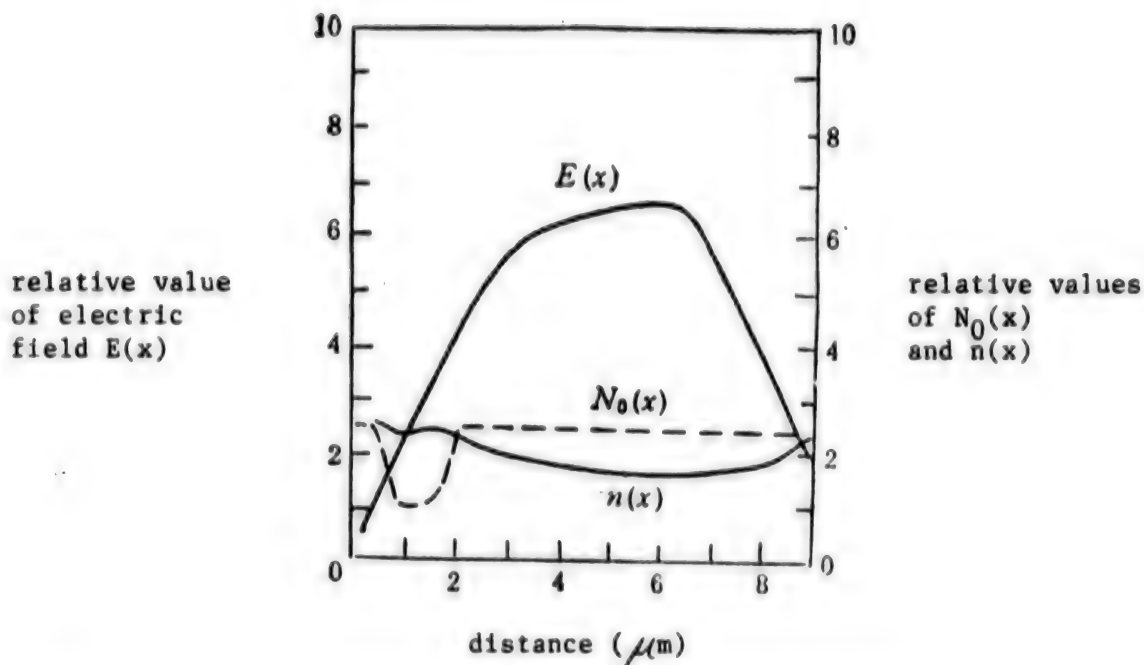
Figure 3. Electric Field and Concentration Distributions in a Stationary Domain Formed at a Deep Notch

III. Experimental Results

We fabricated several Hall devices with the crossed shape shown in Figure 1 and performed experiments with specimens of various lengths. Our results showed that we could not get any high-sensitivity devices when the length exceeds 100 μ m because the depletion layer could not extend to the Hall voltage and even when the voltage exceeds the threshold value. If the bias keep going up, thermal effects of the device become apparent to bring in a great deal of error in the measurement.

The meaningful experiments involved short samples, approximately 4-5 μ m in length or less. It is necessary to use a thin epitaxial layer or a 0.3 μ m ion-implanted GaAs wafer. The current-voltage curve was obtained in three areas, as shown in Figure 4. The normal Hall device operates in Region I, i.e., the ohmic region. The focus of our discussion is Region II where high-sensitivity devices can be obtained. Since short specimens are used, the applied voltage can be quite high, until avalanche oscillation of the domain takes place. That is Region III shown in the figure. As a result of the avalanche, electron-hole pairs will be generated and the bulk concentration will increase; the Hall output will decrease. The Hall device does not operate well in this region.

77
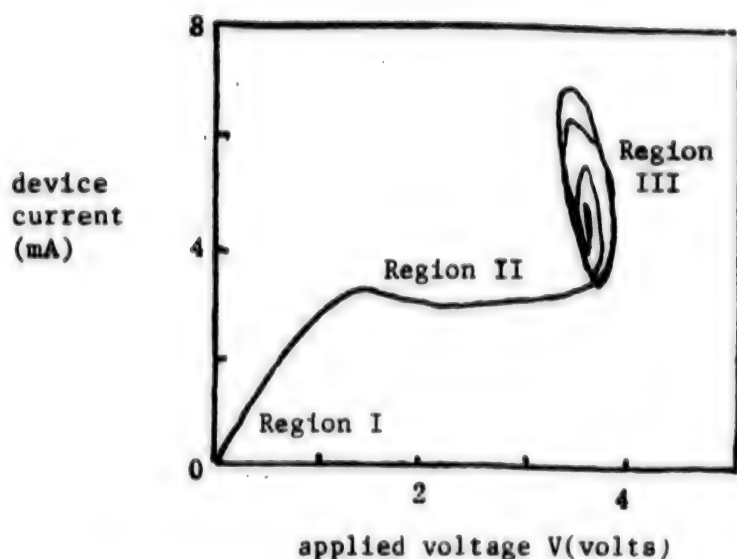
Figure 4. Current-Voltage Curve of the Device in Region I (ohmic),
Region II (negative impedance), and Region III (avalanche)

When the device is biased to operate between regions I and II, the
sensitivity of a short device varies with current in a pattern such as
the one shown in Figure 5. When the current is low, the device is in
the ohmic zone. The output of the Hall device is proportional to
current and sensitivity is constant. However, when current continues to
increase to the point that domain begins to form, as in Region II in
Figure 4, current no longer rises. Increase in voltage expands the
domain. When the depletion layer is extended to the Hall voltage output
terminal, the impedance of the device suddenly increases to raise the
output by an order of magnitude to yield a high-sensitivity Hall device.
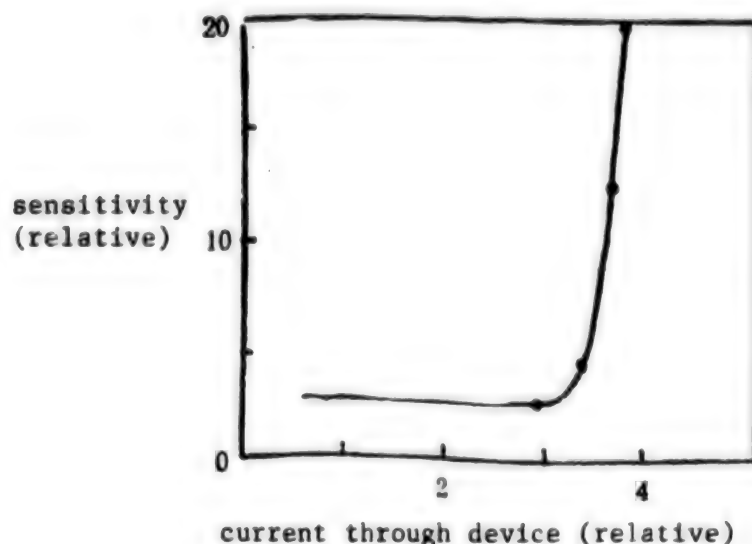
Figure 5. Sensitivity vs. Current Curve for Hall Device

IV. Conclusions

A GaAs Hall device usually operates in the ohmic zone on the current-voltage curve. When it operates in the negative impedance zone, new modes will appear. Particularly, high sensitivity can be achieved in the stationary domain mode because of an increase in bulk impedance. This requires short specimens and sufficiently high applied voltage. It is desirable to choose a high-concentration material in fabricating the device to ease making the ohmic contact. The high sensitivity is achieved by the increase in bulk resistance due to the formation of the depletion layer. This new mode may have some good characteristics. However, further study is required before it can become practical.

REFERENCES

1. T. Kanayama, et al., The 4th International Conference on Solid-State Sensors and Actuators, Tokyo, Japan, June 2-5 (1987), p 532.

2. W. Fawcett and H. D. Rees, PHYS. LETT., Vol 29A, p 578 (1972).

3. K. R. Freeman and G. S. Hobson, IEEE TRANS., Vol ED-19, p 62 (1972).

4. Zheng Yiyang, BANDAOTI XUEBAO [CHINESE JOURNAL OF SEMICONDUCTORS], Vol 6, p 469 (1985).

5. Ibid., p 475.

6. Zheng Yiyang, Modelling, Simulation & Control, A. AMSE Press, Vol 12, No 3, 1987, pp 47-56.

7. Wang Shouwu [3769 1343 2976], Zheng Yiyang, et al., Modelling, Simulation & Control, A (France), Vol 9 No 3, pp 1-11 (1987).

Observation of Structural Defects in Te-Doped GaAs Single Crystal Grown in Space Microgravity

[Article by Jiang Sinan [5592 0934 0589], Fan Tiwen [5400 4895 2429], Li
Chengji [2621 2952 1015], and Lin Lanying [2651 5695 5391] of the
Institute of Semiconductors of the Chinese Academy of Science at
Beijing; manuscript received 4 July 1988: "Observation of Structural
Defects in Te-Doped GaAs Single Crystal Grown in Space"]

[Text] Abstract: The structural integrity of Te-doped GaAs grown in
space microgravity has been studied by X-ray diffraction, electron
microscopy and cathodoluminescence. Striations are apparent in Te-doped
crystals grown on the ground but not in crystals grown in space. There
is a 5-μm-wide defect-free zone at the center on the space-grown side
of the interface between the crystal grown on the ground and that grown
in space. Away from the center, structural perfection of the crystal
grown in space decreases. A large number of dislocations and
microdefects are found. Our experimental results showed that impurity
distribution in the GaAs crystal grown under microgravity in space is
more homogeneous than that grown on the ground. The dislocations and
microdefects in the space-grown crystal were not caused by
weightlessness, but rather by lack of temperature control during crystal
growth in space.

I. Introduction

Studies on impurity-induced defects in doped single-crystal GaAs have
been reported;[1,2] these studies, however, used single crystals of GaAs
grown on the ground. Impurity defects in GaAs single crystals grown in
space microgravity have not yet been reported. In August 1987, China
launched a recoverable satellite for the first time. A Te-doped GaAs
single crystal, approximately 1 cm in diameter and 1 cm long, was grown
in space from melt. This gave us sufficient samples to conduct a
variety of studies on its physical properties, such as the growth
mechanism[3] and the photoelectric behavior.[4] This is a study of the

crystal structure (defects and degree of perfection) of the GaAs single
crystal grown in space microgravity using X-ray diffraction,
transmission electron microscopy and cathodoluminescence.

II.   Sample Preparation

The raw material for growing GaAs single crystal in space from melt was
a ground-grown single-crystal GaAs [ingot] doped with $1 - 3 \times 10^{18}$
atoms/cm^3 of Te.   It was sealed in a special quartz tube.   When the
satellite was in orbit in space, the quartz tube and the GaAs single
crystal inside were weightless (in realty under microgravity).   A 4-cm-
long section at the middle of the single crystal was melted and the heat
was on for 57 minutes (without any temperature-control equipment).   The
current was then turned off to allow it to cool down.   Two torch-shaped
space-grown GaAs single crystals seeded by the two unmelted ends (which
remained in ground-grown state) were obtained.   They have been called A
and B.   Single crystal A is surrounded by a polycrystalline layer and B
is a pure single crystal with an exposed growth plane.   Both A and B
were cut into 0.6-mm-thick {100} wafers.   All wafers to be analyzed
were ground and polished on both sides.   A conventional chemical etching
method was used to remove the 30-50-μm layer damaged by polishing.
Treated samples were analyzed by X-ray diffraction and
cathodoluminescence.   Samples 2 mm in diameter were taken from the
space-grown part, the ground-grown part, and the space-grown/ground-
grown interface for electron microscopy analysis.   They were
mechanically polished to reduce the thickness to below 40 μm and then
placed in an ion milling machine to further reduce the thickness until
the center was perforated.

III.   Experimental Method and Results

Two X-ray diffraction methods were used: (1) anomalous transmission
scanning topography and (2) the X-ray bicrystal oscillation curve
method.

In X-ray topography, the morphology of the (022) diffraction plane was
taken by MoKα_1 radiation.   The morphology of single crystal A is shown
in the photograph in Figure 1 [not reproduced].

In double-diffraction experiments, we used CuKα_1 radiation and used the
reflection from Si(422) as the first crystal of a monochromator.   The
purpose was to eliminate horizontally polarized X-rays to improve
resolution.   All oscillation curves were measured at the (400)
diffraction surface.   Point-by-point measurements were made from the
seed to the space-grown part of single crystals A and B, as shown in
Figures 2(a) and (b).   In the space-grown part, the half-height width of
the oscillation curve was found to vary with the point of measurement,
and some peaks were found to have split.   Peak splitting became more
severe near the edge of the crystal.   In order to observe this effect,
we measured oscillation curves at different ϕ angles at 2 mm on the

space-grown side and 3 mm on the seed side of single crystal A, as shown in Figures 3(a) and (b). As for single crystal B, as shown in Figure 2(b), when the [0$\bar{1}$1] direction is parallel to the axis of rotation of θ at 3 mm, ϕ is zero. It is no longer necessary to measure at different ϕ. The results are shown in Figure 4.
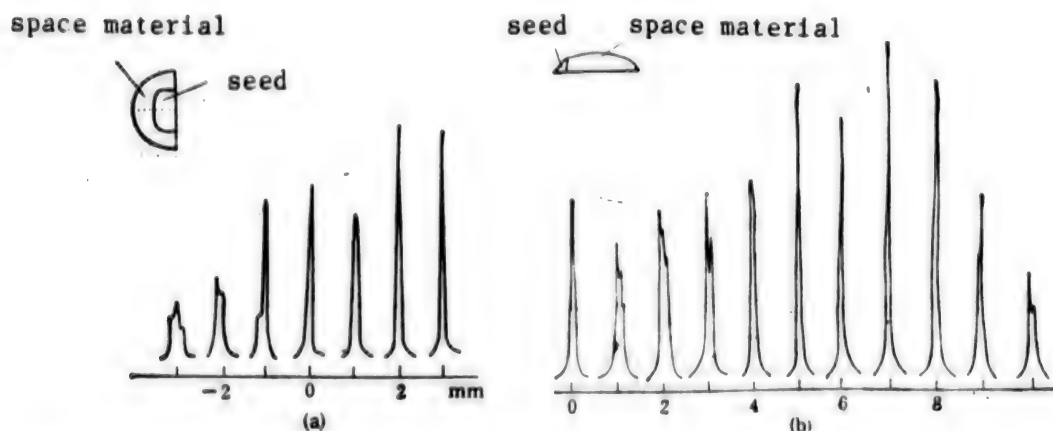
Figure 2

(a) Oscillation curves measured at different points in single crystal A. "0" represents the interface between seed and space-grown material; "-" represents the space-grown portion; "+" represents the seed-crystal portion. (b) Oscillation curves measured at different points in single crystal B. "0" represents the seed-crystal position; "+" represents the space-grown part.
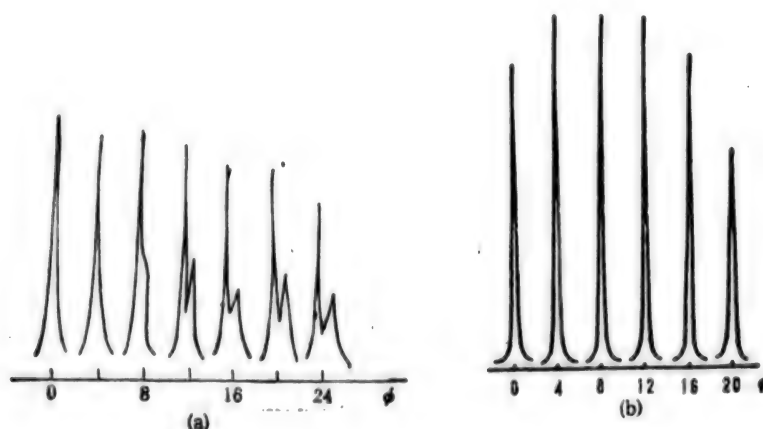
Figure 3

Oscillation curves obtained with single crystal A at different ϕ. (a) space-grown material 2 mm from interface; (b) seed 3 mm from interface.

$(0\bar{1}1)$
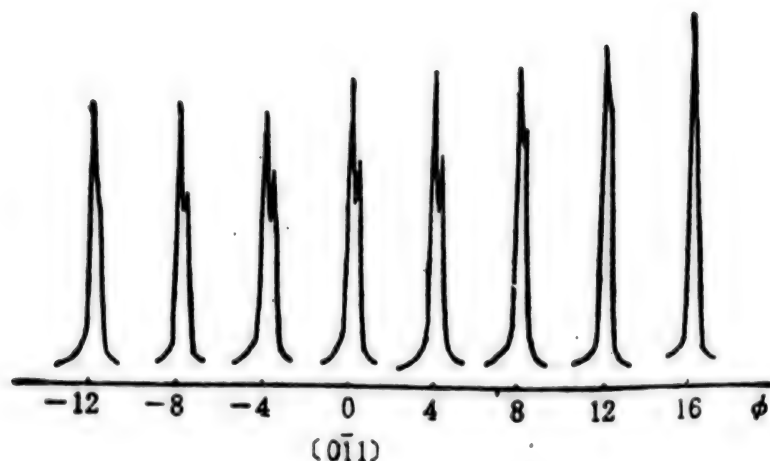
Figure 4

Oscillation curves obtained with single crystal B at different ϕ.
Position is at 3 mm shown in Figure 2(b); ϕ is zero when the axis of
rotation of θ is parallel to $[0\bar{1}1]$ of the crystal.

To observe the specimens, we used Philips EM420 and EM430 transmission
electron microscopes at 120 kV and 300 kV, respectively. Figures 5(a)
and (b) are the electron micrographs taken with single crystals A and B.
Figure 6 is the electron micrograph showing the interface between space-
grown and seed crystal in single crystal B.

Figure 5(a). The thick lines shown in the electron micrograph are the
dislocation network in single crystal A.

83

Figure 5(b). The short thick line shown in the electron micrograph is the distortion wall in single crystal B.

Figure 6. Electron micrographs of the ground/space interface in single crystal B.

Cathodoluminescence experiments were done with a Model JXA-3A electron probe X-ray micro-analyzer. An optical microscope was used to collect cathodoluminescence. The spectroscopic system is a Model H-25 monochromator. The detector system is a Model S-1 photomultiplier operating in liquid nitrogen. The voltage of the electron beam is 25 kV and the current is 2×10^{-7}A. The beam is approximately $1 - 2 \mu$m in size. The cathodoluminescence patterns for single crystals A and B are shown in Figures 7(a) and (b). Figure 7(a) shows that the interface between space-grown and ground grown material is a dark line. This dark line is not obvious in Figure 7(b).

Figure 7(a). Cathodoluminescence of the interface in single crystal A.
F is the interface, G is the seed-crystal region, and S is the space-
grown material (X200).
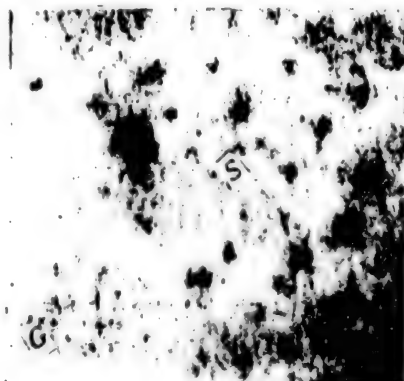
Figure 7(b). Cathodoluminescence of the interface in single crystal B.
G is the seed-crystal region and S is the space-grown material (X200).

IV. Conclusions

From Figure 1, the topographic photograph clearly shows impurity
striations in the seed area, i.e., ground-grown material. In the space-
grown region, however, striations disappeared. Nevertheless, regional
contrast difference was observed. We believe that when the crystal was
grown in space, because of the absence of gravity, the concentration
fluctuation of impurity atoms of different weight at the solid-melt
interface did not exist. Hence, striations could not be detected in
space-grown crystals with X-ray topography. Within the resolution of
the X-ray, impurity distribution is homogeneous. As for the contrast
difference in the space-grown crystal, it indicates that the perfectness
of the crystal differs quite significantly in different regions. This
is especially apparent when we look at the bicrystal oscillation curves.
The point-by-point oscillation curves (see Figure 2) show that near the

center of the crystal, no matter whether it is single crystal A or B, the half-height width of the oscillation curve of the space-grown crystal is not much different from that of the ground-grown crystal. However, away from the center, the half-height width becomes wider and the peak begins to split; the splitting is more serious at the edge and sometimes it splits into three peaks. Figure 2 also shows that single crystal B is more defect-free than single crystal A. Figure 3 points out that the oscillation curve of the space-grown material did not split when the incident angle of the x-ray is set at a specific value. The oscillation peaks of the ground grown seed would not split independently from the direction of incidence of the X-ray (i.e., sample rotation angle ϕ), as shown in Figure 3(b). This suggests that the split is induced by the growth process in space and is not related to the seed. In order to obtain more information on the split, we conducted more rigorous measurements on single crystal B. It was found that the split is symmetric with respect to the [$0\bar{1}1$] direction of the space-grown material. The maximum effect occurred when the axis of rotation of θ is parallel to [$0\bar{1}1$]. The split measured on the (400) plane indicates that there is micro-orientation deviation on the (100) plane of the crystal. This orientation deviation is a result of edge dislocation caused by the slipping of the (100) plane in the [011] direction. There are three types of simple dislocations in the diamond structure:[5] pure screw dislocation, pure edge dislocation, and the 60° dislocation. Other dislocations can be considered as a combination of these three types. Pure screw dislocation would not cause any orientation change. The 60° dislocation is unstable and eventually would become a fault and an incomplete dislocation around the fault. A fault would not cause orientation change. Only edge dislocation could cause certain crystal orientations to change because it is due to an increase (or decrease) or one-and-a-half atomic planes. In the space-grown single crystal, if

there is an edge dislocation whose Burger vector is $\dfrac{\sqrt{2}}{2}a\langle 011\rangle$, with

a dislocation line direction of $\langle 0\bar{1}1\rangle$ and a slip plane of (100), as shown in the dislocation lattice model in Figure 6, then the experimental results would be those shown in Figure 4. Based on Figure 4, when ϕ is equal to zero, the maximum angular difference of the split peak is 2.25." The appropriate equation is:

$$\frac{|b|}{2r} = tg\alpha$$

where b is the Burger vector, r is the radius of the dislocation region, and α is the angular deviation. For GaAs, $|b| = \dfrac{1}{2}\sqrt{2}a$ = 3.96 Å. r

is 316.8 Å. The stress region caused by this dislocation is even bigger. This may be the reason for the contrast difference in X-ray topography despite the fact that the impurity was homogeneously distributed in the space-grown crystal which showed no striations. Since the resolution of the film used in X-ray topography is greater

than 25 μm, it is not possible to identify each individual micro-defect. However, contrast difference might be due to the interaction between dislocation and micro defect.
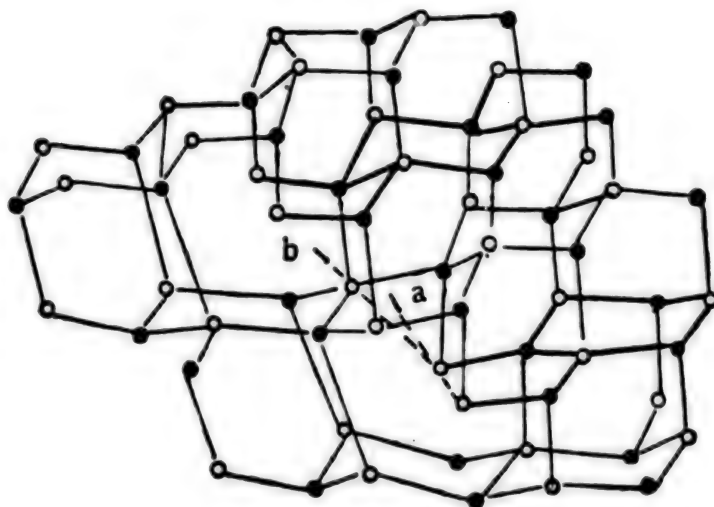
Figure 8. Lattice Model of GaAs with two edge dislocations. a is direction of dislocation, b is direction of Burger vector, and slip plane is (100).

A comparison of Figures 2(a) and (b) shows that oscillation peak splitting is much more serious with single crystal A. This suggests that there are more defects in A than B. We believe that this is because single crystal A is wrapped with a polycrystalline layer. The solid phase volume of GaAs is larger than that of the liquid phase volume. The liquid-to-solid phase transition of the polycrystalline envelope applied an internal stress on the single crystal to create a large number of dislocations. The electron micrograph shown in Figure 5 provides direct evidence to this point. A dislocation network was observed in single crystal A and only a dislocation line was seen in single crystal B. Thus, the severity of the oscillation peak split is an indication of the magnitude of dislocation defects. The number of defects in the space-grown crystal gradually increases from the center to the edge. We believe this was not due to weightlessness. Rather, it was caused by the rapid temperature drop in the growth process. Of course, since the crystal is small, the surface-tension effect becomes more predominant, especially in space microgravity. Therefore, we believe that the gradual increase of dislocation sites from centre to edge is due to a combination of factors, including rapid cooling rate, which created a large number of edge dislocations slipping along the (100) plane, and the surface tension effect which cause the number of dislocations to rise.

Both electron microscopy and cathodoluminescence experiments (Figures 6 and 7) indicate that in either single crystal A or B there is a 5-30 μm defect-free region near the seed/space-grown crystal interface. There is no dislocation and micro-precipitate. The X-ray oscillation curve obtained when the beam (0.2 x 0.01 mm) hit the interface (see Figure 2(a)) is a perfect peak. This illustrates that in the initial growth period in space the crystal was defect-free. After a period of time, the number of defects increased. During sample preparation for electron microscopy, we noticed that ion milling always resulted in a perforation with circular symmetry with these crystals, except at the ground/space interface. Instead, it is a long needle-shaped hole approximately 5 μm wide, as shown in Figure 6. This shows that the space-grown material has a higher resistance to ion bombardment. We believe this is because the cooling rate was very slow in the initial growth period. The atomic-weight difference between Ga and As disappeared in space microgravity which increased the probability of collision and produced an ideal stoichiometric ratio; this generated a distortion-free covalent bond. Therefore, an improved crystal resulted with a stronger bond to resist ion bombardment.

Away from the interface, there are fewer micro-precipitates and more dislocations. A contrast difference was shown in X-ray topography. We believe that this is due to impurity adsorption at the dislocation to reduce the number of centers created by micro-precipitates. Consequently, the number of dislocations increased as that of micro-precipitates decreased.

V. Conclusions

The results from three different techniques used to analyze the space-grown single-crystal GaAs are in agreement. Space microgravity facilitates the homogeneous distribution of impurities in single-crystal GaAs grown in such an environment. With proper temperature control, it may be possible to obtain defect-free single crystal which cannot be grown on earth.

REFERENCES

1. Symposium on GaAs and Related Compounds, Semiconductor Committee of Chinese Society of Metallurgy (1981).

2. Jiang Sinan, BANDAOTI XUEBAO [CHINESE JOURNAL OF SEMICONDUCTORS], Vol 3, p 277 (1982).

3. Zhou Bojun [0719 0130 7486], et al., BANDAOTI XUEBAO [CHINESE JOURNAL OF SEMICONDUCTORS], Vol 9, p 548 (1988) [translated in full in JPRS-CST-89-001-L, 13 Jan 89, pp 82-88].

4. Wang Zhanguo [3769 0594 0948], et al., BANDAOTI XUEBAO [CHINESE JOURNAL OF SEMICONDUCTORS], Vol 9, p 553 (1988) [translated in full in JPRS-CST-89-001-L, 13 Jan 89, pp 88-95].

5. J. Hornstra, J. PHYS. CHEM. SOLIDS, Vol 5, p 129 (1958).

Characteristics of ZrN/n-GaAs Schottky Barriers

[English abstract of article by Zhang Lichun [1728 0448 2504] and Gao Yuzhi [7559 3768 5347] of the Institute of Microelectronics, Beijing University, and N.W. Cheung of the University of California, Berkeley]

[Text] The characteristics of ZrN/n-GaAs Schottky barriers are investigated using RBS [Rutherford backscattering spectrometry], AES [Auger electron spectroscopy] and electrical measurements. The results show that ZrN/n-GaAs Schottky barriers have excellent electrical characteristics and thermal stability. After annealing at 850°C, the corresponding barrier height of 0.90eV and ideality factor of 1.02 are obtained. It is observed that with the increase of annealing temperature from 500°C to 850°C, the electrical characteristics of ZrN/n-GaAs Schottky barriers are improved distinctly: an enhancement of barrier height, reduction of reverse leakage current, reduction of diode capacitance, and increase in reverse breakdown voltage are obtained. Our study suggest that ZrN is promising for self-aligned GaAs integrated circuits.

References

[1] L.C. Zhang, C.L. Liang, S.K. Cheung and N.W. Cheung, APPL. PHYS. LETT., Vol 50, p 445 (1987).
[2] L.C. Zhang, C.L. Liang, S.K. Cheung and N.W. Cheung, J. VAC. SCI. TECHNOL., Vol B5, p 1716 (1987).
[3] Zhang Lichun and N.W. Cheung, DI WU JIE QUANGUO BANDAOTI JICHENG DIANLU GUI CAILIAO XUESHU HUI LUNWEN JI [COLLECTED PAPERS OF THE 5TH NATIONAL ACADEMIC CONFERENCE ON SILICON MATERIALS FOR SEMICONDUCTOR INTEGRATED CIRCUITS], p 346 (1987).
[4] G.P. Schwartz, G.J. Gualtieri and W.A. Bonner, J. ELECTROCHEM. SOC., Vol 133, p 1266 (1986).

Formation, Characterization of Tungsten Silicide GaAs Schottky Contacts

[English abstract of article by Zhu Zhongde [4376 1813 1795], Yu Hong [6079 5725], Ning Baojun [1337 1405 0193] and Li Xiaoguang [2621 2556 0342] of the Institute of Microelectronics, Beijing University]

[Text] The formation process and electrical characteristics of tungsten silicide GaAs Schottky contacts are reported. An excellent WSi_x/GaAs Schottky contact is obtained with a barrier height of 0.8V and an ideality factor equal to unity. High-temperature stability is demonstrated with furnace annealing up to 750°C. It is shown that besides the composition of silicides, the surface cleaning procedure and silicide deposition technique also have a strong effect on the I-V [current-voltage] characteristics of Schottky contacts and their thermal stability. By using sputter-etching on the GaAs substrate surface or applying a negative bias on the substrate during the deposition process, the adhesion between the metal layer and the GaAs substrate can be improved significantly.

References

[1] Zhu Zhongde, Nathan W. Cheung, Zachary J. Lemnios, Michael D. Strathman and James B. Stimmell, J. VAC. SCI. TECHNOL., Vol B4, p 1398 (1986).
[2] H. Nakamura, Y. Sano, T. Nonaka, T. Ishida and K. Kaminishi, IEEE GaAs IC SYMPOSIUM (1983), p 134.
[3] Haruo Yamagishi and Masayoshi Miyauchi, JPN. J. APPL. PHYS., Vol 24, p L841 (1985).
[4] Kazuhiko Matsumoto, Nobuo Hashizume, Hisao Tanoue and Toshihiko Kanayama, JPN. J. APPL. PHYS., Vol 21, p L393 (1982).
[5] Sang-Mo Shin, presented at the Workshop on Refractory Metal and Silicides for VLSI, San Juan Bautista, CA, 1987.
[6] T.N. Jackson and J.F. DeGelormo, J. VAC. SCI. TECHNOL., Vol B3, p 1676 (1985).
[7] J.L. Zilko and R.S. Williams, J. ELECTROCHEM. SOC., Vol 129, p 406 (1982).
[8] S.M. Sze, Physics of Semiconductor Devices, New York: Wiley, 1969.
[9] T. Ohnishi and N. Yokoyama, presented at the Workshop on Refractory Metals and Silicides for VLSI III, San Juan Bautista, CA, May 13-16, 1985.
[10] K. Yamasaki, K. Asai, K. Shimada and T. Makimura, J. ELECTROCHEM. SOC., Vol 129, p 2760 (1982).

Characteristics of TiN/n-GaAs Schottky Barriers

[English abstract of article by Zhang Lichun [1728 0448 2504] and Gao Yuzhi [7559 3768 5347] of the Institute of Microelectronics, Beijing University]

[Text] The characteristics of TiN/n-GaAs Schottky barriers formed by reactive sputtering are investigated using AES [Auger electron spectroscopy] and I-V [current-voltage] and C-V [capacitance-voltage] measurements. The TiN/n-GaAs Schottky contact is thermally stable and maintains excellent rectifying characteristics after rapid thermal annealing (RTA) at 800°C. A corresponding barrier height of 0.80eV and ideality factor of 1.07 are obtained. When the contacts are annealed from 500 to 800°C, major interesting results are observed: enhancement of barrier height, decrease in barrier capacitance, and increase in reverse breakdown voltage of the diode. This is attributed to the incorporation of nitrogen into the GaAs substrate during sputtering deposition. We have invoked the Shannon contact model (i.e., metal/p-GaAs/n-GaAs structure) to account for the above results. Our study suggests that TiN is a suitable gate material for self-aligned GaAs MESFET [metal semiconductor field effect transistor] fabrication.

References

[1] N.W. Cheung et al., J. APPL. PHYS., Vol 52, p 4297 (1981).
[2] I. Suni et al., J. ELECTROCHEM. SOC., Vol 130, p 1215 (1983).
[3] C.Y. Ting, J. VAC. SCI. TECHNOL., Vol 21 (1), p 14 (1982).
[4] M. Wittmer, J. VAC. SCI. TECHNOL., Vol A3 (4), p 1797 (1985).
[5] Thomas Tang et al., IEDM, p 590 (1985).
[6] T.E. Tang et al., IEEE TRANS. ON ELECTRON DEVICES, Vol ED-34, p 682 (1987).
[7] L.C. Zhang (Zhang Lichun) et al., APPL. PHYS. LETT., Vol 50, p 445 (1987).
[8] Hou Zhuang [0186 8369] et al., DI WU JIE QUANGUO DIANZI SHU LIZI SHU GUANGZI SHU XUESHU NIANHUI LUNWEN JI [COLLECTED PAPERS OF THE 5TH ANNUAL NATIONAL ACADEMIC CONFERENCE ON ELECTRON BEAMS, ION BEAMS, AND PHOTON BEAMS], p 4-20 (1988).
[9] J.M. Shannon, SOLID-STATE ELECTRON., Vol 19, p 537 (1976).
[10] Zhang Lichun et al., "Chendi pianya jianshe dui GaAs Xiaoteji shilei xingneng de yingxiang" [The influence of substrate bias sputtering on GaAs Schottky barrier performance] (to be published).

Ceramic Microcasing Developed for GaAs FET's

40080190a Beijing DIANZI SHICHANG [ELECTRONICS MARKET] in Chinese 4 May 89 p 2

[Article by Luan Chunjin [2940 4783 6855]]

[Text] A gallium-arsenide field-effect transistor [GaAsFET] ceramic microcasing, widely used for packaging [such] very-high-speed transistors, was recently developed by the state-run Yixing [1355 5281] Electronic Devices Plant. The GaAs transistor casing has external dimensions of about 1.8mm x 1.8mm, and a metallized internal cavity with a diameter of 1.3mm. Testing of this product has shown that its technical performance indicators all meet or approach advanced standards for similar Japanese products. In particular, the pulling force that the leads can stand up to greatly exceeds that of the Japanese NEC Corporation's product.

Joint Venture Set Up To Produce ASIC's

40080190b Shanghai JIEFANG RIBAO in Chinese 9 May 89 p 1

[Unattributed article: "Shanghai Bei Ling Microelectronics Company in Production: Has Produced First Batch of Integrated Circuits Meeting Standards of Similar Foreign Products"]

[Text] The Sino-foreign joint venture Shanghai Bei Ling ["Bell Mountain" 6296 1545] Microelectronics Manufacturing Ltd.--China's most technologically advanced and largest-capacity center for producing integrated circuits [IC's]--officially went into production yesterday. It successfully turned out the first batch of application-specific integrated circuits [ASIC's] for five-function electronic [wrist]watches.

Located in the Caohejing High-Technology Development Area, Shanghai Bei Ling Co. is a joint-venture high-tech enterprise formed from Shanghai Radio Plant No 14 and the Sino-Belgian joint venture Shanghai Bell Telephone Equipment Manufacturing Co., Ltd.; its capitalization is over US$50 million. Over 70 percent of the total labor force are engineers and technicians. Production equipment and technology meet advanced international standards for the mid-eighties. The greater part of the equipment is being imported by China for the first time, now that approval has been received; an example is the large-beam ion-implant machines. In addition to manufacturing IC's for electronic wrist-watches, the company will also produce five other main varieties of 3-micron large-scale-integration [LSI] ASIC's, including [stored-]program-controlled [SPC] telephone exchanges and 16-bit microcomputers.

According to Zhang Huiquan [1728 1920 3123], General Manager of Bei Ling, the company this year will produce 10-15 million IC's for electronic watches, mainly to supply various joint-venture electronic-watch-manufacturing enterprises in Fujian [Province's] Putian City. These products will be marketed in Hong Kong.

Phototriode, GaAs LED Certified

40080197a Beijing DIANZI SHICHANG [ELECTRONICS MARKET] in Chinese 11 May 89 p 2

[Article by Yu Ruming [0151 3067 2494]]

[Text] The Ministry of Machine-Building & Electronics Industry's Chongqing-Yongchuan [Sichuan Province] Research Institute 44 has developed the GF9410U GaAs LED [gallium arsenide light emitting diode] and the GT5650U phototriode. To meet the need, the institute has set up a trial line and this year will produce over 1 million of each.

The GF9410U GaAs LED is primarily used as a remote-control light source and a smoke-detector light source, but can also be employed in optical encoders, optical repeater circuits, [optical] isolators, etc. Its current is under 100mA dc, and it has a typical light output power in the 5mW-7mW range, with a maximum value of 12mW. Emission peak-value wavelength is 940nm, and the emission spectrum half-width is 50nm.

The GT5650U silicon phototriode is primarily used in remote-control [devices], infrared alarms, optical couplers, optoelectronic converter amplifiers, etc., and is an ideal component for optoelectronic receivers. Sensitivity is high. The crystal triode [i.e., semiconductor triode] B value is greater than 200: the device can convert faint optical signals into electronic signals and internally amplify them by a factor of over 200. The peak-value wavelength of the received light is 940nm, identical to the emission wavelength of the GaAs LED. The receiving photosensitive surface is small ($0.25nm^2$) and cost is low; dark current and noise are also low, in general only several nanoamperes. Performance is stable and reliable, and operating voltage is low (5-10V). The device's performance indicators are superior to those of similar products such as the Matsushita PN150, the Hamamatsu S2829, the KODCSTIMLAR 11 [as printed], and the Texas [Instruments] TLS series.

Domestic Development of GaAs FET's

40080197c Beijing ZHONGGUO DIANZI BAO in Chinese 23 May 89 p 3

[Article by Li Xiaobai [2621 2400 4101]: "A Bright New Star in Electronic Components: Microwave Power Field Effect Transistors"]

[Excerpt] [Passage omitted] In terms of quality, quantity, and performance indicators, the GaAs FET's [gallium arsenide field effect transistors] produced by the Ministry of Machine-Building & Electronics Industry's [MMEI] Research Institute 13 represent the forefront in China today. This institute began developing low-noise GaAs FET's in 1970, and in 1978 finalized the design of the first-generation domestic product; in 1974 it began development of a power GaAs FET, and in 1980 finalized the design of the first-generation domestic product, which has been in batch production for some time.

The institute has finalized designs for C-band, X-band, and K-band microwave GaAs FET amplifier tubes, power oscillator tubes, monolithic power field amplifiers, dual-gate power tubes, and GaAs FET amplifiers, and has taken the first steps to meet the domestic need in this key national project. Some of these products have been successfully employed in satellites, and some batches have been put to effective use in microwave multiplexing systems. The quality of some of the varieties has already caught up with that of advanced products worldwide, but the performance-to-cost ratio still needs a little improvement.

MMEI's Institute 55 also works in a similar area, and is China's main facility for research on GaAs low-noise components. Several series of products it has developed are used in various kinds of microwave systems.

11-Meter Satcom Earth Station Passes Test

[Summary] An 11-meter satellite communications (satcom) earth station, developed in a 3-year effort by the Ministry of Posts & Telecommunications' Research Institute 1, passed ministry-level technical accreditation in Shanghai on 3-5 April 1989. Thirty-nine specialists from 19 units within and outside of the ministry participated in the appraisal.

Designed to meet the need for domestic satcom construction and development, the system will be employed as a regional central station. Maximum capacity of the equipment is 972 circuits. The system has 10 subsystems, including an 11-meter double circularly polarized antenna, a 3kW klystron high-power amplifier, a 55K low-noise amplifier, miniaturized FDM/FM [frequency division multiplexing/frequency modulation] communications equipment, an SCPC [single channel per carrier] data terminal, and a microcomputer control station. Either of two communications modes--FDM or SCPC--may be used. The station incorporates new technologies such as a low-sidelobe antenna, a low-phase-noise microwave frequency synthesizer, a broadband low-threshold demodulator, and a microcomputer-controlled monitor alarm. The performance and technical indicators for all the equipment comply with national standards for satellite earth stations and with 1980's international standards set by Intelsat. The entire system, whose quality is at the forefront in China, is manufactured domestically, with a good performance-to-cost ratio: the actual price is about 1/3 to $\frac{1}{2}$ that of an imported product of like kind. Main components of the equipment have been installed at some domestic earth stations and have met with favorable reaction from users. [See also FBIS-CHI-89-066, 7 Apr 89, p 31, and FBIS-CHI-89-073, 18 Apr 89, pp 30-31.]

After the earth station was certified, the technical specialists also accredited miniaturized satellite television uplink equipment, a 75W traveling wave tube amplifier [TWTA], and the research on a 12GHz satcom system. All indicators for these systems met the planned targets.

Domestically Made Low-Phase-Noise Microwave Frequency Synthesizer for
Satellite Communications

40080171 Shanghai DIANXIN KUAIBAO [TELECOMMUNICATIONS INFORMATION] in
Chinese No 3, Mar 89 pp 2-11

[Article by Ding Yanyan [0002 3508 3508]: "Low-Phase-Noise Microwave
Frequency Synthesizer"]

[Excerpts] Satellite communications [satcom] developed rapidly during
the 1970s. With this proliferation of communications came the need to
regularly transform microwave radio frequencies [RF]; the development of
communications systems has been toward digitization, which produces
strict requirements on the degree of frequency stability for RF systems
and on phase noise. For this reason, for frequency sources, RF systems
equipment must use microwave frequency synthesizers that are highly
frequency-stable and low in phase noise. RF equipment not only requires
high performance from these synthesizers, but it also must be small in
size, low in manufacturing cost, and high in reliability.

The RCA Company completed development of its O-1677/GSC synthesizer in
1976. It is used as the local oscillator source for the American
military strategic satellite [i.e., Milstar] groundstation's up-down
frequency converters.[1] In 1979 a new product was introduced by
Frequency Sources, Inc., West Division--a low-phase-noise satcom
frequency synthesizer.[2] This synthesizer has been used for up-down
frequency converters in the SCPC [single carrier per channel] satcom
system, manufactured by the Canadian Spar Company. In 1980 the Japanese
company NEC Corp. used a NEC microwave frequency synthesizer on the
satcom up-down frequency converter it produces.[3] In 1984 the Philips
Company introduced its most recently developed SCPC up-down frequency
converter for its RS-400 System. This frequency converter uses a
microwave frequency synthesizer.[4]

China began development of the WGQ-102 microwave frequency synthesizer
in 1984. It passed its evaluation by the Beijing Institute of Posts and
Telecommunications Science in December 1985, after which it was put into
batch production.

This paper describes the demand by digital communications regarding phase noise of signals output by microwave synthesizers; it analyzes the phase noise of digital frequency synthesizers; it describes the program for the WGQ-102 microwave frequency synthesizer, as well as the characteristics of the primary components of this synthesizer and ways to lower the phase noise; and finally, this paper provides the technical specifications achieved by this synthesizer.

[Passage omitted]

Primary Components of the Synthesizer and Ways to Lower the Phase Noise

Voltage-Controlled Oscillators (VCO) and Frequency Quadrupler

The VCO of the synthesizer has a manual microwave crystal triode oscillator that can be mechanically tuned and electrically tuned. The oscillator resonating circuit is a high-quality-factor [high-Q] coaxial terminated open-circuit cavity. The length of the guide within the mechanical tuning coaxial cavity is sufficient to rough-tune a frequency. The range of the mechanical tuning frequency is 1.2-1.33 GHz. Because the frequency of the VCO is rough-tuned mechanically and a high-Q coaxial cavity is used for the resonant circuit, phase noise is rather low. Output power of the VCO is greater than 400 mW, and over the entire oscillation band output-power fluctuation is less than 0.5 dB.

The frequency quadrupler of the synthesizer uses a step-recovery-diode SRD] frequency doubler. An accurately designed and adjusted doubler can enable the doubler to put out a stable frequency with little stray output, low phase noise, and stable performance. The specifications reached by the frequency quadrupler are as follows: output frequency range 4.8-5.32 GHz, output power greater than +13 dBm, power fluctuation less than 3 dB, frequency-doubler stray output (namely VCO's 3rd and 5th-order harmonic components) less than -50 dBc, and phase noise as shown in the tables of the previous section [omitted].

Practice has shown that selecting low noise microwave oscillator tubes and SRD's and patiently and carefully adjusting the oscillator and the frequency doubler are the keys to lowering phase noise. The phase noise of the VCO and the frequency quadrupler is directly determined by the phase noise in frequency-range IV of the synthesizer. Lowering the phase noise in frequency-range IV reduces the bandwidth of the main loop of the synthesizer; this diminishes the range of frequency range III, lowering the overall phase noise of the synthesizer.

Mixer

Introduction of a mixer into the synthesizer plan greatly reduces phase noise.

Incorporation of a mixer in the synthesizer will result in the output of stray frequencies. The two input terminals of the mixer cannot be completely isolated, and therefore the 1,155-MHz local-oscillation signal will feed into the VCO, after which it passes through the frequency doubler to be output as stray frequencies. The synthesizer uses lumped-parameter dual-balanced mixers, which have low frequency dissipation and little leakage from the local oscillator. Tests of the synthesizer showed output of stray frequencies to be at levels less than -70 dBc. Experience has shown that the key to achieving good performance from dual balanced mixers is a balanced transformer.

105-MHz Crystal Phase-Locked Frequency Doubler

Using a crystal phase-locked-loop [PLL] frequency doubler in the synthesizer multiplied the 5-MHz frequency standard to 105 MHz. The phase noise of the signal output from the frequency doubler is quite a bit more than the phase noise of the signal output from an ordinary LC-loop frequency doubler.

It is well known that when comparing the 5-MHz frequency standard and the 105-MHz high-frequency crystal oscillator, the long-term frequency stability of the 5-MHz frequency standard will be greater, near-band phase noise will be less, and far-band phase noise will be greater. If the 5-MHz frequency standard is taken as a reference frequency source to lock in the 105 MHz VCO, then the degree of long-term frequency stability for the 105-MHz signal output by the PLL will be equivalent to that of the 5 MHz frequency standard, and near-band and far-band phase noise will both be slight.

Experience has shown that accurate design of all parameters of components of the PLL, and use of high-Q high-frequency crystals and low-noise oscillating transistors is the key to lowering phase noise in region II of the synthesizer.

Eleventh-Order Frequency Doubler

The 11th-order frequency doubler uses an SRD frequency doubler that is composed of a 105-MHz power amplifier, an SRD pulse generator, and a 1,155-MHz filter. The 105-MHz signal is amplified by the amplifier before passing through a matching network on its way to the SRD pulse generator to become a spike with rich harmonics, after which the 11th-order harmonic 1,155-MHz component is filtered out of the spike by the 1,155-MHz filter. With correct design and careful test tuning it can be assured that the power output from the 11th-order frequency doubler will be stable and few stray frequencies will be put out.

Variable Frequency Divider and Discriminator and Loop Filter

The variable frequency divider of the synthesizer uses a tungar pulsed variable frequency divider. Tungar pulse technology can greatly improve the maximum working power of the variable frequency divider. The phase noise introduced by this kind of frequency divider is minimal.

The discriminator of the synthesizer uses a digital frequency and phase discriminator. This kind of discriminator accomplishes phase discrimination when the loop is locked; frequency discrimination is achieved when the loop is released. When the synthesizer unlocks, the frequency and phase discriminator can provide a warning signal to indicate that the VCO needs manual tuning, allowing the frequency to be raised or lowered. As soon as the manually tuned frequency is in the locking band, the frequency phase discriminator can allow the synthesizer to lock quickly.

The loop filter of the synthesizer consists of a low-noise broadband operational amplifier and RC feedback components.

Use of a high-speed frequency discriminator with low trigger delay, a phase discriminator of high working frequency, a digital phase discriminator of high sensitivity, and a low-noise broadband operational amplifier can reduce the phase noise introduced by variable frequency discriminators, phase discriminators, and loop filters, thus lowering loop base noise.

Optimal selection of loop bandwidth can keep phase noise output by the synthesizer to a minimum. Based on loop bandwidth, VCO sensitivity, and phase sensitivity, RC component values can be designed for loop filters.

Low-Pass Filters

In the PLL, the signal output by the digital phase discriminator has not only phase data, but also has the phase discriminant frequency and its harmonic components. These stray components are filtered out with a low-pass filter. Otherwise, when the synthesizer outputs a signal, that will generate spurious modulation, forcing a rise in the output level of stray frequencies. Normally, an LC low-pass filter with a trap is used for the low pass filter. This kind of low-pass filter greatly diminishes stray phase and frequencies, but within the PLL belt there is little shift. For this reason, after insertion into the low-pass filter, the PLL is stable and the performance of the loop is little affected. After switching in the low-pass filter, the spurious output levels of the synthesizer phase and frequency discrimination will be less than -70 dBc.

Conclusions

This paper describes the WGQ-102 microwave frequency synthesizer, concentrating on analyzing the phase noise characteristics of the synthesizer. This synthesizer conveniently transforms frequencies, is highly frequency-stable, and has little phase noise. It can meet various demands of communications control, and since it went into production, more than 200 units have been made, successfully operating in analog and digital satcom up-down frequency converters manufactured by the Ministries of Posts and Telecommunications, Machine-Building and Electronics Industry, and Aeronautics & Astronautics Industry. The synthesizers can also be used as microwave frequency sources in astronomical radio telescopes, radar, and ground digital microwave systems.

Primary technical specifications for the synthesizer:

1.	Frequency Range	4 800--5,320 MHz
2.	Frequency Stability	Determined by an external frequency standard source, where for a 5-MHz source, frequency stability is greater than $\pm 1 \times 10^{-8}$ per day
3.	Frequency Steps	1 MHz or 500 KHz, 250 KHz
4.	Methods of Frequency Selection	Finger-wheel dial is turned to digits representing desired output frequency, manually adjusted by frequency tuning lever until lock-in
5.	Output Power	Greater than +13 dBm; output power fluctuation less than 3 dB
6.	Stray Output	Harmonics of the primary oscillation frequency are less than -50 dBc; other stray output is less than -70 dBc
7.	Phase Noise	Frequency steps at 1 MHz, and for typical single-sideband phase-noise values, see Table 3 [on following page]

Table 3

Shift Frequency (Hz)	100	500	1K	5K	10K	20K	100K
Single-sideband Phase-Noise Spectral Density (dBc/Hz)	-70	-80	-80	-80	-80	-90	-110

8. Power Source   +24 V, 500 mA; +5.5 V   800 mA
   Requirements

9. Ambient Temperature   0-40 degrees [Celsius]

10. Dimensions   120 mm X 110 mm X 100 mm

11. Weight   1.5 kg

[Note: Per advertisement on inside front cover of same source, the WGQ-102 is being marketed by the Satellite Communications Research Dept., Research Institute No. 1 of the Ministry of Posts & Telecommunications, 48 Pingjiang Rd., Shanghai, China; phone 375432, cable 0207b, telex 33330 FRIPT CN]

REFERENCES

1. "Microwave frequency synthesis for satellite communications ground terminals," Proceedings of the 30th Annual Symposium on Frequency Control, 1976, pp 420-437. Chinese translation in GUOWAI DIANZI JISHU, 1977, No 7.

2. "Satcom Source Touts Low Phase Noise," MICROWAVES, Vol 18, No 12, Dec 1979, pp 83...

3. NEC owner's manual handbooks (China No 2 Earth Station) Vol III, Ground Communication Equipment, Part 1-1-4 87946A 5-GHz frequency synthesizer.

4. "An RF Up Down Converter for SCPC Satellite Communications " PTR, Vol 42 No 1, April, 1984, pp 13-22.

5. [In Chinese] "Phase-Lock Technology," Scientific Publishing House.

6. Analysis and Test Methods for Digital Frequency Synthesizer Loop Low-Noise, Institute No 1, the Ministry of Posts and Telecommunications, "Microwave Frequency Synthesizer Identification Materials."

Fiber-Optic Telecommunications Venture Set Up in Shanghai

40100053 Beijing CEI DATABASE in English 30 May 89

[Text] Shanghai (CEI)--A U.S.-Dutch joint venture signed a contract here Monday with Shanghai Municipality to set up a fiber-optic digital telecommunications equipment plant in Shanghai, the first of its kind in China.

Signing the contract for the foreign side was Dr. A. Borsboom, director of finance of AT&T Network Systems International, which was established by AT&T of the U.S. and Philips of the Netherlands.

The plant will be located at the Caohejing high-tech park in Shanghai. According to the contract, advanced technologies will be imported from the United States and the Netherlands. When completed, the plant will produce 16 varieties of fiber-optic and digital telecommunications equipment, which will meet standards for telecommunications both at home and abroad.

Dr. Borsboom said that 25 percent of the products from the plant would be exported while the rest would meet the needs of China's domestic market.

Multipole Giant Resonances in Highly Excited Nuclei

[English abstract of article by Xia Keding [1115 0344 1353] and Cai Yanhuang [5591 1693 3874] of the Institute of Nuclear Research, Chinese Academy of Sciences, Shanghai]

[Text] The isoscalar giant surface resonance and giant dipole resonance in highly excited nuclei are discussed. Excitation energies of the giant modes in ^{208}Pb are calculated in a simplified model, using the concept of energy weighted sum rule (EWSR), and the extended Thomas-Fermi approximation at the finite temperature is employed to describe the finite temperature equilibrium state. It is shown that EWSR and the energy of the resonance depend only weakly on temperature in the system. This weak dependence is analyzed.

References

[1] J.D. Newton et al., PHYS. REV. LETT., Vol 46 (1981), p 1383;
     W. Hennerici et al., NUCL. PHYS., Vol A396 (1983), p 3292;
     A.M. Sandorfi et al., PHYS. LETT., Vol 130B (1983), p 19.
[2] H.M. Sommermann, ANNALS OF PHYS., Vol 151 (1983), p 163.
[3] O. Civitarese, R.A. Broglia and C.H. Dasso, ANN. PHYS., Vol 156 (1984) p 142;
     H. Sagawa and G.F. Bertsch, PHYS. LETT., Vol 146B (1984), p 138.
[4] M. Barranco and A. Polls, NUCL. PHYS., Vol A444 (1985), p 445.
[5] M. Di Toro, Proceedings of the Winter College on Fundamental Nuclear Physics, edited by K. Dietrich, M. Di Toro and H.J. Mang (World Scientific, 1985), Vol 1, p 451.
[6] Cai Yanhuang and Xia Keding, "Rehe de tongji xingzhi he he wuzhi de yeqi xiang bian" ["The statistical nature of thermonuclear [matter] and liquid-gas phase changes in nuclear matter"], to be published.
[7] A. Bohr and B.R. Mottelson, Nuclear Structure, Vol 2, New York: Benjamin, 1975.
[8] M. Brack, C. Guet and H.B. Hakansson, PHYS. REP., Vol 123 (1985) p 275.
[9] M. Barranco and J. Treiner, NUCL. PHYS., Vol A351 (1981), p 269;
     M. Barranco and J.R. Buchler, PHYS. REV., Vol C24 (1981), p 1191.
[10] A. Bohr and B.R. Mottelson, Nuclear Structure, Vol 1, New York: Benjamin, 1969.
[11] J. Bartel, M. Brack, C. Guet and H.B. Hakansson, PHYS. LETT., Vol 139B (1984), p 1.

Photochemical Behavior of Pu(IV)

40090058a Beijing HE HUAXUE YU FANGSHE HUAXUE [JOURNAL OF NUCLEAR AND RADIOCHEMISTRY] in Chinese Vol 11 No 1, Feb 89 pp 1-6, 12

[English abstract of article by Zhou Zhihong [0719 1807 1347], et al., Institute of Atomic Energy, Beijing]

[Text] The effects of H^+ and NO_3^- concentrations on the photochemical behavior of Pu(IV) in perchloric acid solution (ionic strength = 3) have been investigated. The results show that the photochemical oxidation of Pu(IV) to Pu(VI) is obviously promoted th nitrate ions. Results of a study of thermo-disproportionation of Pu(IV) in perchloric acid solution (ionic strength = 3) at 63°C and ultraviolet beam irradiation under the same experimental conditions show that the light irradiation with ultraviolet beams promotes the disproportionation of Pu(IV), and ratios of the reaction concentration quotient $[Pu(III)]^2 \cdot [Pu(VI)]/[Pu(IV)]^3$ are determined as 2.2 x 10^3, 4.15 x 10^2, 1.98 x 10^2 and 3.16 x 10^2 when H^+ is equal to 1.0, 1.5, 2.0 and 3.0 mol/l.

The effects of CH_3OH, C_2H_5OH, UO_2^{2+} and Fe^{3+} on the photochemical behavior of Pu(IV) in nitrate solution have also been studied. The results show that the Pu(IV) oxidation to Pu(VI) is inhibited by ferric ions. The quantity of Pu(VI) can be decreased from 80 percent to 10 percent if the ferric ion concentration is 0.038 mol/l. The probable reason for the inhibition of Pu(IV) oxidation to Pu(VI) by ferric ions is discussed.

References

1. Cleveland, J.M., "Plutonium Chemistry," Science Press, Beijing, 1974.
2. Paley, P.N., RADIOCHEMISTRY, Vol 11, 1969 p 300.
3. Bell, J.T., et al., J INORG NUCL CHEM, Vol 38, 1976 p 831.
4. Friedman, H.A., et al., J INORG NUCL CHEM, Vol 39, 1977 p 123.
5. Gangwer, T., BNL-50147.
6. Toth, L.M., et al., CONF-770506.
7. Kazanjian, A.R., RFP-3113, 1981.
8. Duan Yunfu, et al., JOURNAL OF NUCLEAR AND RADIOCHEMISTRY, Vol 9 No 4, 1987 p 200.
9. Rabideau, S.W., J AM CHEM SOC, Vol 79, 1957 p 3675.
10. Rabinowitch, E., REV MOD PHYS, Vol 14, 1942 p 112.
11. Evans, M.G., et al., NATURE, Vol 77, 1949 p 404.
12. Baxondale, et al., TRANS FARAD SOC, Vol 42, 1946 p 668.

Interaction of 960A MeV ^{238}U Ions with Light Nuclei

[English abstract of article by Cui Huanhua [1508 3183 5478] et al., Institute of High-Energy Physics, CAS, Beijing; Lü Weichun [0712 4850 4783], Qinghua University, Beijing; and R. Brandt, Philipps Universität, FRG]

[Text] A CR-39 track detector was used both as a target and a detector to study the interaction of 960A MeV ^{238}U ions with light nuclei (^{1}H, ^{12}C, ^{16}O). The range, mean free path and cross section of 960A MeV ^{238}U ions in CR-39 have been found to be 6.8 cm, 4.33 cm and 2160 mb [millibarns], respectively. The average multiplicity due to fragmentation of ^{238}U projectiles with light nuclei has been found to be 2.03. It is shown that the most common mode of interaction is binary fission. The reaction products consist of two track peaks according to track diameter distribution. The ratio of track density of each peak to track density of reaction products comes out to be 20 percent and 80 percent, respectively.

References

[1] S.P. Ahlen et al., SCIENCE, Vol 217 (1982), p 1139.
[2] K. Jamil et al, NUCL. INSTR. METH., to be published.
[3] M.H. Salamon et al., NUCL. INSTR. METH. IN PHYS. RES., Vol B6 (1985), p 504.
[4] E.V. Benton, U.S. Naval Radiological Defense Laboratory, TR-68-14 (1968).
[5] W.H. Barkas et al., National Academy of Science/National Research Council Publication 1133, p 103 (1964).
[6] H.L. Bradt et al., PHYS. REV., Vol 77 (1950), p 54.
[7] G.D. Westfall et al., PHYS. REV., Vol C19 (1979), p 1309.
[8] M.L. Tincknell et al., PHYS. REV. LETT., Vol 51 (1983), p 1948.

Mechanism of High-Energy Unequi-Nuclei Collisions, Calculations of Hydrodynamical Model in Energy Region from 200A GeV to 100A TeV

[English abstract of article by Shen Guojin [3088 0948 6855], Wang Enke [3769 1869 4430] and Li Jiarong [2621 1367 2837] of the Institute of Particle Physics, Central China Teachers' University, Wuhan]

[Text] A mechanism for high-energy unequi-nuclei collisions is proposed. The space-time evolution of high-energy unequi-nuclei collisions is discussed with the help of the hydrodynamical model. It explains successfully the characteristic features of the rapidity distribution of the final state particles for the several typical cosmic ray events and the first preliminary results from an experiment with a beam of 200A GeV ^{16}O colliding on emulsion at the CERN SPS [super proton synchrotron].

References

[1] J. Cleymans et al., PHYS. REV., Vol D33 (1986), p 2585; NA35 Collaboration, PHYS. LETT., Vol B184 (1987), p 271.
[2] P.F. Zhuang, Z.Q. Wang, and L.S. Liu, Z. PHYS., Vol C32 (1986), p 93.
[3] Kisei Kinoshita et al., Z. PHYS., Vol C8 (1981), p 205.
[4] EMUO1 Collaboration, Cosmic and Subatomic Physics Report LUIP 8704, Lund (1987).
[5] T.B. Burnett et al., PHYS. REV. LETT., Vol 50 (1983), p 2062; Yoshiyuki Takahashi et al., NUCL. PHYS., Vol A461 (1987), p 263c.
[6] J.D. Bjorken, PHYS. REV., Vol D27 (1983), p 140.
[7] K. Kajantie et al., NUCL. PHYS., Vol B222 (1983), p 152; Vol B214 (1983), p 261.
[8] L.D. Landau, IZV. AKAD. NAUK SSSR, Vol 17 (1953), p 51.
[9] L.S. Liu, L.H. Qi, and P.F. Zhuang, SCIENTIA SINICA, Vol A29 (1986), pp 1063-1072.

Analysis of Error in EXAFS Studies of Metallic Glass

[English abstract of article by Liu Wen [0491 2429] of the Center of Fundamental Physics, University of Science and Technology of China, Hefei; Huang Shengtao [7806 0524 3447] of the Department of Physics, Wuhan University]

[Text] The deviation of the radial distance to a shorter value in EXAFS studies of metallic glass is analyzed in this paper. Simulation calculations show that the current error theory cannot explain the deviating-to-shorter phenomenon satisfactorily. By comparing the phase-shift function of the amorphous state with that of the crystalline state, the authors conclude that in the similar system the slope of the amorphous phase-shift function may be different from that of the crystalline phase-shift function. Normal EXAFS data processing without evaluating this kind of difference is also a cause of the radial distance deviating-to-shorter error in the EXAFS results. A simple method for correcting the slope of the phase-shift function of the reference sample (crystalline state) has been proposed and applied to the EXAFS data processing of $Cu_{55}Zr_{45}$ metallic glass. The results are consistent with those obtained from X-ray abnormal scattering measurement.

<div align="center">References</div>

1. Huang Shengtao, et al., "Structural Analysis of Noncrystalline Materials," Science Press, 1987, Chapter 6.
2. Haensel, R., et al., in "Liquid and Amorphous Metal," ed. by E. Lüscher and H. Coufal, 1980, p 459.
3. Crescenzi, M.D., et al., SOLID STATE COMMUN, Vol 37, 1981 p 921.
4. Wagner, C.N.J., J NON-CRYST SOLIDS, Vol 31, 1978 p 1.
5. Waseda, Y., Chen, H.S., PHYS STAT SOLIDS (A), Vol 49, 1978 p 387.
6. Eissenberger, P., et al., SOLID STATE COMMUN, Vol 29, 1979 p 481.
7. Crozier, E.D., et al., CAN J PHYS, Vol 58, 1980 p 1388.
8. Cargill, G.S., J NON-CRYST SOLIDS, Vol 61, 1984 p 261.
9. Teo, B.K., Lee, P.A., J AM CHEM SOC, Vol 101, 1979 p 2815.
10. Stern, E.A., et al., PHYS REV, Vol B21, 1980 p 5521.
11. Liu Wen, ACTA PHYSICA SINICA, Vol 36, 1987 p 1551.
12. Chen, H.S., Waseda, Y., PHYS STAT SOLIDS (A), Vol 51, 1979 p 593.

Multi-Photon Quantum Statistical Theory of Driven Optical Systems (III).
Improvement of Method of Adiabatic Elimination

[English abstract of article by Lin Renming [2651 0088 2494], et al., of the Department of Physics, Fujian Teachers' University, Fuzhou]

[Text] In this paper, the authors discuss multi-photon systems by employing the adiabatic elimination method following Lugiato's procedure[4]. The authors conclude that, in both the "good cavity case" and the "bad cavity case," their results contain those drawn by Gordon's adiabatic elimination[3]. In addition, the authors' method can directly compute the correlation of the variable that has been adiabatically eliminated. Particularly in the "bad cavity case," the steady state value of the field variable correlation obtained by Lugiato's method is different from that obtained by Gordon's method. Lugiato's method is self-consistent, so it is much better.

In the appendix, the formulae for atomic squeezing and for the multi-photon spectrum of transmitted light are presented.

References

1. Lin Renming, et al., ACTA PHYSICA SINICA, Vol 37, 1988 p 573.
2. Zhang Lin, et al., ACTA PHYSICA SINICA, Vol 37, 1988 p 1438.
3. Gordon, J.P., PHYS REV, Vol 161, 1967 p 367.
4. Lugiato, L.A., PHYS REV, Vol A33, 1986 p 4079.
5. Lugiato, L.A., et al., PHYS REV, Vol A26, 1982 p 3438.
6. Lugiato, L.A., Strini, G., OPT COMM, Vol 41, 1982 p 374.
7. Lugiato, L.A., NUOVO CIMENTO, Vol B50, 1979 p 89.
8. Loudon, R., "The Quantum Theory of Light," Clarendon Press, Oxford, 1983 p 205.
9. Carmicheal, H.J., PHYS REV, Vol A33, 1986 p 3262.

Theory, Experiments Involving Laser Resonator with Low Sensitivity to Thermal Effect

[English abstract of article by Li Shichen [2621 0013 1820], et al., of the Department of Precision Instruments, Tianjin University]

[Text] A theory for laser resonators with low sensitivity to thermal effects is introduced, and a new analytical solution is obtained. The influence of changing cavity parameters has been analyzed, achieving some important results. A monomode Nd:YAG laser has been designed using the authors' procedure and their theory has been tested and verified through experiments. From the experiments, the authors have determined that the laser can operate at two different stable zones with unequal thresholds, and also that the operating state of a reasonably designed resonator, which is stable with regard to thermal effects, corresponds to the optimum TEM mode output.

References

1. Kogelnik, H., BELL SYST TECH J, Vol 44, 1965 p 455.
2. Magni, V., APPL OPTICS, Vol 25, 1986 p 107.
3. Li Shichen, et al., JOURNAL OF TIANJIN UNIVERSITY, No 2, 1989 p 59.
4. Kogelnik, H., Li, T., APPL OPTICS, Vol 5, 1966 p 1550.

Optical, Electrical Properties of Sputtered Amorphous GeN$_x$, GeN$_x$:H Films

[English abstract of article by Chen Guanghua [7115 0342 5478], et al., of the Department of Physics, Lanzhou University]

[Text] The technological conditions and basic photoelectronic properties of a-GeN$_x$ and a-GeN$_x$:H films prepared by an rf-reactive sputtering method are reported. The IR and Raman spectra are presented. The effects of the N content on ΔE and the IR and Raman spectra of a-GeN$_x$:H film are also discussed.

References

1. Carius, R., et al., J NON-CRYST SOLIDS, Vols 97/98, 1987 p 1067.
2. Chen Guanghua, et al., SOLAR ENERGY MATERIALS, Vol 12, 1985 p 471.
3. Yang, J., et al., MAT RES SOC SYMP PROC, Vol 70, 1986 p 475.
4. Honma, I., et al., APPL PHYS LETT, Vol 50, 1987 p 276.
5. Tauc, J., "Amorphous and Liquid Semiconductors," Plenum Press, 1984, Section 4.4.
6. Scuzmann, M., et al., PHYS REV, Vol B35, 1987 p 5666.
7. Kaicher, R., et al., PHYS REV, Vol B30, 1984 p 1896.
8. Bermejo, D., Cardona, M., J NON-CRYST SOLIDS, Vol 32, 1979 p 405.
9. Finger, F., et al., J NON-CRYST SOLIDS, Vols 97/98, 1987 p 1015.

Infrared, Far-Infrared Spectra of Oxide Superconductors--Ti$_x$Y$_{1-x}$Ba$_2$Cu$_3$O$_{7-\delta}$

[English abstract of article by Ye Hongjuan [0673 4767 1227], et al., of Shanghai Institute of Technical Physics, Chinese Academy of Sciences; Li Guangyuan [2621 0342 6678] of the Department of Physics, East China University of Chemical Technology, Shanghai; Cai Peixin [5591 1014 2450], et al., of Shanghai Institute of Metallurgy, Chinese Academy of Sciences]

[Text] This paper reports the infrared and far-infrared spectra of Ti$_x$Y$_{1-x}$Ba$_2$Cu$_3$O$_{7-\delta}$ (x = 0.2, 0.4) superconductors in the temperature range of from 300K to 4.2K. Seven reflection peaks have been observed in the range of 50-360 cm^{-1}, and have been identified as associated with the vibrations of Ba, Cu, O ions, Y, O ions, Ti, O ions, and Cu-O bonds, respectively. For x = 0.2, two inversion structures were observed, but only one was observed for x = 0.4. In the infrared spectra, six reflection and three absorption peaks were observed, with their intensities increasing with an increase in Ti content. The authors discuss the origin of the peaks and the inversion structures, comparing them to those for YBa$_2$Cu$_3$O$_{7-\delta}$.

References

1. Izumi, F., et al., J APPL PHYSICS, Vol 26, 1987 p L649.
2. Sigrist, T., et al., PHYS REV, Vol B35, 1987 p 7137.
3. Ye Hongjuan, et al., ACTA PHYSICA SINICA, publication pending.
4. Ye Hongjuan, et al., PHYS REV, Vol B36, 1987 p 8802.
5. Ye Hongjuan, et al., CHIN PHYS LETT, Vol 5, 1988 p 162.
6. Bonn, D.A., et al., PHYS REV, Vol B37, 1988 p 1574.

Roles of Cu-O Planes, Chains in $YBa_2Cu_3O_{7-y}$

[English abstract of article by Zhao Yong [6392 0516], et al., of the Department of Physics, Zhejiang University, Hangzhou; Zhang Han [1728 6799], et al., of the Department of Physics, University of Science and Technology of China, Hefei]

[Text] The crystal structure, electronic transport properties in normal states and superconductivity of a series of sample $YBa_2Cu_{3-x}M_xO_{7-y}$ (M = Zn, Ni, $0 \leq x \leq 0.3$) have been studied, and a more direct evidence of preferential substitution of Zn for Cu(2) is obtained. In addition, an orthorhombic (I)-to-orthorhombic (II) structural transition in the Zn-doped system, as well as the effect of electronic localization in the Ni-doped system, is observed. The investigation shows that the Zn^{3+} may replace Cu(2) preferentially, but no such replacement for Cu by Ni has been found. The role of Cu-O planes and chains on superconductivity is discussed. The importance of the coupling between Cu-O sheets and chains for high T_c superconductivity is noted.

References

1. Gang Xiao, et al., PHYS REV LETT, Vol 60, 1988 p 1446.
2. Tarascon, J.M., et al., PHYS REV, Vol B37, 1988 p 7458.
3. Jorgensen, J.D., et al., PHYS REV, Vol B36, 1987 p 5731.
4. Beech, F., et al., PHYS REV, Vol B35, 1987 p 8778.
5. Cava, R.J., et al., NATURE, Vol 329, 1987 p 423; PHYS REV, Vol B36, 1987 p 5719.
6. Tokumoto, M., et al., preprint.
7. Takagi, H., et al., PHYSICA, Vol 148B, 1987 p 349.
8. Mooij, J.H., PHYS STATUS SOLIDI, Vol A17, 1973 p 521.
9. Maeno, Y., et al., JPN J APPL PHYS, Vol 26, 1987 p L774.
10. Maeno, Y., et al., JPN J APPL PHYS, Vol 26, 1987 p L1982.
11. Santoro, A., et al., MAT RES BULL, Vol 22, 1987 p 1007.
12. Miceli, P.F., et al., preprint.
13. Zhao, Y., et al., PHYSICA C, Vol 152, 1988 p 513.

Stability of Collisionless Drift Waves in Hot Electron Plasma

[English abstract of article by Huang Chaosong [7806 2600 2646] of the Institute of Plasma Physics, Chinese Academy of Sciences, Hefei; Wu Guangxue [0702 1639 1331], et al., of the Department of Physics, Southern-Central Institute for Nationalities, Wuhan]

[Text] The low frequency interchange mode and drift wave in a hot electron plasma are analyzed by using the Vlasov equation, and the effect of hot electrons is discussed. The stabilization of the drift wave occurs when $\alpha \sim 30$ percent, and the stabilization of the interchange mode occurs when $\alpha \sim 10$ percent, where α is the fraction of hot electrons. The influences of the ion Larmor radius, density gradient and temperature of the plasma, wavelength of perturbation, and the magnetic curvature on the stability are discussed. Compared with the results of the strongly collisional drift wave derived from the MHD approximation, the collisionless drift wave can be stabilized by the hot electrons more easily.

References

1. Van Dam, J.W., et al., "Proceedings of the Workshop on Advanced Bumpy Torus Concepts," California, 1983, p 167.
2. Miller, R.L., Van Dam, J.W., NUCL FUSION, Vol 27, 1987 p 2101.
3. Chen Yanping, et al., ACTA PHYSICA SINICA, Vol 37, 1988 p 546.
4. Nelson, D.B., Hedrick, C.L., NUCL FUSION, Vol 19, 1979 p 283.
5. Nelson, D.B., PHYS FLUIDS, Vol 23, 1980 p 1850.
6. Chen, X., et al., "MIT Report," PFC/JA-87-43, 1987.
7. Huang Chaosong, et al., ACTA PHYSICA SINICA, Vol 37, 1988 p 1284.
8. Krall, N.A., "Advances in Plasma Physics," Wiley, New York, 1968, p 153.
9. Batchelor, D.B., Hedrick, C.L., NUCL FUSION, Vol 19, 1979 p 235.
10. Huang Chaosong, et al., ACTA PHYSICA SINICA, Vol 36, 1987 p 1112.

Spectroscopic Measurement of Electron Temperature in Current Rising Phase on CT-6B Tokamak

[English abstract of article by Li Zanliang [2621 6363 5328], et al., of the Institute of Physics, Chinese Academy of Sciences; Liu Xiang [0491 5046], et al., of the Institute of High Temperature and High Pressure Physics, University of Science and Technology of Chengdu]

[Text] The time evolution of the electron temperature in the plasma current rising phase on the CT-6B Tokamak is estimated by the historical method for oxygen impurity lines. The time variations of line emissions of OII-OVI in the VUV region are measured by a 1-meter grazing incidence vacuum spectrometer, and the electron density is measured using the FIR HCN laser interferometer. The switch-on time of each line emission is used to estimate the electron temperature. The influences of the oxygen impurity influx rate and confinement time on the intensity and switch-on time of the line emissions are surveyed numerically. The estimated electron temperatures are approximately 3.6, 5.6, 7.3, 10.8 and 21 eV, respectively, at 0.36, 0.56, 0.66, 0.90 and 1.4 ms after the start of discharge, and indicate the plasma temperature in the central region.

References

1. Equipe TFR, NUCLEAR FUSION, Vol 5, 1978 p 647.
2. Goldman, L.M., Kilb, R.W., PLASMA PHYSICS, Vol 6, 1964 p 217.
3. Equipe TFR, NUCLEAR FUSION, Vol 15, 1975 p 1053.
4. Ohasa, K., et al., JPN J APPL PHYS, Vol 15, 1976 p 2403.
5. Mimura, M., et al., JPN J APPL PHYS, Vol 25, 1986 p 458.
6. Li Zanliang, et al., CHINESE PHYSICS LETTERS, Vol 6, 1989 p 47.
7. Wang Wenshu, et al., ACTA PHYSICA SINICA, Vol 36, 1987 p 712.
8. Bell, K.L., et al., J PHYS AND CHEM REFERENCE DATA, Vol 12, 1983 p 891.
9. Equipe TFR, PLASMA PHYS, Vol 20, 1978 p 207.
10. Suckewer, S., et al., PHYS REV, Vol A20, 1978 p 207.
11. Hinnov, E., et al., NUCLEAR FUSION, Vol 22, 1982 p 325.
12. Bates, D.R., "Atomic and Molecular Processes," Academic Press, 1962.

Optical Characteristics of ZnWO$_4$ Single Crystals

[English abstract of article by Wang Hong [3076 3126], et al., of Beijing Polytechnic University; Zhou Tang [0719 2768], et al., of the Institute of Physics, Chinese Academy of Sciences]

[Text] The transmittance curves of ZnWO$_4$ single crystals grown by the Czochralski method have been measured. The authors suggest that the existence of an oxygen vacancy is the basic reason for the rosy color of the crystal. The position of the optical indicatrix, the refractive indices in the visible wavelength region and Sellmeier's equations have been determined more accurately.

References

1. Filipenko, O.S., et al., CRYSTALLOGRAPHY, Vol 13, 1968 p 163.
2. Oi, T., et al., APPL PHYS LETT, Vol 36, 1980 p 278.
3. Zhu, Y.C., et al., NUCL INSTR METH, Vol A244, 1986 p 579.
4. Zhou Yadong, et al., JOURNAL OF THE CHINESE CERAMIC SOCIETY, Vol 14, 1986 p 479.
5. Takagi, K., et al., J CRYST GROWTH, Vol 52, 1981 p 580.
6. Zhou Yadong, et al., Chinese patent, GK 85104053.
7. Lammers, M.J.J., et al., PHYS STAT SOL, Vol (a)63, 1981 p 569.
8. Hu Boqing, et al., ACTA PHYSICA SINICA, Vol 32, 1983 p 1098.
9. Wang Hong, et al., ACTA PHYSICA SINICA, Vol 37, 1988 p 43.
10. Bond, W.L., J APPL PHYS, Vol 36, 1965 p 1674.

XPS Study of YBa-Cu-Al-O System

[English abstract of article by Zhang Han [1728 6799], et al., of the Department of Applied Chemistry, University of Science and Technology of China, Hefei; He Zhenhui [0149 2182 6540], et al., of the Department of Physics, University of Science and Technology of China, Hefei]

[Text] The XPS, oxygen content and resistance-temperature relationship of a $YBa_2Cu_{3-x}Al_xO_{7-y}$ single phase system have been determined. The experimental results show that Al can possibly serve as a partial substitute for the Cu and Y positions in the 1-2-3 phase. Because of the existence of Al^{3+}, the oxygen content increases, the oxygen environment tends to be uniform and the difference between the two states of O_{1s} in XPS is indistinct. The presence of Cu^{3+} is clearly observed.

References

1. Hazen, R.M., et al., PHYS REV, Vol B35, 1987 p 7238.
2. Daharma-Wardana, M.W.C., PHYS LETT, Vol A126, 1987 p 205; Vol A126, 1987 p 61.
3. Steiner, P., et al., Z PHYS B, Vol 66, 1987 p 275.
4. Steiner, P., et al., Z PHYS B, Vol 67, 1987 p 497.
5. Werfl, F., et al., Z PHYS B, Vol 70, 1988 p 317.
6. Ji Mingrong, et al., SOLID STATE COMMUN, Vol 63, 1987 p 511.
7. Zhang Han, et al., SOLID STATE COMMUN, Vol 66, 1988 p 291.
8. Siegrist, T., et al., PHYS REV, Vol B36, 1987 p 8365.
9. Kirby, P.B., et al., PHYS REV, Vol B36, 1987 p 8315.
10. Frank, J.P., et al., PHYS REV, Vol B36, 1987 p 2038.
11. Steiner, P., et al., Z PHYS B, Vol 69, 1988 p 449.
12. Tarascon, J.M., et al., PHYS REV, Vol B37, 1988 p 7458.
13. Jorgensen, J.D., et al., PHYS REV, Vol B36, 1987 p 5731.

Superconducting Current-Carrying Properties of $Yb_xY_{1-x}Ba_2Cu_3O_{7-y}$

[English abstract of article by Zhao Yong [6392 0516], et al., of the Department of Physics, Zhejiang University, Hangzhou; Sun Shifang [1327 1709 2455], et al., of the Department of Physics, University of Science and Technology of China, Hefei]

[Text] The microstructure, superconductivity and superconducting current-carrying properties of $Yb_xY_{1-x}Ba_2Cu_3O_{7-y}$ are investigated systematically. The authors find that, when the Yb content increases, T_c changes slightly, but the critical current density decreases with the grain size. The results suggest that decreasing the grain size alone cannot increase the critical current density of granular superconductors in which the couplings among grains are weak.

References

1. Müller, K.A., et al., PHYSICA C, Vol 148B, 1987 p 149.
2. Zhao Yong, et al., publication pending.
3. Sun, S.F., et al., EUROPHYS LETT, Vol 6, 1988 p 359.
4. Yu Daoqi, et al., ACTA PHYSICA SINICA, Vol 37, 1988 p 1048.
5. Zhao Y., et al., SOLID STATE COMMUN, Vol 66, 1988 p 31.
6. Zhao Y., et al., J APPL PHYS, in press.
7. Zhao Y., et al., SOLID STATE COMMUN, Vol 66, 1988 p 35.
8. Zhang, Q.R., et al., PHYS LETT, Vol Z124, 1987 p 457.
9. Zhao, Y., et al., SOLID STATE COMMUN, Vol 64, 1987 p 885.
10. Zhao, Y., et al., Z PHYS B, Vol 71, 1988 p 53.
11. Chen, Z.Y., et al., PHYSICA C, Vols 153-155, 1988 p 409.
12. Podder, A., et al., PHYSICA C, Vols 153-155, 1988 p 924.
13. Zhao, Y., et al., PHYSICA C, Vols 153-155, 1988 p 304.
14. Murakami, M., et al., PHYSICA C, Vol 153-155, 1988 p 994.

First Pulsed Nuclear Pile To Go Critical

40080159a Beijing RENMIN RIBAO in Chinese 20 Apr 89 p 1

[Article by Cheng Jian [2052 1696] and Hu Jie [5170 2638]: "First Pulsed Nuclear Pile to Go Critical, Another Major Achievement in Nuclear Technology"]

[Text] Chengdu, 19 Apr (XINHUA)--On 6 April the first pulsed nuclear pile designed and constructed by China reached critical state in zero power operation. Self-sustained chain reaction and the first experimental results were successfully obtained. This is another major technical accomplishment following the pressurized-water power pile and high-flux experimental pile. This accomplishment is the result of 10 years of hard work by the technical staff at the First Research Institute of the Ministry of Nuclear Industry.

A pulsed nuclear pile is a uniquely promising nuclear pile for research use. Compared to a conventional pile, it can rapidly raise the power by a factor of several thousand in a very short period of time without any danger. Because it is very safe, it can be built in densely populated areas. Its structure is relatively simple and the safety-equipment requirement is relatively low. The amount of fuel required is low and the core life is long. The construction and operating costs are approximately one half of those of a conventional pile of the same power level. A pulsed pile has a wide range of applications in industry, agriculture, medicine, basic science, archaeology and forensic science.

Developed nations have built many pulsed nuclear piles. However, the market is monopolized by General Electric. The fact that our nuclear pile has gone critical signifies that China's nuclear technology is among the leaders in the world.

Room-Temperature Fusion Experiments Hailed as Success

40080159b Beijing RENMIN RIBAO in Chinese 23 Apr 89 p 3

[Article by Jiang Zaizhong [1203 0961 1813], Chen Zujia [7115 4371 3946] and Wang Yougong [3769 3645 1872]: "Cold Fusion Experiments Successful"]

[Text] Beijing, 22 Apr (XINHUA)--Chinese scientists have made significant progress in "room-temperature nuclear fusion" (cold fusion), according to the State Scientific Commission.

A report signed and released by nuclear physicists, electrochemists and radiochemists at Beijing Normal University revealed that a large number of neutrons were detected 20 hours after they began to pass a current between a palladium tube cathode and platinum wire anode in heavy water at 2 pm on 18 April. Approximately 700 neutrons were detected by a liquid scintillation counter in 80 minutes. At 10 pm on 19 April, they replaced the palladium cathode with an identical new tube and added a tritium collector to continue the experiment under the same conditions. At 6 pm on 20 April, a high neutron count was observed again. The results are similar to the "cold fusion" effect.

The Beijing Normal University work has four major findings. First, in both attempts it took approximately 20 hours to obtain a high neutron count. There seems to be a certain pattern. Next, the signal-to-noise ratio of the neutron detector is 100:1. Hence, the count ought to be reliable. The neutron energy measured is approximately 2.45 MeV which is close to that of the neutron released from the fusion of two deuterium atoms to form helium 3. Last, tritium, a product of the deuterium-deuterium reaction, was detected.

Scientists in China are very concerned about cold fusion. There are more than a dozen institutions involved in this type of experiment which have observed some of the so-called cold-fusion phenomenon. The research group at the Institute of Chemistry of the Chinese Academy of Sciences detected a very strong radiation signal with a nuclear detector from the cell with a palladium cathode which they designed to

electrolyze heavy water on 18 April. There was excessive cell
temperature rise and significant increase in tritium content in the
electrolyte. Different from the apparatus used by Fleischmann, the
Chinese apparatus did not use a platinum anode, and also did not use a
lithium deuteroxide electrolyte and pure palladium cathode.

The China Nuclear Engineering Corporation announced that researchers at
the Institute of Nuclear Physics and Chemistry of the Chinese Applied
Physics Institute successfully duplicated room-temperature fusion on
21 April.

Researchers detected high-energy neutrons with two different methods. A
research group inserted a palladium electrode and a platinum electrode
in heavy water, and up to 100 neutrons per second were found after a
current was impressed for 120 hours. Another group used deuterium gas
(an isotope of hydrogen which exists in abundance in seawater) and two
palladium electrodes to yield high-energy neutrons as well. Experts
said that various methods were used to ascertain that those neutrons
came from nuclear fusion. Nuclear fusion at room temperature was first
disclosed by Professor Fleischmann of the University of Southampton,
England, and Professor Pons of the University of Utah, U.S.A., on
23 March 1989.

Recently, scientists in Hungary, the USSR, Poland, Italy, Japan and
South Korea all announced the successful confirmation of this
experiment.

First Synchrotron Radiation Facility Completed

40080167   Shanghai JIEFANG RIBAO in Chinese 27 Apr 89 p 1

[Article by Xuan Fenghua [1357 1144 5478] and Tian Wenxi [3944 2429 0823]: "First Synchrotron Radiation Facility Completed"]

[Text] Hefei, 26 Apr (XINHUA)--The China University of Science and Technology reported on 26 April that the first synchrotron radiation device was officially completed and operational at 1:08 Beijing daylight savings time. It only took 23 hours from the injection of an electron beam into the storage ring to obtaining intense synchrotron radiation. Experts believed that this kind of speed was rare for similar devices in the world.

This facility is another major accomplishment in high technology following the success of the Beijing Positron-Electron Collider project. It signifies that China is one of the leaders in the construction of synchrotrons.

The construction of this national synchrotron radiation laboratory began in 1984. It is located on the new campus of China University of Science and Technology in the southern suburb of Hefei. It has approximately 150 mu of land. The building is 12900 square meters. It principally consists of three parts; a 35-meter-long 200 MeV linear accelerator which is used as the injector, a 66-meter-circumference 800 MeV electron storage ring with an average current of 100-300 mA, and a synchrotron radiation experiment area with 27 windows and over 50 experimental stations.

This facility was completely designed, constructed, installed and adjusted by Chinese technical staff. The speed of construction, quality of engineering work and cost are at least comparable to those of similar facilities built in the world. It fully illustrates the wisdom and hard working spirit of the Chinese scientists involved.

The backbone force behind this major project is a number of young and middle-aged technical staff at the China University of Science and Technology. Their average age is 38. The work was done with a shortage

of manpower, experience funding and materials. However, a strong
feeling of responsibility to make a contribution to high technology in
China drove them to struggle through this project. In the ten-year
period from development to completion, they did not receive any special
material reward. They voluntarily gave up vacation. They did not have
time to take care of their sick relatives and help their children's
homework. They also turned down opportunities to work or study abroad.

This synchrotron radiation project has received a great deal of
attention from the leadership of the Chinese Communist Party and the
government. Deng Xiaoping has always supported this project. General
Secretary Zhao Ziyang has personally inspected the facility. A number
of comrades in leadership position have been concerned about its
progress and assisted in solving difficulties encountered in its
construction.

Many famous scientists such as Yang Zhengning, Lee Zhengdao, Wu
Jianxiong, Yuan Jialiu and Samuel Ding overseas and Wang Ganchang [3769
3227 2490] and Zhang Wenyu [1728 2429 5940] in China have given their
support and praise to this project.

Vice President Bao Zhongmo of China University of Science and Technology
indicated that as an open national laboratory this synchrotron radiation
facility will be available to all institutions in China and the world
after it is completed. At the present moment, it has five windows for
five experimental stations, i.e. soft x-ray lithography, x-ray
microscopy, x-ray electron energy spectrum, time sharing spectroscopy
and photochemistry. Additional windows and experimental stations will
be opened as the number of users increases in the future.
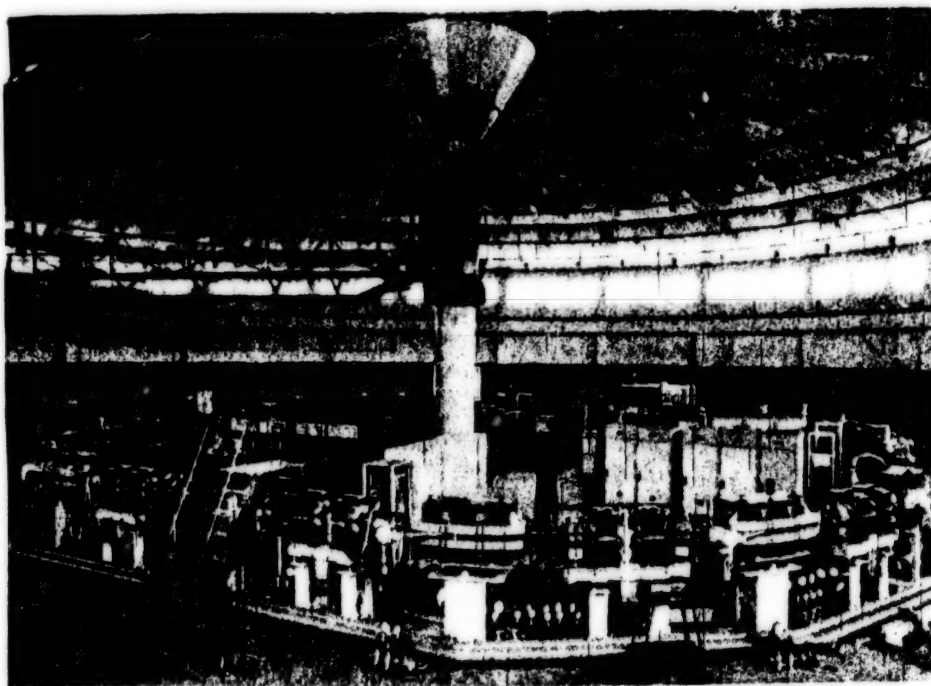
- END -

Foreign Broadcast Information Service (FBIS) and Joint Publications Research Service (JPRS) publications contain political, economic, military, and sociological news, commentary, and other information, as well as scientific and technical data and reports. All information has been obtained from foreign radio and television broadcasts, news agency transmissions, newspapers, books, and periodicals. Items generally are processed from the first or best available source; it should not be inferred that they have been disseminated only in the medium, in the language, or to the area indicated. Items from foreign language sources are translated; those from English-language sources are transcribed, with personal and place names rendered in accordance with FBIS transliteration style.

Headlines, editorial reports, and material enclosed in brackets [ ] are supplied by FBIS/JPRS. Processing indicators such as [Text] or [Excerpts] in the first line of each item indicate how the information was processed from the original. Unfamiliar names rendered phonetically are enclosed in parentheses. Words or names preceded by a question mark and enclosed in parentheses were not clear from the original source but have been supplied as appropriate to the context. Other unattributed parenthetical notes within the body of an item originate with the source. Times within items are as given by the source. Passages in boldface or italics are as published.

SUBSCRIPTION/PROCUREMENT INFORMATION

END OF
FICHE

DATE FILMED

1 AUG 89